AD-A230 955

91 1 15097

REPORT DOCUMENTATION PAGE

1a. REPORT SECURITY CLASSIFICATION	1b. RESTRICTIVE MARKINGS
Unclassified	

2a. SECURITY CLASSIFICATION AUTHORITY	3. DISTRIBUTION/AVAILABILITY OF REPORT
2b. DECLASSIFICATION/DOWNGRADING SCHEDULE	Approved for public release; distribution unlimited.

4. PERFORMING ORGANIZATION REPORT NUMBER(S)	5. MONITORING ORGANIZATION REPORT NUMBER(S)
	ARO 24626.117 PH-UIR

6a. NAME OF PERFORMING ORGANIZATION	6b. OFFICE SYMBOL (If applicable)	7a. NAME OF MONITORING ORGANIZATION
		U. S. Army Research Office

6c. ADDRESS (City, State, and ZIP Code)	7b. ADDRESS (City, State, and ZIP Code)
	P. O. Box 12211 Research Triangle Park, NC 27709-2211

8a. NAME OF FUNDING/SPONSORING ORGANIZATION	8b. OFFICE SYMBOL (If applicable)	9. PROCUREMENT INSTRUMENT IDENTIFICATION NUMBER
U. S. Army Research Office		DAAL03 86-K-0173

8c. ADDRESS (City, State, and ZIP Code)	10. SOURCE OF FUNDING NUMBERS			
P. O. Box 12211 Research Triangle Park, NC 27709-2211	PROGRAM ELEMENT NO.	PROJECT NO.	TASK NO.	WORK UNIT ACCESSION NO.

11. TITLE (Include Security Classification)
Effects of source correlations on the spectrum of radiated fields

12. PERSONAL AUTHOR(S)
Avshalom Gamliel

13a. TYPE OF REPORT	13b. TIME COVERED	14. DATE OF REPORT (Year, Month, Day)	15. PAGE COUNT
Technical	FROM _____ TO _____	September 1990	200

16. SUPPLEMENTARY NOTATION The view, opinions and/or findings contained in this report are those of the author(s) and should not be construed as an official Department of the Army position, policy, or decision, unless so designated by other documentation.

17.	COSATI CODES		18. SUBJECT TERMS (Continue on reverse if necessary and identify by block number)
FIELD	GROUP	SUB-GROUP	Coherence; correlation-induced spectral changes; radiation efficiency

19. ABSTRACT (Continue on reverse if necessary and identify by block number)

Please see Abstract on pages iv-v.

20. DISTRIBUTION/AVAILABILITY OF ABSTRACT	21. ABSTRACT SECURITY CLASSIFICATION
☐ UNCLASSIFIED/UNLIMITED ☐ SAME AS RPT. ☐ DTIC USERS	Unclassified

22a. NAME OF RESPONSIBLE INDIVIDUAL	22b. TELEPHONE (Include Area Code)	22c. OFFICE SYMBOL
Nicholas George	716-275-2417	

DD FORM 1473, 84 MAR 83 APR edition may be used until exhausted. All other editions are obsolete.

EFFECTS OF SOURCE CORRELATIONS ON THE SPECTRUM OF RADIATED FIELDS

by

Avshalom Gamliel

Submitted in partial fulfillment

of the

Requirements for the Degree

DOCTOR OF PHILOSOPHY

Supervised by: **Professor Nicholas George**

Professor Emil Wolf

The Institute of Optics

University of Rochester

Rochester, New York

Vita

Avshalom Gamliel was born ███████████████. In 1984 he received a B.S. degree in Mathematics and in Physics from the University of Illinois at Chicago, and later that year joined the Ph.D. program at The Institute of Optics.

Acknowledgments

First and foremost I am obliged to Zafi Gamlieli who brought me to this country and facilitated my studies here since 1981. His encouragements and support have been invaluable at all times.

Special thanks to Professors Nicholas George and Emil Wolf for their support and guidance in the last six years.

Abstract

It has long been assumed that the normalized spectrum of a radiated field remains invariant on propagation. Recent developments in coherence theory have demonstrated that, in general, the normalized spectrum of a radiated field changes on propagation depending on the state of coherence and the original spectrum of the source. In this thesis we examined the effect of the spatial correlations of the source fluctuations on the radiated fields.

We first considered the effect of source correlations on the total radiated power using the concept of "radiation efficiency". For a class of planar sources, known as Schell-model sources we showed that the radiation efficiency and hence also the total emitted power increase with increasing source size or increasing source correlation length. Interestingly enough, our results indicate that any source of this class whose linear dimensions are larger than about a wavelength has a radiation efficiency that exceeds 90%.

In investigating the radiation efficiency of three-dimensional, partially coherent, primary sources we develop a method for finding the correlation function that maximizes the radiation efficiency and the total power emitted by such sources. In the case of quasi-homogeneous sources we show that the optimal degree of spatial coherence is $\sin kr'/kr'$ where r' is the spatial offset and k is the wave number. The significance of this result is discussed in connection with blackbody radiation.

In considering the effects of the source correlation on the spectrum of the radiation we analyze a simple physical configuration of two small sources. Our calculations demonstrate that one can choose correlation functions that give rise to line narrowing, line broadening, line shifting and line splitting. Similar results are also obtained when the full electromagnetic nature of the sources is taken into account. We illustrate this fact by considering radiation from two partially correlated linear dipoles.

To gain a different perspective for the effects of the spatial correlations on the spectrum we consider an example in coherent-mode representation. In this example we introduce the concept of "spectral modifier" to show the small spectral changes that occur on propagation of single coherent modes, and we then examine the spectral effects when several modes are present.

In the final part of the thesis we consider the spectral effects arising from source correlations when the fields propagate in homogeneous or inhomogeneous media. Our calculations elucidate the development of spectral shifts as a function of the propagation distance and illustrate the various spectral effects for light propagation in graded-index fibers.

Table of contents

1. Introduction

2. Radiation efficiency

3. Spectral modulation with scalar sources

4. Spatial and spectral effects with electromagnetic sources

5. Spectral effects in coherent mode representation

6. Spectral changes on propagation of partially coherent light in media

7. Summary

List of figures

1

Introduction

Introduction

The term *spectrum* plays an important role in most areas of science. In optics it refers to the distribution of energy as a function of frequency. This concept has deep roots in the development of optical physics. The first reported experiments demonstrating that sunlight consists of multi-color contributions were performed by Sir Isaac Newton and published as early as 1666.[1] Since the days of Newton, observations and measurements of spectra have became a leading research tool that was largely responsible for the development of quantum mechanics and has made significant contributions to areas such as thermodynamics, chemistry, astronomy and metrology.

In spite of the fact that relatively accurate measurements of spectra were made as early as 1817[2], only rough guesses, intuition and an ample measure of luck made the experimental results useful for the development of the various sciences that were based on spectroscopy.[3] Implicit in all spectroscopic measurements is the assumption that the spectrum of the field measured by various means is equal to the spectrum of the source generating it, even when the light has propagated a significant distance from the source This assumption, as was demonstrated recently, is valid only in special cases. In general, the spectrum of partially coherent light changes on propagation. The extent and type of the changes are determined by the state of coherence of the source and separately by the propagation medium.

Although the concept of coherence was recognized many years ago, it appears that scientists have not considered the effects of coherence on the spectrum until recently.[4] Experimentally, it is known that the most common sources of light do indeed produce a spectrum that does not vary appreciably on propagation. Although several cases of spectral changes were encountered, they were either attributed to the Doppler effect[5] or left as an experimental uncertainty.[6] Theoretically, the main

reason that coherence effects on the spectrum have not been investigated earlier may be due to the fact that for many years the main quantities used in coherence theory were space-time correlations. In particular, the second order correlation function most widely used was the mutual coherence function.[7] One of the major developments of statistical optics in the last decade was the formulation of coherence theory in the space-frequency domain, which shifted the emphasis from the mutual coherence function to the cross-spectral density function. The transition to space-frequency domain simplifies some of the theoretical techniques used to solve boundary value problems and focuses the emphasis on the frequency-dependence of all the relevant physical quantities.

Wolf first derived conditions under which the spectrum of light generated by a quasi-homogeneous source remains invariant after propagation.[3b] According to that analysis, planar secondary quasi-homogeneous sources whose degree of correlation obeys a certain scaling law produce light whose spectrum is independent of the direction of observation and is equal to the source spectrum. Additional investigations have since shown the effects of spatial correlations in various physical situations.

The simplest physical system that was considered was that of two small radiating sources.[8] The simplicity lies in the fact that both sources are assumed to be essentially point sources and the spatial correlation is a function that depends on the position of the two sources and on the frequency. It has been shown that even this simple system can produce spectral line shifts as well as actual modulation of the radiated spectrum. These theoretical predictions have since been verified experimentally by several groups.[9]

In considering different spatial correlations, the next level of complexity is that of extended secondary planar sources. Here the spatial correlations are taken

between any two points in the source plane. Most of the investigations relating to planar sources examined the spectral shifts occurring on the propagation of light from the source plane.[10] Additional work explored more general spectral changes such as line broadening, line narrowing and line distortion in partially coherent sources whose cross-spectral density consists of several Hermite-Gaussian modes.[11] A number of experiments in this area have also been reported.[12]

When the radiating sources are three-dimensional, the spatial correlations have additional degrees of freedom compared with the spatial correlations of planar sources.[13] The effects of the spatial correlations on the spectrum of the light produced by three-dimensional sources are, however, similar to those produced by planar sources.[14]

The investigation of changes in the spectrum of partially coherent light on propagation have dealt so far mainly with propagation in free space. In many practical applications light propagates in dispersive media that are homogeneous or inhomogeneous. In these cases it is important to estimate, for example, the changes in the spectrum after propagating a certain distance in the medium.[15]

The spectrum of the field is not the only physical quantity affected by source correlations. Closely related quantities are the radiated power at a given frequency, the directivity of a radiating system and the shape of intensity profile of light beams produced by partially coherent sources. The effects of source correlations on the spatial distribution of the radiated intensity have been investigated for several years.[16] Of interest in this thesis are the radiation efficiency, the directivity and the shape of the intensity profile of partially coherent optical beams.

The radiation efficiency of partially coherent sources is a concept that has been developed as a measure for the amount of light generated by a source of a given intensity profile and with varying forms of spatial correlations. Most of the early

work on radiation efficiency involved quasi-homogeneous sources.[16] Other types of partially coherent sources including planar and three-dimensional sources have since been investigated.[17] Considering the effects of the correlation on the radiation efficiency, it is natural to look for the spatial correlation that maximizes the radiation efficiency and hence the total power emitted by a source of a prescribed intensity profile.[18]

The total emitted power does not give much information about the distribution of the radiation in space. The radiant intensity at a given frequency is important for the characterization of the directivity of fields produced by partially coherent sources and in calculations of the intensity profiles of partially coherent beams. Since the radiant intensity depends on spatial correlation, so do the directivity and the intensity profile. Of particular interest in this respect are the intensity profiles of the so-called Gaussian Schell-model sources[19] that are closely related to certain laser radiators.

1.2   Organization of the thesis

This thesis describes several investigations on the effect of source correlation on the physical properties of the radiated field. Specifically, we discuss the dependence of the spectrum of light produced by partially coherent sources on the spatial correlations of the source fluctuations. Most of the material included in the following chapters has already been reported in papers that are already published or have been submitted to publication. The pertinent references are listed in Appendix E. Each chapter is concerned with a specific aspect of the theory, and the presentation does not always follow the chronological development of the work. Throughout this thesis attempts have been made to thoroughly document the relevant literature. End notes to every chapter contain extensive lists of references in addition to supplemental statements that could not be incorporated in the main text. Since much of the research concentrates on closely related areas, some of the fundamental papers may be referenced more than once, where appropriate.

In the second part of this chapter we review some elements of coherence theory and establish the notation and conventions used throughout the rest of the thesis. Our treatment is based on classical statistical optics and on the consideration of statistically stationary fields. Most of the formal treatment is based on space-frequency representation so that quantities such as the radiant intensity, the total power and the directivity refer to their respective values at a single frequency. We also present some of the basic relations in the space-time domain in order to illustrate the advantages of using the space-frequency representation. Following the discussion of the cross-spectral density function we describe model sources which are frequently used in the theory as well as in the formulation of coherent-mode representation.

Chapter 2 contains a description of investigations of the radiation efficiency and directivity of fields produced by partially coherent planar and three-dimensional sources. Specifically we examine the radiation efficiency of planar Gaussian Schell-model sources. We determine the spatial correlation which maximizes the radiation efficiency for three-dimensional sources of prescribed intensity profiles. While we show that the maximum radiation efficiency of planar sources is obtained when the source is fully coherent, three-dimensional coherent sources are, in general, highly inefficient. Since the radiation efficiency and the directivity are evaluated at a single frequency, it is necessary to account for the original source spectrum to obtain the total efficiency or directivity. Some of the spectral effects are considered in the following chapters.

In chapter 3 we begin our discussion of correlation induced spectral changes. We consider a simple physical configuration of two small sources and describe some of the possible ways in which the spectrum of light can be modulated by appropriately modifying the spatial correlations. The analysis up to this point is based on scalar theory. In chapter 4 the analysis is extended to the full electromagnetic fields, by considering the radiation produced by two linear electric dipoles. This chapter expands the analysis of the spectral modulation technique to include directional effects and the vector properties of the field. A comparison between the results of chapter 3 and chapter 4 shows, as one might perhaps expect, that the electromagnetic treatment reduces to the results of scalar theory in certain limits.

The theoretical predictions of spectral changes in chapters 3 and 4 are discussed without suggesting any possible mechanism that can produce the required spatial correlations. In chapter 5 we consider the radiation from a secondary planar source whose cross-spectral density consists of several coherent modes. The choice

of the Hermite-Gaussians as the functional form of the coherent modes makes the analysis relevant to applications where independent laser modes are present in a source. The theory developed in this chapter shows the spectral changes that occur on propagation of individual coherent modes. When the radiation consists of several coherent modes the changes in the spectrum can be attributed to correlation effects which are manifested by the relative strengths of the individual modes present in the source.

The analysis presented in chapters 2 through 5 concerned propagation of light in free space. In most practical applications light passes through optical elements and through media whose response is frequency-dependent. In chapter 6 we consider propagation of partially coherent light through homogeneous and inhomogeneous media, as well as the effects of dispersion. In particular, we consider propagation through optical fibers whose index of refraction has a quadratic profile (so-called Selfoc fibers). As one may expect, spectral changes that take place on propagation in free space are somewhat enhanced by propagation in a medium characterized by a frequency dependent index of refraction.

Throughout this thesis various symbols were used to denote numerous physical and mathematical entities. We made every effort to define all symbols the first time that they occur in the text. In Appendix F we present a list of the main symbols and their definitions.

1.3   Elements of coherence theory

In this section we summarize some basic results of coherence theory which are essential to the development of the material presented in the rest of the thesis. We focus our attention on the development of space-frequency representation, and we discuss properties of the cross-spectral density and the so-called coherent-mode representation. This review also includes short derivations of the main relations involving various physical quantities of interest.

The concept of spatial correlation

Consider an aperture in an opaque screen[20] that is illuminated by a light source as shown in Fig. 1.1. The field distribution in the plane of the aperture is known as a *secondary source*. The concept of a secondary source is useful in describing practical situations where one considers the light incident on the entrance or exit pupil of an optical system, or when describing a particular distribution of light without regard to the physical system which produces the radiation in the first place. We denote the field strength at two typical points in the plane of the aperture and at two different times by complex analytic signals[21] $V(P_1, t_1)$, $V(P_2, t_2)$ respectively. The correlation between the fluctuations of the field at the two points is characterized by the average

$$C(P_1, P_2; t_1, t_2) = \left\langle V^*(P_1, t_1) V(P_2, t_2) \right\rangle . \qquad (1.1)$$
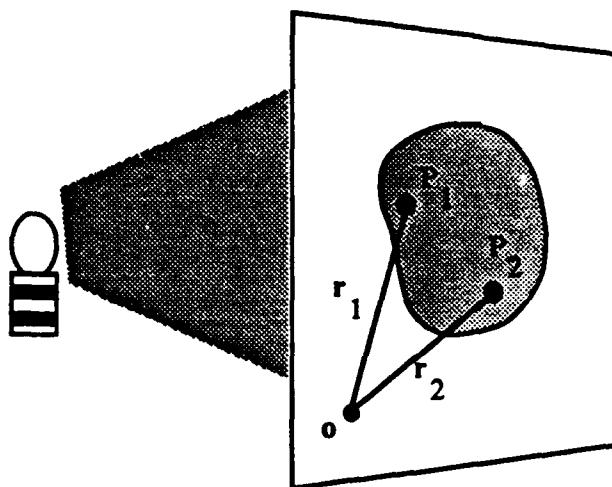
Figure 1.1:   A secondary source consisting of an aperture in a planar opaque
screen. P_1 and P_2 are two typical points in the plane of the aperture.

This type of average, which occurs frequently in our analysis, is taken over an ensemble of realizations of similar systems, and it is denoted by the angular brackets.[22]

In this document we consider only fields which are stationary in the wide sense, i.e. fields whose average is a constant which is independent of time, and whose two-point correlation Γ depends on the two time arguments only through the difference $t_2 - t_1$, namely

$$\Gamma(r_1, r_2; \tau) = \left\langle V^*(r_1, t)V(r_2, t+\tau) \right\rangle .$$ (1.2)

The space-time correlation $\Gamma(r_1, r_2, \tau)$ is called the *mutual coherence function*.[23] which had been widely used together with its normalized form, the *complex degree of coherence*

$$\gamma(r_1, r_2; \tau) = \frac{\Gamma(r_1, r_2; \tau)}{\sqrt{\Gamma(r_1, r_1; \tau)}\sqrt{\Gamma(r_2, r_2; \tau)}} , \qquad (1.3)$$

whose magnitude satisfies the constraint

$$\left|\gamma(r_1, r_2; \tau)\right| \leq 1 . \qquad (1.4)$$

In Eq. (1.4) the lower limit, zero, is obtained for a temporally incoherent field and the upper limit corresponds to a temporally coherent field.

The mutual coherence function conveniently facilitates calculations involving interference of partially coherent light. For calculations involving the propagation of partially coherent light it is usually better to use the cross-spectral density function. Before we define it, we consider the generalized[24] Fourier representation for the field $V(r, t)$ in the form

$$V(r,t) = \int_0^\infty v(r; \omega) e^{-i\omega t} d\omega . \qquad (1.5)$$

The cross-spectral density function is defined by the ensemble average

$$W(r_1, r_2; \omega) \delta(\omega - \omega') = \left\langle v^*(r_1; \omega) v(r_2; \omega') \right\rangle , \qquad (1.6)$$

where $\delta(\omega - \omega')$ is the Dirac delta function. Its appearance in Eq. (1.6) arises from the assumption of stationarity of the field. I is important to observe that the cross-spectral density function defined by Eq. (1.6) is a measure of the spatial correlation of

the field fluctuations at a single frequency ω. Because of our assumption of stationarity, the cross-spectral density function has no information about the spatial correlation of the fluctuations of the field at different temporal frequencies. As we show below, the fact that the cross-spectral density is a spatial correlation at a single frequency makes it particularly suitable for calculations where the frequency dependence of the variables is important.

The cross-spectral density function and the mutual coherence function are related by the generalization of the well known Wiener-Khintchine theorem[26]

$$W(r_1,r_2;\omega) = \int_{-\infty}^{\infty} \Gamma(r_1,r_2,\tau)e^{i\omega\tau}\,d\tau \ , \qquad (1.7)$$

$$\Gamma(r_1,r_2,\tau) = \int_{0}^{\infty} W(r_1,r_2;\omega)e^{-i\omega\tau}\,dv \ . \qquad (1.8)$$

This relatively simple relation is justified on the basis of a substantial amount of mathematical analysis that is outside the scope of this manuscript.[27]

Before leaving the subject of the mutual coherence function we compare the expressions governing the propagation of the mutual coherence function and of the cross-spectral density function to the far zone. This comparison illustrates one of the advantages of using the cross-spectral density in propagation calculations. In free space, the mutual coherence function is given by

$$\Gamma(r_1,r_2,\tau) = \frac{1}{(2\pi)^2} \iint_\sigma \frac{\cos\theta_1 \cos\theta_2}{R_1^2 R_2^2}$$

$$\times \hat{\mathcal{D}}\Gamma\left(s_1,s_2,\tau-\frac{R_2-R_1}{c}\right)d^2s_1\,d^2s_2 \ , \tag{1.9}$$

where s_j are position vectors in the source plane σ, θ_j are the angles which the vectors r_j make with the positive z-direction, c is the vacuum speed of light and $\hat{\mathcal{D}}$ is the differential operator

$$\hat{\mathcal{D}} = 1 - \frac{R_1-R_2}{c}\frac{\partial}{\partial\tau} - \frac{R_1 R_2}{c^2}\frac{\partial^2}{\partial\tau^2} \ , \tag{1.10}$$

with R_j given by

$$R_j = \left|r_j - s_j\right| \ . \tag{1.11}$$

Equation (1.9) should be compared with the expression for W, the cross-spectral density of the field in the far zone[27], i.e.,

$$W^{(\infty)}(Ru_1,Ru_2;\omega) = (2\pi k)^2 \cos\theta_1 \cos\theta_2$$

$$\times \tilde{W}^{(0)}(-ku_{1\perp},ku_{2\perp})\frac{\exp\left[ik(R_2-R_1)\right]}{R_2 R_1} \ , \tag{1.12}$$

where $u_{j\perp}$ are projections of the unit vectors u_j on the source plane[28], and $\tilde{W}^{(0)}$ is the four-dimensional Fourier transform of the cross-spectral density in the source plane

$$\tilde{W}^{(0)}(\mathbf{f}_1,\mathbf{f}_2) = \frac{1}{(2\pi)^4}\iint\limits_{\sigma} W^{(0)}(\mathbf{r}_1,\mathbf{r}_2;\omega)e^{-i(\mathbf{f}_1\cdot\mathbf{r}_1+\mathbf{f}_2\cdot\mathbf{r}_2)}\,d^2r_1\,d^2r_2 \ . \tag{1.13}$$

In this notation k in Eq. (1.12) is the wavenumber associated with frequency ω,

$$k = \frac{2\pi}{\lambda} = \frac{2\pi v}{c} = \frac{\omega}{c} \ , \tag{1.14}$$

and λ is the wavelength of the field.

It is clear from Eqs. (1.9)-(1.12) that, in general, it is simpler to use the cross-spectral density function when calculating the propagation of partially coherent fields in free space. In the rest of this section we review the properties of the cross-spectral density and summarize some of the relationships between the cross-spectral density and various physically measurable quantities.[29]

The first measurable quantity that we consider is the spectrum $S(r, \omega)$ which is simply the 'diagonal' component of the cross-spectral density, i.e.,

$$S(r;\omega) = W(r,r;\omega) \ . \tag{1.15}$$

$S(r, \omega)$ may represent the spectrum of the field or the spectrum of the source. It is usually supplemented by a subscript or superscript giving it the proper designation, e.g., $S^{(\infty)}(r, \omega)$ denotes the far-zone spectrum whereas $S^{(0)}(r, \omega)$ denotes the source

spectrum. We note that although most of our interest is in the diagonal component of the cross-spectral density function, no propagation calculation can be performed without the explicit knowledge of the full, complex-valued, cross-spectral density.

A quantity closely related to the spectrum is the radiant intensity[30] $J(u; \omega)$ which is a measure of the amount of energy per unit frequency radiated at frequency ω in a solid angle $d\Omega$ about a direction specified by unit vector u. It is defined by

$$J(u;\omega) = \lim_{R\to\infty} R^2 W(Ru, Ru;\omega) \ . \qquad (1.16)$$

It is clear from the last two equations that the only difference between the spectrum in the far zone $S^{(\infty)}(r; \omega)$ and the radiant intensity $J(u; \omega)$ is the scaling factor R^2. For this reason we will use both the spectrum and the radiant intensity when investigating spectral effects.

The radiated power at frequency ω is given by the formula

$$P(\omega) = \int_{(4\pi)} J(u;\omega) d\Omega \ , \qquad (1.17)$$

where (4π) denotes integration over all solid angles. The radiated power is an important quantity that we encounter in calculations of radiation efficiency and directivity. We will sometimes refer to this quantity as the *total power*[31] *at frequency* ω.

The spectrum, the radiant intensity and the power are the main quantities of interest in this thesis. Unless otherwise noted, we will be concerned with their values for observation points in the far zone. According to Eqs. (1.15), (1.16) and (1.12)

we may express the far-zone spectrum, and the radiant intensity in terms of the cross-spectral density of the source, viz.,

$$S^{(\infty)}(Ru;\omega) = \frac{(2\pi k)^2 \cos^2\theta}{R^2} \tilde{W}^{(0)}(-ku,ku;\omega) \ , \qquad (1.18)$$

$$J(u;\omega) = (2\pi k)^2 \cos^2\theta \ \tilde{W}^{(0)}(-ku,ku;\omega) \ . \qquad (1.19)$$

For general propagation in source-free region, it follows from Eqs. (1.5) and (1.6) that the cross-spectral density function satisfies the double Helmholtz equation

$$\left(\nabla_1^2 + k^2\right)\left(\nabla_2^2 + k^2\right)W(r_1,r_2;\omega) = 0 \ , \qquad (1.20)$$

where ∇_j^2 is the Laplacian operator with respect to r_j. It is straightforward to show that a general solution of Eq. (1.20) expressing the cross-spectral density of the field in terms of the cross-spectral density of the source is given by

$$W(r_1,r_2;\omega) = \iint W^{(0)}(s_1,s_2;\omega)G^*(r_1,s_1;\omega)G(r_2,s_2;\omega)d^n s_1 \, d^n s_2 \ , \qquad (1.21)$$

where $n = 1, 2, 3$, according to the dimensionality of the problem, and G is the free space Green's function for the given boundary conditions. In particular, for propagation in a linear system, we simply replace in Eq. (1.21) the Green's function $G(r, s; \omega)$ by the impulse response of the system.

Representations and models of the cross-spectral density

Another item of resemblance between the cross-spectral density and the mutual coherence function is that the cross-spectral density can be normalized in a way similar to Eq. (1.3). The normalized form is known as the *complex degree of spatial coherence* which is defined by[32]

$$\mu(r_1, r_2; \omega) = \frac{W(r_1, r_2; \omega)}{\sqrt{W(r_1, r_1; \omega)}\sqrt{W(r_2, r_2; \omega)}} , \qquad (1.22)$$

and which satisfies the constraint

$$\left| \mu(r_1, r_2; \omega) \right| \le 1 . \qquad (1.23)$$

Here the lower limit corresponds to spatial incoherence at frequency ω while the upper limit corresponds to complete spatial coherence at that frequency. It follows from Eqs. (1.15) and (1.22) that the cross-spectral density can be expressed in the general form

$$W(r_1, r_2; \omega) = \sqrt{S(r_1; \omega)}\sqrt{S(r_2; \omega)}\mu(r_1, r_2; \omega) . \qquad (1.24)$$

Three special cases that are often encountered in coherence theory are derived from Formula (1.24): the cross-spectral densities of the homogeneous[33], Schell-model[34] and quasi-homogeneous[35] sources.

A homogeneous source is represented by the cross-spectral density

$$W(r_1, r_2; \omega) = F(r_2 - r_1; \omega) \ . \tag{1.25}$$

This expression implies that the source is, in principle, infinitely large. We point out that this difficulty can be removed if we assume that the function F vanishes outside a finite domain σ.

A Schell-model source is characterized by a cross-spectral density whose degree of correlation depends on the two spatial arguments only through their difference, i.e.,

$$W(r_1, r_2; \omega) = \sqrt{S(r_1; \omega)} \sqrt{S(r_2; \omega)} \mu(r_2 - r_1; \omega) \ . \tag{1.26}$$

This form of the degree of correlation is a natural choice in most practical situations. When we describe secondary sources, it is reasonable to assume that the *fluctuations of a source in a given neighborhood are a result of the radiation from a single, spatially coherent, primary radiator.*[36] When the separation between the points r_2 and r_1 is larger, the fluctuations reflect contributions from more than one primary radiator and hence the fields are only partially correlated. A similar argument can be made regarding primary sources. Here one has to take into account cooperative effects that depend on the nature of the radiating system.[37] Supplementing the choice of the degree of correlation in this model, the choice of the spectral intensity $S(r; \omega)$ as a function of position effectively determines the physical size of the source.

Quasi-homogeneous sources are a very popular special case of the Schell-model class. They are used in many investigations in coherence theory for reasons that become apparent from their mathematical and physical properties. Their cross-spectral density is characterized by a sharply peaked degree of correlation and a

broad intensity profile that does not change appreciably over a typical correlation length (see Fig. 1.2). As a result of this relation between the intensity profile and the degree of correlation, the cross-spectral density may be approximated by the following expression

$$W(r_1, r_2; \omega) = S\left(\frac{r_2 + r_1}{2}; \omega\right)\mu(r_2 - r_1; \omega) .$$

(1.27)

This approximation may not appear advantageous until one employs it in calculating far-zone expressions for the cross-spectral density, the spectrum or the radiant intensity. Using the transformation

$$r = (r_2 + r_1)/2 , \quad r' = r_2 - r_1 ,$$

(1.28)

with unity Jacobian, it is easy to show that the spatial Fourier transform of the cross-spectral density can be factored in the form

$$\tilde{W}(f_1, f_2; \omega) = \tilde{S}(f_1 + f_2)\tilde{\mu}\left(\frac{f_2 - f_1}{2}; \omega\right) .$$

(1.29)

In Eq. (1.29) $\tilde{S}$ and $\tilde{\mu}$ are the spatial Fourier transforms of the intensity and correlation respectively, which for planar sources are given by

$$\tilde{S}(f) = \frac{1}{(2\pi)^2}\int S(r; \omega)e^{-if \cdot r}d^2r ,$$

(1.30)
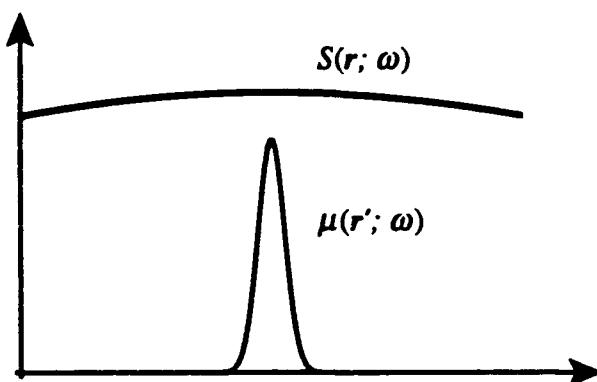
Figure. 1.2: The relation between the intensity profile and the spatial correlation of a quasi-homogeneous source.

and

$$\bar{\mu}(f;\omega) = \frac{1}{(2\pi)^2} \iint \mu(r';\omega) e^{-if \cdot r'} d^2r' .$$ (1.31)

The fact that the spatial Fourier transform of the cross-spectral density of a quasi-homogeneous source factorizes into a product of two spatial Fourier transforms of half the dimensions is a significant simplification of the mechanics of the propagation calculation, but at this point we should also point out that a large class of physical sources can actually be characterized as quasi-homogeneous sources. In particular, all sorts of thermal sources have relatively short spatial correlation length and at the same time possess an almost uniform intensity profile, which is precisely the description of a quasi-homogeneous source.

The different model sources we have described represent some of the physical properties of common light sources. Another description of partially coherent sources can be made using *coherent-mode representation*,[38] which is based on the expansion of the cross-spectral density into a sum of mutually uncorrelated coherent fields (modes). Before we proceed with the formulation of coherent-mode representation, we point out some of the properties of the cross-spectral density function on which the representation is based.

The cross-spectral density is an hermitian quantity, i.e.,

$$W(r_1, r_2; \omega) = W^*(r_2, r_1; \omega) .$$
(1.32)

It is also a non-negative definite quantity[39], explicitly,

$$\iint_\sigma W(r_1, r_2; \omega) f^*(r_1) f(r_2) d^n r_1 d^n r_2 \geq 0 ,$$
(1.33)

where n has the dimensionality of the source and f is any square integrable function. Under very general conditions (in fact, in all known practical cases) the cross-spectral density also satisfies the relation

$$\iint_\sigma |W(r_1, r_2; \omega)|^2 d^n r_1 d^n r_2 < \infty .$$
(1.34)

When a continuous function of two variables (r_1 and r_2) satisfies conditions (1.32), (1.33) and (1.34) it can be expressed as an absolutely and uniformly convergent series known as the Mercer expansion

$$W(r_1, r_2; \omega) = \sum_m \lambda_m(\omega) \phi_m^*(r_1; \omega) \phi_m(r_2; \omega) , \qquad (1.35)$$

where the index m has the same dimensionality as that of r_1 and r_2, λ_m are the non-negative eigenvalues and ϕ_m are the orthogonal eigenfunctions of the Fredholm integral equation

$$\int_\sigma W(r_1, r_2; \omega) \phi_m(r_1; \omega) d^n r = \lambda_m(\omega) \phi_m(r_2; \omega) . \qquad (1.36)$$

The eigenfunctions can be made orthonormal, i.e.,

$$\int_\sigma \phi_i^*(r; \omega) \phi_j(r, \omega) d^n r = \delta_{ij} , \qquad (1.37)$$

where δ is the Kronecker symbol.

It follows from the definition of the degree of correlation Eq. (1.22) that a corss-spectral density which consists of a single eigenfunction is fully coherent, i.e.

$$\left| \mu(r_1, r_2; \omega) \right| = \left| \frac{\phi_m^*(r_1; \omega) \phi_m(r_2; \omega)}{\left| \phi_m(r_1; \omega) \right| \left| \phi_m(r_2; \omega) \right|} \right| = 1. \qquad (1.38)$$

The magnitude of the degree of correlation of a source consisting of several modes reduces with increasing number of modes. The rate of decrease depends on the particular distribution of the eigenvalues.[40]

Coherent-mode representation which we discussed earlier seems to be a more complicated formulation than the closed form representation of partrially coherent fields which we considered earlier. It is however important to note the essential differences between these representations. Whenever both representations are available, it is usually simpler to handle most calculations using the full functional form of the model source. However, when the coherent-mode representation is available and the source is relatively spatially coherent, the number of eigenfunctions in the sum is manageable and it not only gives a picture of the source in terms of a superposition of coherent fields but it also facilitates somewhat simpler calculations because each one of the eigenfunctions can be propagated separately as a fully coherent field.[42] The advantage of propagating each eigenfunction separately is used in inverse problems,[43] and in analyzing the spatial content of the illumination.[44] In chapter 5 we consider a partially coherent source and analyze correlation effects on the spectrum using coherent-mode representation.

References

[1] a.   I. Newton, Phil. Trans. **80**, 3075 (1672).

    b.   Isaac Newton, *Optiks*, (Dover, New York) p. 26.

[2] J. Fraunhofer, Gilberts Ann., **56**, 264 (1817).

[3] a.   A. A. Michelson and Morely, "On the method of making the wave length of sodium light the actual and practical standard of length".

    b.   See also, A. A. Michelson, *Studies in Optics*, (University of Chicago Press, Chicago, 1968), Chap. IV.

4   a.   L. Mandel, "Concept of Cross-Spectral Purity in Coherence Theory", J. Opt. Soc. Amer. **51**, 1342-1350 (1961).

     b.   E. Wolf, "Invariance of spectrum of light on propagation", Phys. Rev. Lett. **56**, 1370-1372 (1986).

5   For many years astronomers have been struggling to explain large spectral shifts in the radiation of certain quasars.

6   The most striking aspect of coherence effects on the radiated spectrum were present in experimental results of national standards laboratories. A discussion of the discrepancies in measurements of several labs can be found in J.R. Moore, "Sources of error in spectroradiometry", *Lighting Res. and Tech.*, **12**, (1980) 213-220.

7   M. Born and E. Wolf, *Principles of Optics*, (Pergamon Press New York, 1982), Chapter 10.

8   a.   E. Wolf, "Red Shifts and Blue Shifts of Spectral Lines Emitted by Two Correlated Sources", Phys. Rev. Lett. **58**, 2646-2648 (1987).

     b.   A. Gamliel and E. Wolf, "Spectral Modulation by Control of Source Correlations", Opt. Commun., **65**, 91-96 (1988).

9   a.   M. F. Bocko, D. H. Douglass and R. S. Knox, "Observation of frequency shifts of spectral lines due to source correlations", Phys. Rev. Lett. **58**, 2649-2651 (1987).

     b.   F. Gori, G. Guattari, C. Palma and G. Padovani, "Observation of optical redshifts and blueshifts produced by source correlations", Opt. Commun., **67**, 1-4 (1988).

10   a.   Z. Dacic and E. Wolf, "Changes in the spectrum of a partially coherent light beam propagating in free space", J. Opt. Soc. Amer. A **5**, 1118-1126 (1988).

     b.   J. T. Foley, "The effect of an aperture on the spectrum of partially coherent light", Opt. Commun., in press.

11   A. Gamliel, "Mode analysis of spectral changes in light propagation from sources of any state of coherence", J. Opt. Soc. Amer. A, in press.

12   See, for example:

     a.   G. M. Morris and D. Faklis, "Effects of source correlations on the spectrum of light", Opt. Commun. **62**, 5-11 (1987).

     b.   D. Faklis and G. M. Morris, "Spectral shifts produced by source correlations", *Opt. Lett.* **13**, 4-6 (1988).

     c.   G. Indebetouw, "Synthesis of polychromatic light sources with arbitrary degrees of coherence: Some experiments", J. Mod. Opt. **36**, 251-259 (1989).

d.   H.C. Kandpal, J.S. Vaishya and K.C. Joshi, "Wolf shift and its applications in spectroradiometry", Opt. Commun. **73**, (1989).

[13]   In general, the spatial correlation $\mu(\mathbf{r}_1, \mathbf{r}_1; \omega)$ depends on the two position vectors $\mathbf{r}_1$ and $\mathbf{r}_1$. The additional degrees of freedom are due to the fact that the two vectors now span a three-dimensional space.

[14]   E. Wolf, "Redshifts and blueshifts of spectral lines caused by source correlations", *Opt. Commun.* **62**, 12-16 (1987).

[15]   A. Gamliel and G.P. Agrawal, "The Wolf effect in homogeneous and inhomogeneous media, Submitted to J. Opt. Soc. Amer. A.

[16]   A. T. Friberg, "Radiation from partially coherent sources", Opt. Eng. 21, 362-369 (1982).

[17]   a.   W. H. Carter and E. Wolf, "On the Radiation Efficiency of Quasi-homogeneous Sources of Different Degrees of Spatial Coherence", in **Coherence and Quantum Optics, IV**, ed. L. Mandel and E. Wolf (Plenum, New York, 1978), 415-430.

     b.   E. Wolf and W. H. Carter, "Coherence and Radiometry with Quasihomogeneous Planar Sources" , J. Opt. Soc. Amer. **67**, 785-796 (1977).

18   a.   A.T. Friberg, "Radiation efficiency of three-dimensional, partially coherent, primary sources", J. Opt. Soc. Amer. A **3**, 1219-1223 (1986).

       b.   A. Gamliel, "Radiation efficiency of planar Gaussian Schell-model sources", Opt. Commun. **60**, 333-337 (1986).

       c.   A. T. Friberg, "Radiation from partially coherent sources", Opt. Eng. **21**, 362-369 (1982).

19   A. Gamliel and A. T. Friberg, "Spatial correlations that maximize the radiation efficiency of three-dimensional primary sources", Submitted to J. Opt. Soc. Amer. A.

20   A.C. Schell, "A technique for the determination of the radiation pattern of a partially coherent aperture", IEEE Trans. Antennas Propag. AP-15, 187-188 (1967).

21   We will ignore here all edge effects.

22   We are using the complex analytic signal to represent fields in space-time domain. For a full discussion of this representation see M. Born and E. Wolf, *Principles of Optics*, (Pergamon Press New York, 1982), Chapter 10.

23   A. M. Yaglom, *An Introduction to the Theory of Stationary Random Functions*, (Prentice-Hall, New York, 1952) Chapter 1.

24   For an example of two-space, two time correlation function see, R.L. Fante, "Two-position, two-frequency mutual-coherence function in turbulance", J. Opt. Soc. Amer. **71**, (1981) 1446-1451.

25   Strictly speaking, the Fourier transform of a stationary random process $V(\mathbf{r}, t)$ does not exist since $V(r, t)$ is not square integrable over the infinite time domain. The only condition on $V(\mathbf{r}\ t)$ required for our purposes is that it is measurable. A short discussion of this issue that is outside the scope of this thesis can be found in Ref 38 a, section 2.

26   A nice discussion of this theorem in reference to real valued random processes can be found in C. Kittel, *Elementary Statistical Physics*, (J. Wiley & Sons, Inc., New York 1958), pp. 133-136.

27   For a detailed discussion of this aspect see, for example, E. Wolf, "New theory of partial coherence in space-frequency domain. Part I: spectra and cross spectra of steady-state sources", J. Opt. Soc. Amer. **72**, (1982) 343.

28   E.W. Marchand and E. Wolf, "angular Correlations and the Far-zone behavior of Partially Coherent Fields", J. Opt. Soc. Amer. **62**, (1972) 379

29   The projections of the unit vectorr **u** on the x, y plane are the vectors $\mathbf{u}_{j\perp} = (u_x, u_y)$.

30   Although the cross-spectral density is the primary function in calculations involving partially coherent fields, it is not *directly* measurable. Specifically, since it is a complex valued function one needs to measure both its magnitude and its phase. By comparison, the spectrum of the field can be measured directly in a single step.

31   E.W. Marchand and E. Wolf, "Radiometry with sources of any state of coherence", J. Opt. Soc. Amer. **64**, (1974) 1219.

32   The reader should not confuse the *total power at frequency* ω with the *total power* which takes into account the contribution from all frequencies.

33   Sometimes it is also referred to as the *complex degree of spectral coherence*.

34   E. Wolf and W.H. Carter, "Angular distribution of radiant intensity from sources of different degrees of spatial coherence", Opt. Commun., **13**, (1975) 205-209.

35   A.C. Schell, "A technique for the determination of the radiation pattern of a partially coherent aperture", IEEE Trans. Antennas Propag. AP-15, 187-188 (1967).

36   W.H. Carter and E. Wolf, "Coherence and Radiometry with quasihomogeneous planar sources", J. Opt. Soc. Amer. **67**, (1977) 785-796.

37   Here a primary radiator can also be understood in the sense of Huygens'
      construction of a wavefront.

38   G.V. Varada, "Cooperative effects in four wave mixing, two photon absorption
      and in radiation from atoms at high temperatures", Ph. D. thesis, University of
      Hyderabad, India, June 1990, Chapter 7, " A microscopic model for the Wolf
      effect-frequency shift in the emmited radiation due to atomic correlations", 118-
      142.

39   Coherent mode representation was introduced by Wolf in:

      a.   "New theory of partial coherence in space-frequency domain. Part I:
            spectra and cross spectra of steady-state sources", J. Opt. Soc. Amer.
            72, (1982) 343.

      b.   "Part II: Steady-state fields and higher-order correlations", ibid. A 3,
            (1986) 76.

      See also B.E.A. Saleh and M. Rabbani, "Simulation of partially coherent
            imagery in the space and frequency domains and by modal expansion",
            Applied Opt., **21**, (1982) 2770-2777.

40   See Appendix A of ref 26 .

41   a.   A. Starikov and E. Wolf, "Coherent-mode representation of Gaussian
            Schell-model sources and their radiation fields", J. Opt. Soc. Amer. **72**,
            (1982) 923-928.

b.   A. Starikov, "Effective number of degrees of freedom of partially coherent sources", J. Opt. Soc. Amer. **72**, 1538-1544 (1982).

42   E. Wolf, "Coherent-mode propagation in sptially band-limited wave fields", J. Opt. Soc. Amer. A **3**, (1986) 1920-1924.

43   T. Habashy and E. Wolf, "Application of Coherent-mode representation to invrse propagation problems", Annual meeting, Optical Society of America, Rochester, NY, Abstract ThT1 J. Opt. Soc. Amer. A4, p 103 (1987).

44   Certain aspects of matched filtering can be handled by representing the illuminating field as a sum of coherent modes and optimizing the filter for each one of the coherent spatial distributions. This research topic is described in private notes that are outside the scope of this document.

2

Radiation efficiency

Introduction

The concept of radiation efficiency is used extensively in various fields of electromagnetic theory.[1] It is usually a measure of the effectiveness of the production of radiation by a given mechanism which is taken as the ratio of the emitted energy to the energy used by the system. In many applications the radiation efficiency also takes into account the spatial or spectral distribution of the fields.

In this chapter we consider the total flux emitted by a partially coherent source at a fixed frequency ω, and compare it with the source integrated intensity at that frequency. We begin our discussion with the analysis of the radiation efficiency of planar Gaussian Schell-model sources. This example gives a unique insight into the relationship between the size of the source intensity profile and the spatial correlation length of the light fluctuations. We then examine the radiation efficiency of three-dimensional primary sources. The treatment of certain aspects of quasi-homogeneous sources requires the extension of the mathematical definition of the radiation efficiency. After considering the radiation efficiency of a uniform coherent spherical source we conclude this chapter by presenting a method for choosing the optimal spatial correlation which maximizes the radiation efficiency of a three-dimensional, primary sources of a prescribed intensity profile.

2.2   The radiation efficiency of planar Gaussian Schell-model sources

The radiation efficiency of partially coherent sources was studied by several investigators.[2] Initial work focused on quasi-homogeneous planar sources. Among planar sources, the properties of Gaussian Schell-model sources have been studied most extensively.[3] This fact may be attributed to two main reasons: physically this class of sources is closely related to the radiation from certain types of lasers[4] and mathematically the Gaussian intensity profile and Gaussian correlation functions are convenient forms in the analysis.

We define the radiation efficiency of secondary planar sources by the formula

$$C(\omega) = \frac{\Phi(\omega)}{\int_D S(r;\omega)d^2r} , \qquad (2.1)$$

where D is the domain occupied by the source and Φ is the total emitted flux at a frequency ω, i.e.,

$$\Phi(\omega) = \int_{(2\pi)} J(u;\omega)d\Omega . \qquad (2.2)$$

In Eq. (2.2) J is the radiant intensity and (2π) denotes integration over the half space $z > 0$ as shown in Fig. 2.1.

The Gaussian Schell-model source is characterized by the cross-spectral density
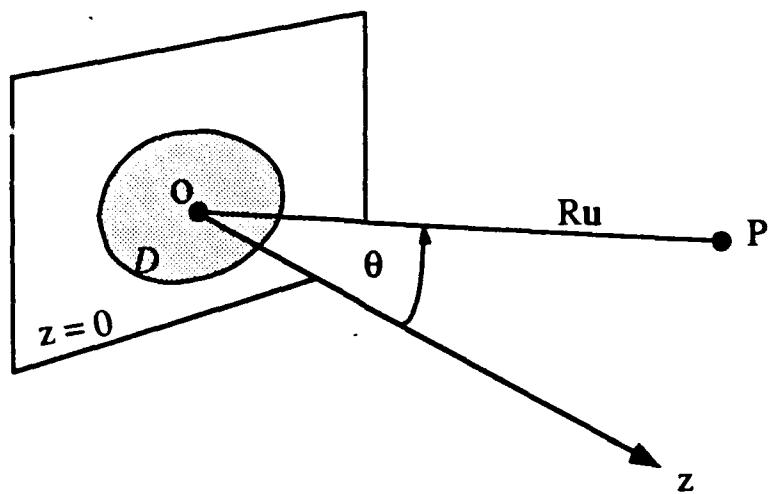
Figure 2.1: Illustrating the notation used in this chapter. The source is located in the plane z = 0 and a typical observation point P is in a direction specified by unit vector u and at a distance R (from the origin) assumed to be in the far zone.

$$W(r_1, r_2; \omega) = S^{(0)}(\omega) \exp\left[-\frac{r_2^2 + r_1^2}{4\sigma_I^2}\right] \exp\left[-\frac{(r_2 - r_1)^2}{2\sigma_c^2}\right], \qquad (2.3)$$

where σ_I is the rms width of the intensity profile and σ_c is the rms correlation length and $S^{(0)}(\omega)$ is the source spectral distribution. Although the cross-spectral density in Eq. (2.3) implies, in principle, an infinite source, we note that whenever the maximum physical extension of the source L say, satisfies the relation $L \gg \sigma_I$ then the Gaussian intensity profile is essentially the blocking function which defines the size of the effective source.

To obtain an expression for the radiation efficiency of the Gaussian Schell-model source we first evaluate the denominator of Eq. (2.1). Using Eq. (2.3) with $r_1 = r_2 = r$, we have

$$\int_D S(r;\omega)d^2r = S^{(0)}(\omega)\int_0^{2\pi}d\theta\int_0^\infty r\exp\left[-r^2/2\sigma_I^2\right]dr$$

$$= 2\pi\sigma_I^2 S^{(0)}(\omega) .$$

(2.4)

Next we derive an expression for the radiant intensity $J(u;\omega)$ using the four-dimensional spatial Fourier transform of the cross-sepctral density [cf. Eq. (1.19)]. We obtain

$$\tilde{W}(-ks_\perp,ks_\perp;\omega) = \frac{1}{(2\pi)^2}S^{(0)}(\omega)\sigma_I^2\sigma^2\exp\left(-k^2\sigma^2\sin^2\theta/2\right) ,$$

(2.5)

where

$$\frac{1}{\sigma^2} = \frac{1}{4\sigma_I^2} + \frac{1}{\sigma_c^2} .$$

(2.6)

On substituting Eq. (2.5) in Eq. ('.19) we find that the radiant intensity generated by the source is given by

$$J(u;\omega) = S^{(0)}(\omega)k^2\sigma_I^2\sigma^2\cos^2\theta\,\exp\left(-k^2\sigma^2\sin^2\theta/2\right) .$$

(2.7)

The expression for the total flux is obtained by substituting Eq. (2.7) into Eq. (2.2), it is then given by the formula

$$\Phi(\omega) = S^{(0)}(\omega)(k\sigma\sigma_I)^2\int_{(2\pi)}\cos^2\theta\,\exp\left(-k^2\sigma^2\sin^2\theta/2\right)d\Omega .$$

(2.8)

To perform the integration we define

$$\cos\theta = x$$
$$k\sigma/\sqrt{2} = \xi \ . \tag{2.9}$$

Using Eqs. (2.9) in Eq. (2.8) we obtain

$$\Phi(\omega) = 2\pi S^{(0)}(\omega)\left(k\sigma\sigma_I\right)^2 \int_0^1 x^2 \exp\left[-\xi^2\left(1-x^2\right)\right]dx \ , \tag{2.10}$$

which can be simplified to the form

$$\Phi(\omega) = 2\pi S^{(0)}(\omega)\sigma_I^2\left[1 - \frac{e^{-\xi^2}}{\xi}\int_0^\xi e^{t^2}dt\right] \ . \tag{2.11}$$

On substituting Eqs. (2.4) and (2.11) into Eq. (2.1) we finally obtain the following expression for the radiation efficiency of planar Gaussian Schell-model sources:

$$C(\omega) = 1 - D(\xi)/\xi \ , \tag{2.12}$$

where

$$D(\xi) = \exp\left(-\xi^2\right)\int_0^\xi \exp\left(t^2\right)dt \tag{2.13}$$

is the Dawson integral[5] (see Fig. 2.2).
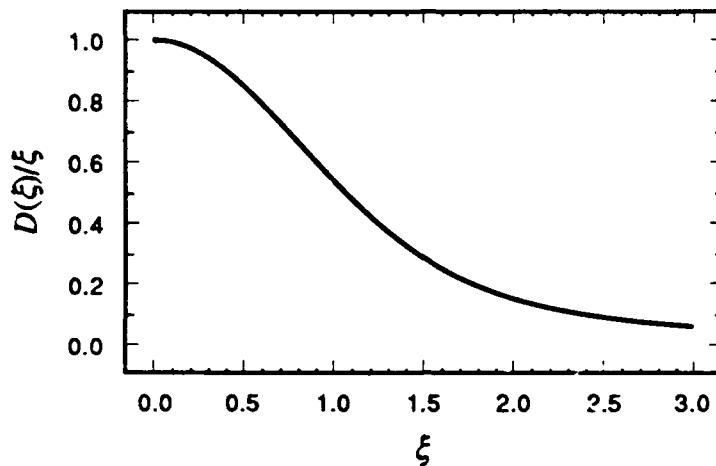
Figure 2.2: Graphical representation of $D(\xi)/\xi$ where $D(\xi)$ is the Dawson integral.

The radiation efficiency given by Eq. (2.12) is a function of the source intensity profile and its spatial correlation length through Eqs. (2.6) and (2.9). In particular, we note from Eq. (2.6) that there are classes of different Gaussian Schell-model sources that have the same radiation efficiency. Specifically, the characteristic quantity σ which determines the radiation efficiency is a sum of a term corresponding to the source rms intensity and a term corresponding to the correlation length of the source fluctuations. It is clear from this equation that there are many combinations of different correlation lengths and different intensity profiles that lead to the same value of σ and hence to the same radiation efficiency. These equivalent classes of partially coherent sources were first discussed in connection with the spatial distribution of the radiation produced by Gaussian Schell-model sources.[6] The radiation efficiency in Eq. (2.12) is independent of the spectrum. Its only dependence on frequency is due to the wavenumber k and the possible frequency dependence of the parameters σ_c and σ_I. In this chapter we take these parameters to be independent of frequency.
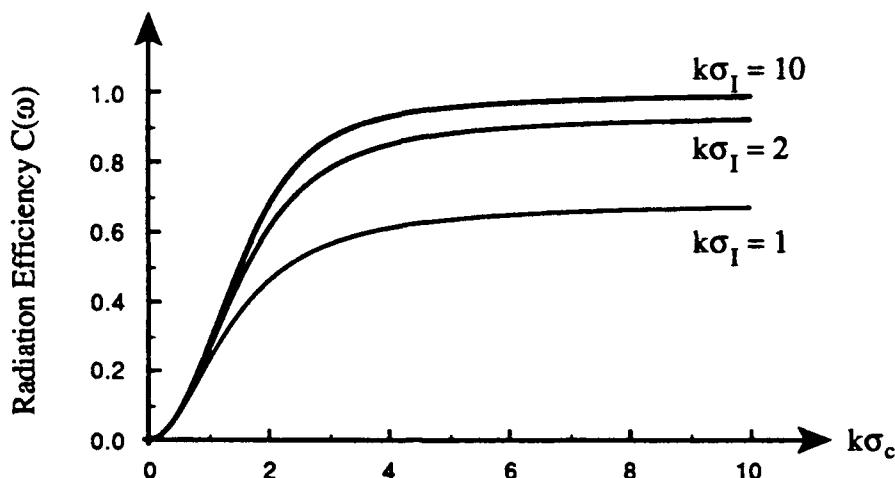
Figure 2.3: The radiation efficiency $C(\omega)$ as a function of the normalized spatial correlation length $k\sigma_c$. The three curves indicate that the radiation efficiency increases rapidly with an increase in the source rms width.

Before we examine the equivalent classes of planar Gaussian Schell-model radiators we consider separately the effects of the source size (rms intensity) and the spatial correlation length on the radiation efficiency. In Fig. 2.3 we show curves representing the radiation efficiency of three small sources. The intensity profiles are characterized by rms widths $\sigma_I = 1/k$, $2/k$, and $10/k$ respectively. We note that for each one of the sources the radiation efficiency increases with increasing correlation length. The asymptotic value of the radiation efficiency in each case may be obtained directly from Eqs. (2.6) and (2.9), by setting

$$\xi^2 \to 2\left(k\sigma_I\right)^2 .$$ (2.14)

In a similar manner we show in Fig. 2.4 the radiation efficiency as a function of the source intensity profile (or the effective source size). We note that the radiation
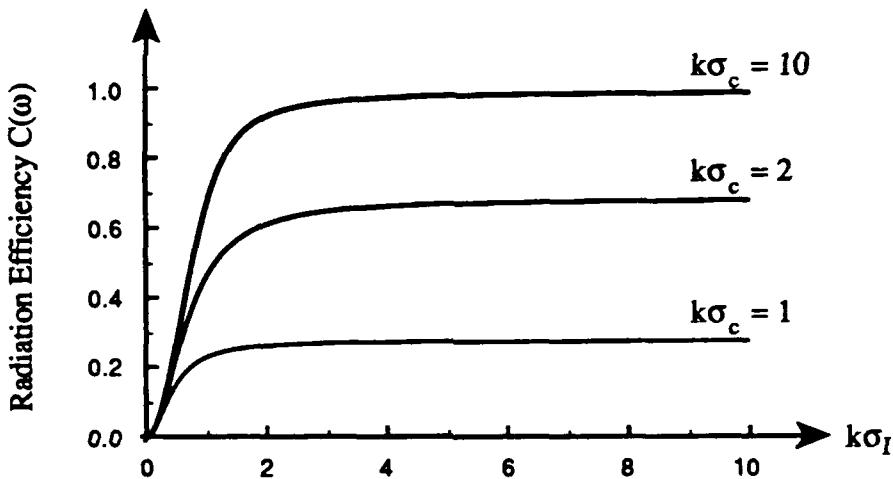
Figure 2.4: The radiation efficient $C(\omega)$ as a function of the width of the source intensity profile $k\sigma_I$. The three curves indicate that the radiation efficiency increases rapidly with an increase in the source correlation length.

efficiency increases rapidly with increasing width of the intensity profile and effectively reaching its asymptotic value for a relatively small source.

The results shown in the last two figures are combined in Fig. 2.5 where the radiation efficiency is shown as a function of both parameters $k\sigma_I$ and $k\sigma_c$. In this picture an equivalent class of Gaussian Schell-model sources is represented by the infinite number of sources specified by pairs of values of $k\sigma_I$ and $k\sigma_c$ that lie on the intersection of any plane parallel to the $k\sigma_I$–$k\sigma_c$ plane and the plotted radiation efficiency surface. Several such curves are shown in Fig. 2.6.

Before we conclude the discussion of the radiation efficiency of planar sources we point out a few physical considerations. Most secondary sources of practical interest are likely to have spatial dimensions that are much larger than a wavelength.[7] If we denote a typical source dimension by L, we then have $L \gg \lambda$, and according to Fig. 2.4 the radiation efficiency is nearly independent of the intensity profile for this range of rms source intensity. In addition, if we note that the smallest natural spatial
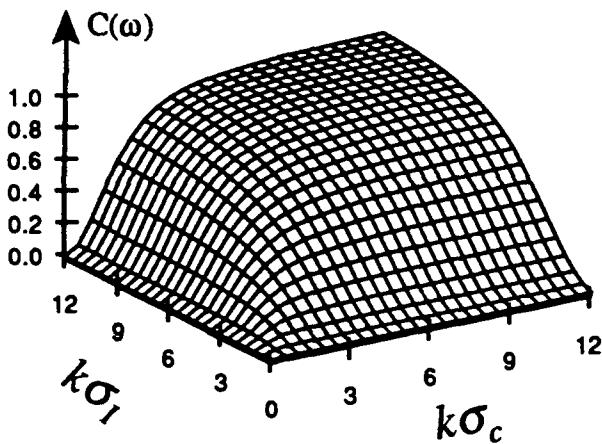
Figure 2.5:   The radiation efficiency of Gaussian Schell-model sources as a function of the rms intensity and the correlation length.

correlation length[8] is on the order of $\lambda/2$ corresponding to $k\sigma_c > 3$, then it follows from Fig. 2.3 that the radiation efficiency of most planar Gaussian Schell-model sources is over 80%.
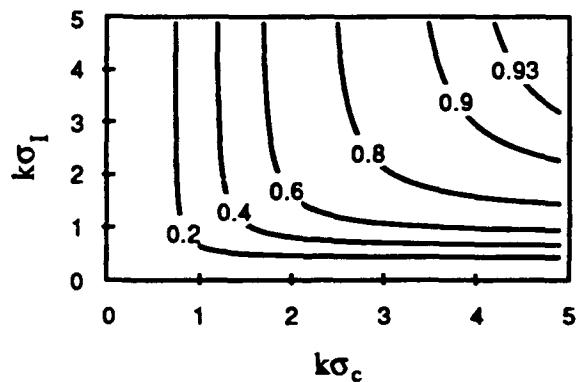
Figure 2.6:   Contours of constant radiation efficiency of Gaussian Schell-model sources. Each curve corresponds to a class of different partially coherent sources that have the same radiation efficiency.

2.3   Optimal radiation efficiency of three-dimensional primary sources

In this section we analyze the radiation produced by arbitrary three-dimensional scalar source distributions, whose degree of correlation at any pair of points depends only on the (oriented) separation between the points. Working in a Fourier transform space, we establish an operational method for calculating the spatial correlations that maximize the radiation efficiency of such sources. The optimal correlation function which we derive is, in general, not unique, and it is found to depend on the distribution of the optical intensity across the source.

We begin the analysis by generalizing the definition of the radiation efficiency Eq. (2.1) to the form

$$C(\omega) = \frac{\Phi(\omega)}{4\pi N \mathcal{D}} , \qquad (2.15)$$

where

$$N = \int_D S_Q(\mathbf{r}) d^3 r . \qquad (2.16)$$

Here D is the source domain and $\mathcal{D}$ is given by

$$\mathcal{D} = \frac{1}{N} \left[\int_D \sqrt{S_Q(r)} d^3 r \right]^2 . \qquad (2.17)$$

The use of the effective volume $\mathcal{D}$, rather than the actual volume D, enables us to discuss infinite sources whose optical intensity distribution falls off sufficiently rapidly.[9] The advantage of this formulation will become apparent later. In Eqs. (2.16) and (2.17) the subscript Q represents a primary source distribution.

Another difference between the calculations of the radiation efficiency of planar and three-dimensional sources is in the evaluation of the total flux which, in the present case, is given by the formula

$$\Phi(\omega) = \int\limits_{(4\pi)} J(u;\omega)\,d\Omega\,, \qquad (2.18)$$

where (4π) denotes integration over *all* solid angles.

The radiant intensity generated by three-dimensional primary sources of any state of coherence is given by Eq. (3.9) of Ref 11 (a).

$$J(u;\omega) = (2\pi)^6\,\tilde{W}(-ku,ku;\omega), \qquad (2.19)$$

where $\tilde{W}$ is the six-dimensional spatial Fourier transform of the source cross-spectral density i.e.,

$$\tilde{W}(f_1,f_2;\omega) = \frac{1}{(2\pi)^6}\iint W_Q(r_1,r_2;\omega)\exp\left[-i\left(f_1\cdot r_1 + f_2\cdot r_2\right)\right]d^3r_1\,d^3r_2. \quad (2.20)$$

The definition of the radiation efficiency in Eq. (2.15) is consistent with that given in Eq. (2.1) in that the efficiency of primary sources is also bounded by

$$0 \leq C(\omega) \leq 1 \ . \tag{2.21}$$

This relation can be derived by considering any source cross-spectral density of the form

$$W_Q(r_1, r_2; \omega) = \sqrt{S_Q(r_1; \omega)} \sqrt{S_Q(r_2; \omega)} \mu_Q(r_1, r_2; \omega) \ . \tag{2.22}$$

Since the degree of correlation is normalized so that

$$\left| \mu_Q(r_1, r_2; \omega) \right| \leq 1 \ , \tag{2.23}$$

it follows from Eqs.(2.17), (2.19) and (2.20) that

$$\left| J(u; \omega) \right| \leq \iint \sqrt{S_Q(r_1; \omega)} \sqrt{S_Q(r_2; \omega)} \, d^3r_1 \, d^3r_2 = 2N \ . \tag{2.24}$$

The normalization of the radiation efficiency Eq. (2.21) can now be obtained on substituting Eq. (2.24) in Eqs. (2.18) and (2.15).

The result expressed by Eq. (2.21) is valid for all primary sources regardless of their state of coherence or the distribution of their optical intensity. It is clear that the lower limit $C(\omega) \to 0$ is obtained, for example, in the limit of complete spatial incoherence[10] since, according to Eqs. (2.19)–(2.20), for such a source the radiant
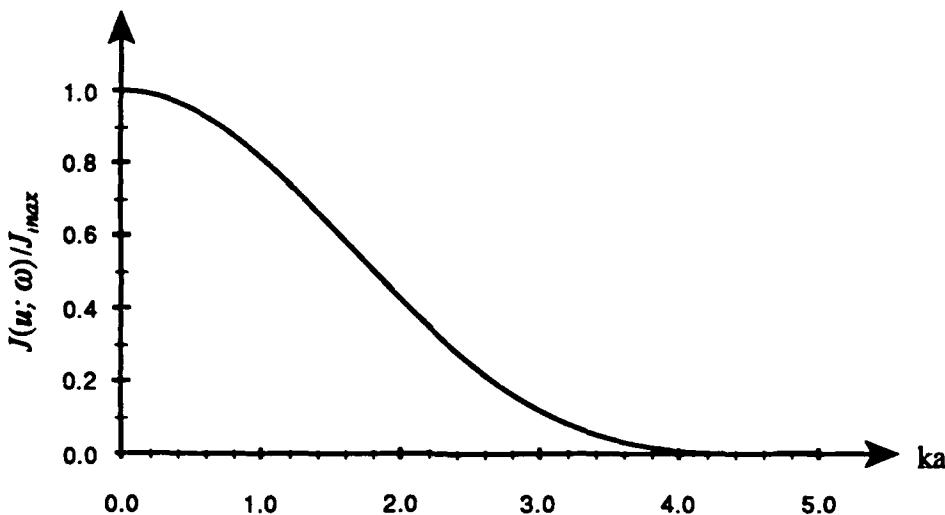
Figure 2.7: Normalized radiant intensity produced by a uniform, co-phasal, fully coherent spherical source of radius a.

intensity $J(u; \omega)$ vanishes. Other examples of this type are certain fully coherent and partially coherent non-radiating source distributions.[11]

We note that lower limit of the radiation efficiency for three-dimensional primary sources occurs, as in the case of secondary planar sources, in the limit of very short spatial correlation lengths. However, as we show in the following example, unlike secondary planar sources, the radiation efficiency is not always maximized in the limit of long correlation length.

Consider a uniform, co-phasal, fully coherent spherical source of radius a. The radiant intensity produced by such a source is given by [Ref. 11(a) Eq. (4.15)]

$$J(u; \omega) = \left(4\pi a^3/3\right)^2 S_Q(\omega)\left[3j_1(ka)/ka\right]^2 , \qquad (2.25)$$

see Fig. 2.7. In Eq. (2.25) $j_1(x)$ is the spherical Bessel function of the first order i.e.,

$$j_1(x) = \frac{\sin x}{x^2} - \frac{\cos x}{x} . \tag{2.26}$$

In the limit of small argument $x \ll 1$ we have $j_1(x) \approx x/3$. It then follows from Eq. (2.25) that the radiant intensity generated by a spherical source of this type, whose radius a is smaller than the wavelength is

$$J(u;\omega) = \left(4\pi a^3/3\right)^2 S_Q(r;\omega) = D^2 S_Q(r;\omega) , \quad (a \ll \lambda) , \tag{2.27}$$

where D is the volume of the source. On the other hand, for a source of this type $N = D S_Q(\omega)$ and $\mathcal{D} = D$. Then according to Eq. (2.15), the radiation efficiency $C(\omega) \to 1$ as $a \to 0$. This result shows that the maximum radiation efficiency is achieved by a uniform coherent source in the limit as its linear dimensions are small compared with the wavelength. When the dimensions of the source increase the radiation efficiency decreases and actually vanishes for radii a such that ka is a zero of the Bessel function j_1.[12] This result is in contrast with the result for the radiation efficiency of planar secondary sources that achieve maximum efficiency for fully coherent field distributions and large spatial dimensions (see Fig. 2.3).

We now wish to find the spatial correlation function $g_Q(r_1 - r_2; \omega)$ which maximizes the radiation efficiency $C(\omega)$ for a given primary source with an arbitrary (but known) intensity distribution $S_Q(r; \omega)$ and domain D. Since the quantities N and D are then fixed, we may confine ourselves, in view of Eq. (2.15), merely to the optimization of $g_Q(r_1 - r_2; \omega)$ in such a way that the total flux $\Phi(\omega)$ radiated by the source attains its absolute maximum value.

According to Eqs. (2.18)-(2.20) the radiated flux at frequency ω is given by the expression

$$\Phi(\omega) = \int\limits_{(4\pi)D} \int\limits_{D} \int \sqrt{S_Q(r_1;\omega)} \sqrt{S_Q(r_2;\omega)} g_Q(r_1 - r_2;\omega)$$

$$\times \exp\left[-iku \cdot (r_1 - r_2)\right] d^3r_1 d^3r_2 d\Omega \ . \qquad (2.28)$$

On introducing the average and difference variables[13]

$$r = (r_1 + r_2)/2 \ , \qquad r' = r_1 - r_2, \qquad (2.29)$$

as well as the auxiliary source function

$$R(r';\omega) = \int\limits_{D_1} \sqrt{S_Q(r + r'/2;\omega)} \sqrt{S_Q(r - r'/2;\omega)} \, d^3r \ , \qquad (2.30)$$

we may simplify Eq. (2.28) and obtain the following expression for the radiated flux:

$$\Phi(\omega) = \int\limits_{(4\pi)} \int\limits_{D_2} R(r') g_Q(r';\omega) \exp(-iku \cdot r') d^3r' \, d\Omega \ . \qquad (2.31)$$

In Eqs. (2.30) and (2.31) the spatial integrations are performed over the domains D_1 and D_2 which are determined from the original source domain D through the coordinate transformation Eq. (2.29). For example, it is evident from Eq. (2.28) that the modulus of r' does not exceed the maximum linear dimension of D. The function $R(r'; \omega)$ is related to the source-averaged correlation function employed in earlier studies of radiation by partially coherent planar sources.[14]

The next step in the analysis is the integration of Eq. (2.31) with respect to Ω. Since the integral

$$I = \int\limits_{(4\pi)} \exp(-iku \cdot r') d\Omega \qquad (2.32)$$

has no preferred direction in space, we can rotate the coordinate system so that r' is in the direction of the polar axis of a spherical polar coordinate system, and the integral is readily performed,

$$\int\limits_{(4\pi)} \exp(-iku \cdot r') d\Omega = \int\limits_0^{2\pi} d\phi \int\limits_0^{\pi} \exp(-ikr'\cos\theta) \sin\theta \, d\theta$$

$$= 2\pi \int\limits_{-1}^{1} \exp(-ikr'x) dx \qquad (2.33)$$

$$= 4\pi \frac{\sin kr'}{kr'} \, ,$$

where $r' = |r'|$. On substituting Eq. (2.33) into Eq. (2.31) we find that

$$\Phi(\omega) = \int\limits_{D_2} Q(r') g_Q(r') d^3 r' \, , \qquad (2.34)$$

in which we have defined the auxiliary function $Q(r'; \omega)$ by

$$Q(r';\omega) = 4\pi R(r';\omega) \frac{\sin kr'}{kr'} \, . \qquad (2.35)$$

Here the functions $R(r'; \omega)$ and $Q(r'; \omega)$ depend explicitly on the frequency ω, but we will suppress this dependence in the rest of this chapter.

Since the source-averaged intensity function $R(r')$ vanishes outside the domain D_2, the same holds true for $Q(r')$ and the integration in Eq. (2.34) can be formally taken over the infinite three-dimensional r'-space.

We now introduce the three-dimensional spatial Fourier transforms of $Q(r')$ and $g_Q(r')$ by the formulas

$$\tilde{Q}(K) = \frac{1}{(2\pi)^3} \int Q(r') \exp(-iK \cdot r') d^3 r' , \qquad (2.36)$$

$$\tilde{g}_Q(K) = \frac{1}{(2\pi)^3} \int g_Q(r') \exp(-iK \cdot r') d^3 r' . \qquad (2.37)$$

On invoking Parseval's theorem[15] in Eq. (2.34), we may then express the total radiated flux by[16]

$$\Phi(\omega) = (2\pi)^3 \int \tilde{Q}(K) \tilde{g}_Q(K) d^3 K . \qquad (2.38)$$

At this stage we focus our attention on the mathematical properties of the functions $\tilde{Q}$ and $\tilde{g}_Q$. Because the function $Q(r)$ is real and inversion symmetric with respect to the origin, we can establish the relations

$$\tilde{Q}^*(K) = \tilde{Q}(-K) = \tilde{Q}(K) . \qquad (2.39)$$

It follows from Eq. (2.39) that $\bar{Q}$ is also real and inversion symmetric function of K with respect to the origin in K–space. The other factor in the integrand of Eq. (2.38), $\tilde{g}_Q$, is the Fourier transform of the complex degree of spatial coherence of the source fluctuations. According to Bochner's theorem[17], a necessary and sufficient condition for $g_Q(r')$ to be a correlation coefficient[18] is that it is non-negative definite and it is equal to unity at the origin. In the Fourier domain these requirements are equivalent to

$$\tilde{g}_Q(K) \geq 0 ,\tag{2.40}$$

and

$$g_Q(0) = \int \tilde{g}_Q(K)d^3K = 1 .\tag{2.41}$$

It follows from Eq. (2.38) and from the properties of the two factors in the integrand of that equation, that there is a simple operational method for finding a spatial correlation function $g_Q(r')$ which maximizes the total radiated flux $\Phi(\omega)$ and consequently also maximizes the radiation efficiency $C(\omega)$. In its simplest form, the basic principle of this method is to determine the point $K = K_0$ at which $\bar{Q}(K)$ assumes its absolute maximum value; the optimal correlation function then corresponds to

$$\tilde{g}(K) = \delta^{(3)}(K - K_0) .\tag{2.42}$$

where $\delta^{(3)}$ is the three-dimensional Dirac delta function. This is only a particular solution of the maximization problem which has several interesting consequences.

The first consequence of this solution is that an upper bound on the amount of flux that a partially coherent source can generate is given by

$$\Phi_{max}(\omega) = (2\pi)^3 \tilde{Q}(K_0) \ . \tag{2.43}$$

The radiation efficiency corresponding to this maximum flux is readily obtained by substituting Eq.(2.43) into Eq. (2.15).

The second consequence of Eq. (2.42) is that at least one solution to the maximization problem is a fully coherent source. This follows from taking the inverse Fourier transform of Eq. (2.42), i.e.,

$$g_Q(r') = \exp(iK_0 \cdot r') \ . \tag{2.44}$$

It is important to note at this stage that the optimal correlation indeed corresponds to a coherent source, but the phase of the correlation is not uniform as can be seen from Eq. (2.44). The linear phase factor $K_0 \cdot r'$ in this equation depends on the optical intensity distribution $S_Q(r)$ through the maximum point K_0 of the function $\tilde{Q}$.

The third consequence of our solution to the maximization problem is that the optimal spatial correlation is, in general, not unique. Different source correlation coefficients $g_Q(r')$ may yield the same maximum radiation efficiency. Moreover, as we pointed out earlier, $\tilde{Q}$ is inversion symmetric and hence the point $K = -K_0$ corresponds to a maximum whenever $K = K_0$ does. Consequently $\delta^{(3)}(K + K_0)$ is also a particular solution of the maximization problem. Either one of the two unimodular source correlation functions $g_Q(r')$ can then be regarded as the optimal complex degree of spatial coherence. Similarly, a linear combination of the form

$$\tilde{g}(K) = p\delta^{(3)}(K - K_0) + q\delta^{(3)}(K + K_0) \ , \qquad (2.45)$$

where $p + q = 1$, is also in agreement with Eqs. (2.40) and (2.41) and produces, according to Eq. (2.38), the maximum possible radiant flux $\Phi(\omega)_{max}$. This choice of $\tilde{g}(K)$ however does not correspond to spatially fully coherent source distribution. In fact, Eq. (2.45) corresponds to a degree of correlation of the form

$$g_Q(r') = p\exp(iK_0 \cdot r') + q\exp(-iK_0 \cdot r') \ , \qquad (2.46)$$

whose magnitude is given by[19]

$$\left| p\exp(iK_0 \cdot r') + q\exp(-iK_0 \cdot r') \right| = \sqrt{p^2 + q^2 + 2pq\cos(2kr')} \ . \qquad (2.47)$$

In general, $\tilde{Q}(K)$ may take on its maximum value over an extended domain such as a surface in the three-dimensional K–space. In such a case the maximizing $\tilde{g}(K)$ may be distributed arbitrarily throughout the domain provided only that the conditions of Eqs. (2.40) and (2.41) are met. Hence an infinite number of optimal correlations with varying degrees of spatial coherence can then be specified. In the following paragraphs we consider several physically important applications where these situations occur.

The first case that we consider is that of quasi-homogeneous sources. The cross-spectral density of such sources may be expressed in the form

$$W(r_1, r_2; \omega) = S[(r_1 + r_2)/2; \omega)]g_Q(r_1 - r_2) \ . \qquad (2.48)$$

We note that for quasi-homogeneous sources we may effectively set $D_1 \approx D$ and

$$\sqrt{S(r + r'/2; \omega)}\sqrt{S(r - r'/2; \omega)} \approx S(r; \omega) , \qquad (2.49)$$

in Eq. (2.30). The source-averaged quantity $R(r')$ then assumes a constant value

$$R(r') = \int_D S_Q(r) d^3r = N. \qquad (2.50)$$

It follows from Eqs. (2.50) and (2.35), that the function $Q(r')$ is, in this case, independent of the source domain D; and it is given by the spherically symmetric (isotropic) formula

$$Q(r') = 4\pi N \frac{\sin kr'}{kr'} . \qquad (2.51)$$

We note, however, that strictly speaking there should be a finite (generally non-isotropic) cut-off in the values of r' in Eqs. (2.50) and (2.51) due to the domain D_2. In the quasi-homogeneous approximation all contributions to the radiant flux $\Phi(\omega)$ arise from a small neighborhood $D_c \subset D_2$ around the origin $r' = 0$ in which $g_Q(r')$ differs appreciably from zero. We therefore let the function $Q(r')$ extend over the entire space without altering the situation physically.

Allowing for an infinite domain $(D_2 \rightarrow \infty)$ the spatial Fourier transform of $Q(r')$ is found by substituting from Eq. (2.51) into Eq. (2.36). One then finds that

$$\tilde{Q}(K) = \frac{N}{k^2}\left[\delta(|K| - k) - \delta(|K| + k)\right] . \qquad (2.52)$$

The second term in Eq. (2.52) makes no contribution to the flux $\Phi(\omega)$. We therefore set

$$\tilde{Q}(K) = \frac{N}{k^2} \delta(K - k) , \qquad (2.53)$$

where $K = |K|$. We observe that for quasi-homogeneous sources $\tilde{Q}(K)$ is isotropic and vanishes identically except on the energy shell $K = k$ in the three-dimensional K-space. Hence, in view of Eq. (2.38), the quasi-homogeneous source will be totally non-radiating if its complex degree of spatial coherence is such that $\tilde{g}(K) = 0$ when $K = k$. This result is in agreement with earlier investigations [see, for example, Eq. (3.11) of Ref. 11(b)].

When the finite size of the quasi-homogeneous source is taken into account, it is evident that $\tilde{Q}(K)$ will no longer be simply proportional to a δ-function as in Eq. (2.53). Instead it will be a sharply peaked, generally non-isotropic function, centered around the shell $K = k$. In such a case the optimal correlations can be found by using the general method we described above. Nevertheless, we show that physically interesting results are readily obtained with the help of Eq. (2.53) for limitingly large quasi-homogeneous sources.

Since the function $\tilde{Q}(K)$ in Eq. (2.53) is spherically symmetric, the values of the Fourier transform $\tilde{g}_Q(K)$ on the shell $K = k$ can be chosen in a number of ways. Specifically, in view of Eqs. (2.41) and (2.53), one may set as the optimal correlation function

$$\tilde{g}_Q(K) = \frac{1}{k^2} F(u) \delta(K - k) , \qquad (2.54)$$

where $K = Ku$ and $F(u)$ is an arbitrary non-negative function that satisfies the condition

$$\int\limits_{(4\pi)} F(u)d\Omega = 1 . \tag{2.55}$$

Using the inverse of Eq. (2.37), it follows from Eq. (2.54) that the spatial correlation is given by

$$g(r') = \int\limits_{(4\pi)} F(u)\exp(iku \cdot r')d\Omega. \tag{2.56}$$

In the case of an isotropic correlation $F(u) = 1/4\pi$ and Eq. (2.56) yields [cf. Eq. (2.33)] the spatial correlation

$$g(r') = \frac{\sin kr'}{kr'} . \tag{2.57}$$

This is an interesting result. It implies that in the limit as the size of a quasi-homogeneous source approaches infinity, the optimal correlations that are isotropic and that maximize the radiation efficiency of the source are given by the universal function $\sin(x)/x$ with $x = kr'$. Since the correlation distance associated with the degree of coherence given by Eq. (2.57) is about $\lambda/2$, the efficient radiation characteristics of such a source can be physically understood on the basis of an interference model.[20]
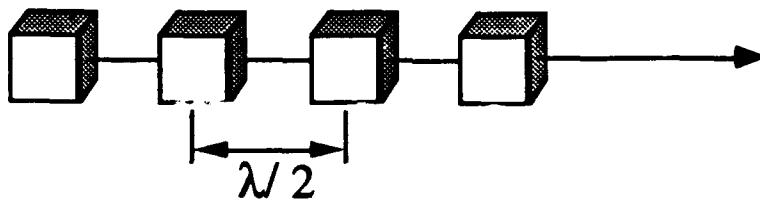
Figure 2.8:   Physical model explaining the reduced radiation efficiency of correlated primary sources as a result of destructive interference [cf. Ref. 5(d)].

Consider a three dimensional source distribution in which several small radiating volume elements are equally spaced on an arbitrary axis (see Fig. 2.8). When all the volume elements are radiating coherently and in phase, it follows that the radiation from any pair of elements that are separated by a distance of $\lambda/2$ cancels everywhere on the axis. If, however, the spatial correlation of the source fluctuations has an effective length shorter than $\lambda/2$, the destructive interference effects do not take place.

The result given by Eq. (2.57) is also closely related to the radiation produced by a source that is in thermal equilibrium with its surroundings, i.e., a blackbody radiator. It was shown recently,[21] that a fluctuating source with this form of spatial correlations gives rise within the source medium to a field whose complex degree of spatial coherence is also given by the function $sin(kr')/kr'$. This, in turn, is the correlation function that is known to be associated with blackbody radiation fields.[22] Hence our results are consistent with the notion that a large uniform source in thermal equilibrium has isotropic spatial correlations that lead to maximum radiation efficiency.

As another illustration of the operational method for finding the spatial correlation function which maximizes the radiation efficiency, we consider three spherically symmetric Schell-model sources, all of which have identical Gaussian optical intensity distributions:

$$S_Q(r;\omega) = I(\omega)\exp\left(-r^2/2\sigma_Q^2\right) .$$ (2.58)

Here $I(\omega)$ characterizes the spectral content of the source and σ_Q is a positive constant.

We now compare three types partially coherent sources having this intensity profile. The sources are: (a) fully coherent, (b) Gaussian correlated (optimal correlation length as in Ref. 2(d), and (c) optimally correlated as discussed in this section.

For the fully coherent source we take $g_Q(r') = 1$, whereas the Gaussian correlated source is specified by

$$g_Q(r') = \exp\left(-r'^2/2\sigma_g^2\right) ,$$ (2.59)

and the optimal correlation length is given by

$$\left(k\sigma_g\right)^2 = \frac{12\left(k\sigma_Q\right)^2}{4\left(k\sigma_Q\right)^2 - 3} \qquad \text{when} \qquad k\sigma_Q > \frac{\sqrt{3}}{2} ,$$ (2.60)

$$k\sigma_g \rightarrow \infty \qquad \text{when} \qquad k\sigma_Q \leq \frac{\sqrt{3}}{2} .$$ (2.61)

The general optimal correlations can be found by determining the points where the spatial Fourier transform of the function $Q(r')$ corresponding to Eq. (2.58) attains its absolute maximum value. The first step in the procedure is to obtain an expression for the auxiliary function $R(r')$ by substituting Eq. (2.58) into Eq. (2.30). After performing the indicated integration we obtain the formula

$$R(r') = \frac{\left(\sqrt{2\pi}\,\sigma_Q\right)^3}{\sqrt{2}} \exp\left(-r'^2/8\sigma_Q^2\right) . \tag{2.61}$$

Next we substitute Eq. (2.61) in Eqs. (2.35) and (2.36) to obtain the spatial Fourier transform $\bar{Q}(K)$:

$$\bar{Q}(K) = 4\pi J(\omega)\frac{\sigma_Q^4}{kK}\left\{\exp\left[-2(k-K)^2\,\sigma_Q^2\right] - \exp\left[-2(k+K)^2\,\sigma_Q^2\right]\right\} . \tag{2.62}$$

For $k\sigma_Q < \sqrt{3}/2$ this function assumes its maximum value at the origin $K = 0$. When $k\sigma_Q \geq \sqrt{3}/2$, the radius K corresponding to the maximum of $\bar{Q}(K)$ for any given σ_Q can be readily found using numerical methods. We will denote this radius by K_0.

Making use of Eqs. (2.17) and (2.58) we find that for all the three model sources that we are considering

$$\mathcal{D}N = (4\pi)^3 I(\omega)\sigma_Q^6 . \tag{2.63}$$

The total radiant flux generated by a Gaussian Schell-model source is given by[2d]

$$\Phi(\omega) = 4\pi(2\pi\sigma_Q\sigma)^3 I(\omega)\exp\left[-(k\sigma)^2/2\right] , \tag{2.64}$$

where

$$\frac{1}{\sigma^2} = \frac{1}{(2\sigma_Q)^2} + \frac{1}{\sigma_g^2} . \tag{2.65}$$

and σ_g is to be chosen as described above [Eqs. (2.60) and (2.61)] for maximum radiated power. In the case of the optimally correlated source, the radiated flux is given by Eq. (2.43),

$$\Phi(\omega) = (2\pi)^3 \tilde{Q}(K_0) \ . \tag{2.66}$$

Because of the isotropy of $\tilde{Q}(K)$ in this case, the correlations that lead to this radiant flux can, in general, be chosen in many different ways. However, when $k\sigma_Q < \sqrt{3}/2$, the value $K_0 = 0$ is the unique solution. This leads to $\tilde{g}_Q(K) = \delta^3(K)$ and consequently the source is fully coherent and co-phasal, i.e., $g_Q(r') = 1$. On combining Eqs. (2.62) and (2.66) and taking the limit as $K_0 \to 0$, we indeed see that the resulting radiant flux $\Phi(\omega)$ is identical to that given by Eq. (2.64) with $k\sigma_g \to \infty$. Here we have used the fact that

$$\lim_{K \to 0} \frac{1}{K} \left\{ \exp\left[-2\sigma_Q^2 (k-K)^2 \right] - \exp\left[-2\sigma_Q^2 (k+K)^2 \right] \right\} = 4k\sigma_Q \ . \tag{2.67}$$

Making use of the above results we may now calculate the radiation efficiency defined by Eq. (2.15). For the fully coherent and optimally Gaussian correlated sources we find from Eqs. (2.63) and (2.64) the formula

$$C(\omega) = \left(\frac{\sigma}{2\sigma_Q} \right)^3 \exp\left[-(k\sigma)^2/2 \right] \ ,$$

$$\tag{2.68}$$
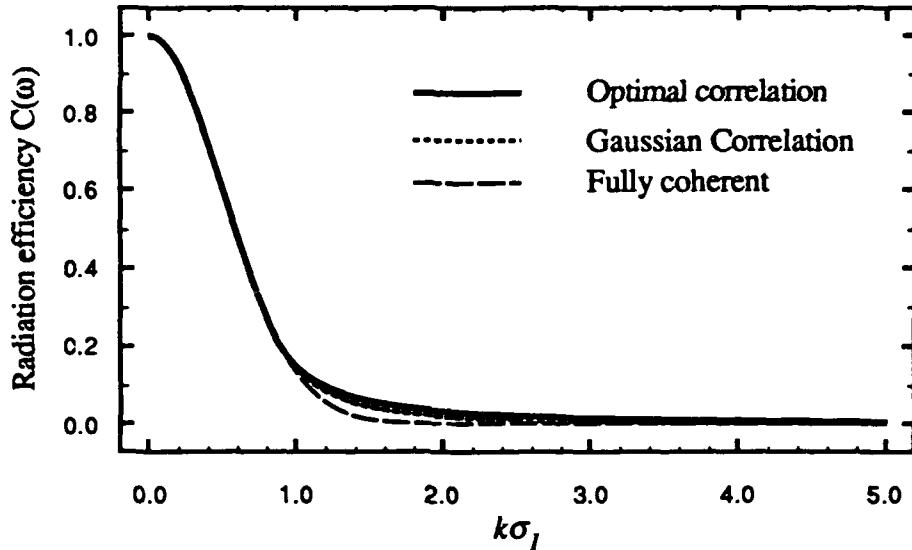
Figure 2.9: The radiation efficiency of the three sources. Note that the radiation efficiency of the sources decreases significantly with increasing source size, and that the three sources have identical efficiency for values of $k\sigma_I \leq 0.86$.

where σ is given by Eq. (2.64). The radiation efficiency of the coherent source is obtained in the limit $k\sigma_g \to \infty$, and it is given by

$$C(\omega) = \exp\left[-2\left(k\sigma_Q\right)^2\right].\qquad(2.69)$$

Similarly, for the radiation efficiency of an optimally correlated source we obtain from Eqs. (2.62), (2.63) and (2.65) the expression

$$C(\omega) = \frac{1}{8\sigma_Q^2 kK_0}\left\{\exp\left[-2\sigma_Q^2(k-K_0)^2\right] - \exp\left[-2\sigma_Q^2(k+K_0)^2\right]\right\},\qquad(2.69)$$

where K_0 is the location of the maximum of $\bar{Q}(K)$ which is determined by numerical evaluation. These results are plotted in Figs. 2.9 and 2.10 as a function of $k\sigma_Q$. As
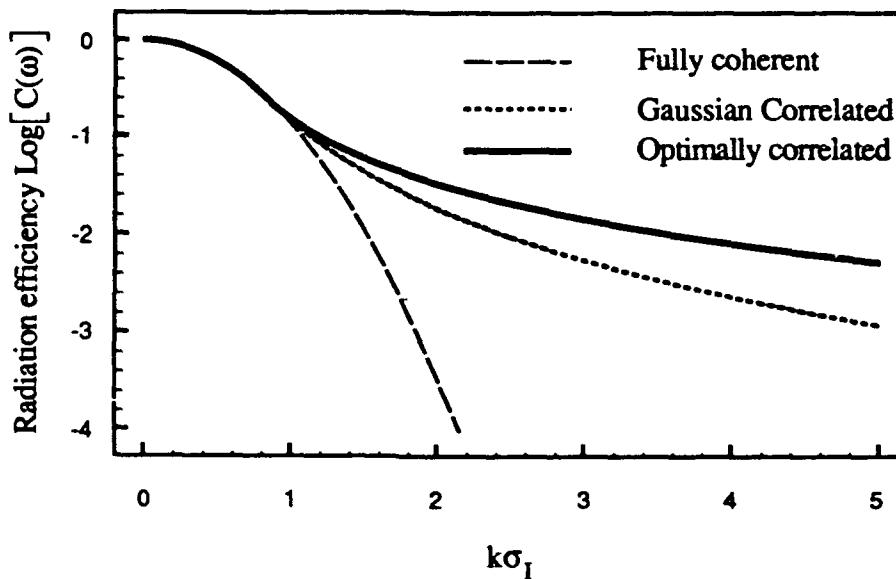
Figure 2.10: Logarithmic plot of the radiation efficiency of the three sources.

shown in Fig. 2.9, the three curves are identical in the region $k\sigma_Q < \sqrt{3}/2$, and take on the maximum value of unity as $k\sigma_Q \to 0$. Figure 2.10 illustrates the differences between the radiation efficiencies of the three model sources in the region $k\sigma_Q > \sqrt{3}/2$.

Taking the correlations that maximize the radiation efficiency to be isotropic, i.e., choosing

$$\tilde{g}_Q(K) = \delta(K - K_0)/4\pi K^2 \; , \qquad (2.70)$$

we readily find on taking the inverse Fourier transform of Eq. (2.70) that the optimal degree of spatial coherence is given by

$$g_Q(r') = \frac{\sin K_0 r'}{K_0 r'} \; . \qquad (2.71)$$

As we pointed out, for small sources that satisfy $0 < k\sigma_Q < \sqrt{3}/2$, we have $K_0 = 0$ and Eq. (2.71) corresponds to full coherence. On the other hand, for sufficiently large sources, we see from Eq. (2.62) that the maximum radiation efficiency is attained for $K_0 \approx k$ (but always $K_0 < k$). Hence in the limit as $k\sigma_Q \to \infty$, the optimal correlations given by Eq. (2.71) reduce to the universal result [Eq. (2.57)], derived in the context of quasi-homogeneous sources.

2.4 Summary

In this chapter we discussed the radiation efficiency of secondary and primary partially coherent sources. We examined the dependence of the radiation efficiency and the radiated flux on the spatial correlations of the source. We showed that typical planar secondary Gaussian Schell sources have high radiation efficiency which increases with an increase in the spatial correlation length of the source fluctuations. On the other hand we demonstrated that three-dimensional primary coherent sources are not necessarily characterized by high radiation efficiency. In particular, an isotropic source that is characterized by a Gaussian intensity profile has maximum radiation efficiency for a spatial correlation given by Eq. (2.71).

The method for choosing the spatial correlation which maximizes the radiation efficiency of three-dimensional primary sources is significant in two aspects. First it shows from the point of view of coherence theory that the spatial correlation of blackbody radiators maximize the radiation efficiency of the source. The second aspect has to do with the possibility of producing more efficient light sources. Most of the light sources currently in use for illumination purposes are partially coherent and hence even a small improvement in their efficiency has great significance for the energy

market. At present, most of the practical methods for controlling source correlations that we are aware of pertain to secondary planar sources, but new approaches to controlling the spatial correlations of primary sources are currently being introduced.

Practical methods for controlling source correlations are also important for the discussion in the next chapter were we consider the effects of the source correlations on the spectrum of the radiation.

References

[1]   For examples of radiation efficiency outside the domain of coherence theory, see:

a.   B. Forssen and M.J. Crocker, "Estimation of acoustic velocity, surface velocity and radiation efficiency by use of the two-microphone technique", J. Acoust. Soc. Amer., **73**, 1047-53 (1983).

b.   M.M. Dawoud and A.P. Anderson, "Design of superdirective arrays with high radiation efficiency", IEEE Trans. Antennas & Propag., **AP 26**, 819-23 (1978).

[2]   a   E. Wolf and W. H. Carter, "Coherence and radiometry with quasihomogeneous planar sources" , J. Opt. Soc. Amer. **67**, 785-796 (1977).

b.   W. H. Carter and E. Wolf, "On the radiation efficiency of quasi-homogeneous sources of different degrees of spatial coherence", in **Coherence and Quantum Optics, IV**, ed. L. Mandel and E. Wolf (Plenum, New York, 1978), 415-430.

c.   A. T. Friberg, "Radiation from partially coherent sources", Opt. Eng. **21**, 362-369 (1982).

d.   A.T. Friberg, "Radiation efficiency of three-dimensional, partially coherent, primary sources", J. Opt. Soc. Amer. A **3**, 1219-1223 (1986).

e.   A. Gamliel, "Radiation efficiency of planar Gaussian Schell-model sources", Opt. Commun. **60**, 333-337 (1986).

3   a.   J.T. Foley and M.S. Zubairy, "The directionality of Gaussian Schell-model beams", Opt. Commun. , **26**, 297-300 (1978).

b.   A.T. Friberg and J.R. Sudol, "Propagation parameters of gaussian Schell-model beams", Opt. Commun., **41**, 383-7, (1982).

c.   Li Yajun and E. Wolf, "Radiation from anisotropic Gaussian Schell-model sources", Opt. Lett., **7**, 256-8 (1982).

d.   A. Starikov and E. Wolf, "Coherent-mode representation of Gaussian Schell-model sources and of their radiation fields", J. Opt. Soc. Amer., **72**, 923-8 (1982).

e.   A. Starikov, "Effective number of degrees of freedom of partially coherent sources", J. Opt. Soc. Amer., **72**, 1538-44 (1982).

f.   J. Deschamps, D. Courjon and J. Bulabois, "Gaussian Schell-model sources: an example and some perspectives", J. Opt. Soc. Amer., **73**, 256-61 (1983).

g.   A.T. Friberg and R.J. Sudol, "The spatial coherence properties of Gaussian Schell-model beams", Opt. Acta, **30**, 1075-97 (1983).

h.   F. Gori and G. Guattari, "A new type of optical fields", Opt. Commun., **48**, 7-12 (1983).

i.   R. Simon, E.C.G. Sudarshan and N. Mukunda, "Generalized rays in first-order optics: transformation properties of Gaussian Schell-model fields", Phys. Rev. A, **29**, 3273-9 (1984).

j.   R. Simon, E.C. G. Sudarshan and N. Mukunda, "Anisotropic Gaussian Schell-model beams: passage through optical systems and associated invariants", Phys. Rev. A, **31**, 2419-34 (1985).

k.   A.T. Friberg, "Coherent-mode representation of lambertian and non-lambertian sources", Opt. Eng., **473**, 230-3 (1984).

l.   N. Mukunda, "Group theoretical methods in optics", Pramana, **25** 497-503 (1985).

m.   P. De-Santis, F. Gori, G. Guattari and C. Palma, "Anisotropic Gaussian Schell-model sources", Opt. Acta, **33**, 315-26 (1986).

n.   R. Simon, "Generalized rays in statistical wave optics: application to anisotropic Gaussian Schell-model beams", J. Opt., **14**, 92-102 (1985).

o.   T. Yoshimura, "Statistical properties of dynamic speckles", J. Opt. Soc. Amer., **3**, 1032-54 (1986).

p.   A.T. Friberg and J. Turunen, "Algebraic and graphical propagation methods for Gaussian Schell-model beams", Opt. Eng., **25**, 857-64 (1986).

q.   R. Simon, N. Mukunda and E.C.G. Sudarshan, "Partially coherent beams and a generalized ABCD-law", Opt. Commun., **65**, 322-8 (1988).

r.   A.T. Friberg and J. Turunen, "Imaging of Gaussian Schell-model sources", Opt. Soc. Amer. A, **5**, 713-20 (1988).

s.   R. Simon and T. Tamir, "Nonspecular phenomena in partly coherent beams reflected by multilayered structures", J. Opt. Soc. Amer. A, **6**, 18-22 (1989).

4   Planar Gaussian Schell-model sources are applicable also to scattering problems where the incident radiation is a coherent Gaussian beam and the scattering medium is characterized by a Gaussian correlation function. See, for example

a.   F. Scudieri, M. Bertolotti and R. Bartolino, Appl. Opt. **13** 181 (1974).

b.   M. Bertolotti, F. Scudieri and S. Verginelli, Appl. Opt. **15**, 1842 (1976)

c.   J. D. Farina, L. M. Narducci and E. Collet, Opt. Commum. **32**, 203 (1980).

5   M. Abramowitz and I.A. Stegun, *Handbook of mathematical functions* (National Bureau of Standards, U.S. Government Publishing Office, Washington. D.C. 1964) p. 319.

6   a.   E. Collett and E. Wolf, "Partially coherent sources which produce the same far-field intensity distribution as a laser", Opt. Commun. **25**, 293-296 (1978).

b.   E. Collett and E. Wolf, "New Equivalence Theorems for Planar Sources which Generate the Same Distributions of Radiant Intensity", J. Opt. Soc. Amer. **69**, 942-950 (1979).

c.   E. Collett and E Wolf, "Beams Generated by Gaussian Quasi-homogeneous Sources", Opt. Commun. **32**, 27-31 (1980).

7   Possible exceptions are secondary sources which are produced by focusing a beam and creating a secondary source in the location of the beam waist.

8   The shortest correlation length that we are aware of is that of a blackbody radiator. Its spatial correlation function is $\sin(kr)/kr$. Since spatial correlations increase on propagation, it follows that we may take the blackbody correlation as the lower spatial correlation limit for secondary sources.

9   We emphasize that the infinite size of the source is only used for the mathematical convinience of extending certain integration limits. See also the discussion following Eq. (2.3).

10   We note that the source correlation for the incoherent case is taken as the limit of a properly normalized correlation function, e.g. a Gaussian, as distinguished from a Dirac delta function.

11   a.   W.H. Carter and E. Wolf, "Correlation theory of wavefields generated by fluctuating, three-dimensional, scalar sources, Part I: General theory", Optica Acta 28, 227-244 (1981).

        b.   A. J. Devaney and E. Wolf, "Non-radiating stochastic scalar sources", in Coherence and Quantum Optics V, eds. L. Mandel and E. Wolf (Plenum, New York, 1984), pp. 417-421.

        c.   A. Gamliel, K. Kim, A. I. Nachman and E. Wolf, "New method for specifying non-radiating, monochromatic, scalar sources and their fields", J. Opt. Soc. Amer. A6, 1388-1393 (1989).

12   K. Kim and E. Wolf, "Non-radiating monochromatic sources and their fields", Opt. Commun. **59**, 1-6 (1986).

13   The Jacobian of this transformation is unity as noted in chapter 1.

14   E. Wolf, "The radiant intensity from planar sources of any state of coherence", J. Opt. Soc. Amer. **68**, 1597-1605 (1978).

15   R. Bracewell, The Fourier Transform and Its Applications (McGraw-Hill, New York, 1965), Chap. 6.

16   The method of maximizing the radiant flux $\Phi(\omega)$ in terms of spatial frequency variables, rather than in real space, was first suggested by F. Gori and G. Guattari (private communication).

17   R. R. Goldberg, Fourier Transforms (Cambridge University Press, Cambridge, 1965), p. 6.

18   By a correlation coefficient we mean a normalized, continuous, non-negative definite function.

19   The magnitude of the degree of correlation Eq. (2.46) is smaller than unity except when $r' = n\lambda/2$ (for positive integer n), by virtue of the triangle inequality.

20   This model was first suggested by A.T. Friberg in reference [2 (d)].

21   H. M. Nussenzveig, J. T. Foley, K. Kim and E. Wolf, "Field correlations within a fluctuating homogeneous medium", Phys. Rev. Lett. 5?, 218-221 (1987).

22   a.   L. D. Landau and E. M. Lifshitz, Electromagnetics of Continuous Media (Addison, Wesley, Reading, MA, 1960), Secs. 88 and 89.

        b.   W. H. Carter and E. Wolf, "Coherence properties of lambertian and non-lambertian sources", J. Opt. Soc. Amer. 65, 1067-1071 (1975).

3

Spectral modulation with scalar sources

3.1 Introduction

Techniques for modifying of the spectrum of radiation have been known for some time both in optics and in antenna theory. The main method for changing the spectrum of field is to vary the spectrum of the source itself, assuming that the spectrum of the radiation is simply proportional to the source spectrum. As we now know, this assumption is, in general, not valid in the case of partially coherent sources, where the spectrum may change on propagation.

In this chapter we show that source-correlations can give rise to interesting modifications of spectra. We consider a simple physical configuration, consisting of two small sources which generate fields of identical spectra, and we analyze the effects of correlation between the two sources on the spectrum of the emitted radiation. We show that spectral lines can be frequency-shifted, made narrower or broader and that several lines may be generated from a single line by this mechanism. These results suggest a new technique for modifying spectra in a desired manner by controlling source correlations. In fact, since these results were first published, there have been two reports of spectral modulation by control of source correlations.[1]

The analysis presented in this chapter refers to a simple configuration and to observation points on the axis of symmetry. The more general case of arbitrary observation point is discussed in Chapter 4.

3.2 Radiation from two small scalar sources[2]

Consider light generated by two small fluctuating sources located at points P_1 and P_2. We assume that the fluctuations are statistically stationary. Let $\{Q_1(\omega)\}$ and $\{Q_2(\omega)\}$ be the ensembles that represent the source fluctuations at frequency ω. Further let

$\{V(P;\omega)\}$ be the ensemble that represents the field at P, generated by the two sources (see Fig.3.1). We assume that the spectra of the two source-distributions are identical and we denote them by $S_Q(\omega)$. Specifically

$$S_Q(\omega) = \left\langle Q_1^*(\omega)\ Q_1(\omega) \right\rangle = \left\langle Q_2^*(\omega)\ Q_2(\omega) \right\rangle, \tag{3.1}$$

where the angular brackets denote the ensemble average.

The field produced by the two sources at a point P is given by

$$V(P;\omega) = Q_1(\omega)\frac{e^{ikR_1}}{R_1} + Q_2(\omega)\frac{e^{ikR_2}}{R_2}, \tag{3.2}$$

where R_1 and R_2 denote the distance from the two sources to the observation point P
The spectrum of tne field at the point P is then given by

$$S_V(P;\omega) = S_Q(\omega)\left\{ R_1^{-2} + R_2^{-2} + 2\Re\left[\mu_Q(\omega)e^{ik(R_2-R_1)}\big/R_1R_2\right]\right\}, \tag{3.3}$$

where $\Re$ denotes the real part and $\mu_Q(\omega)$, known as the degree of spatial coherence, characterizes the correlation between the two fluctuating sources. Explicitly,

$$\mu_Q(\omega) = \left\langle Q_1^*(\omega)Q_2(\omega) \right\rangle\big/ S_Q(\omega). \tag{3.4}$$
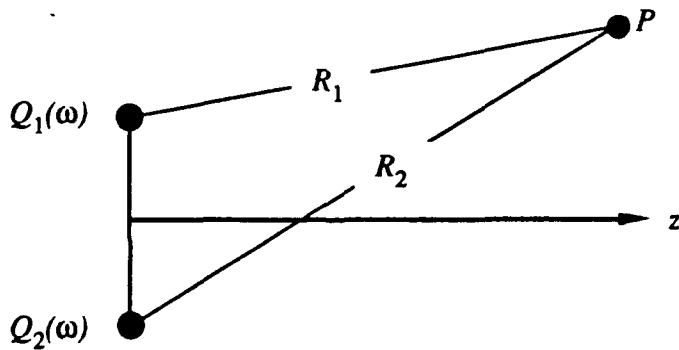
Figure 3.1: Illustrating the configuration. The two small sources Q_1 and Q_2 are place symmetrically about the axis. A typical observation point P is at a distance R_1 and R_2 respectively from the two sources.

As we have explained above [cf. Eq. (1.23)], the degree of spatial coherence satisfies the inequality

$$\left|\mu_Q(\omega)\right| \leq 1 , \tag{3.5}$$

for all frequencies. This condition is the main constraint on the possible types of spectral effects that can be achieved with the present system.

For simplicity we will consider the spectrum of the emitted radiation at points located on the perpendicular bisector, which we will refer to as the axis, of the line joining the two sources. In this case $R_2 = R_1$ (= R say) and Eq. (3.3) reduces to[2]

$$S_V(P;\omega) = \frac{2}{R^2} S_Q(\omega)\left[1 + \Re\mu_Q(\omega)\right] . \tag{3.6}$$

We note that when $\Re\mu_Q(\omega)$ is independent of ω, the spectrum of the field at all axial points will be proportional to the source spectrum $S_Q(\omega)$. This includes the case where

the two sources are mutually incoherent at each frequency [$\mu_Q(\omega) \equiv 0$]. It also includes the case when $\Re\mu_Q(\omega) \equiv 1$, which corresponds to two sources that are mutually fully coherent at each frequency. These are, however, exceptional cases. In general, $\Re\mu_Q(\omega)$ will be frequency-dependent and Eq. (3.4) shows that the field spectrum $S_V(\omega)$ will then be no longer proportional to the source spectrum $S_Q(\omega)$. Hence, in general, not only the source spectrum but also the correlation between the two sources will determine the spectrum of the emitted light.

Before we proceed to examine the effect of the degree of spatial correlation on the spectrum of the radiation we simplify our notation by setting

$$s_V(\omega) = \frac{R^2}{2} S_V(\omega) \ . \tag{3.7}$$

We will refer to $s_V(\omega)$ as the *reduced* field spectrum. For the sake of simplicity we will consider source-correlations that are characterized by a real degree of coherence. Equation (3.4) then becomes

$$s_V(P;\omega) = S_Q(\omega)\left[1 + \mu_Q(\omega)\right] \ . \tag{3.8}$$

It follows at once from this formula, that in terms of s_V and S_Q,

$$\mu_Q(\omega) = \frac{s_V(\omega)}{S_Q(\omega)} - 1 \ . \tag{3.9}$$

From the inequality (3.5) and from Eq. (3.9) it follows that only those reduced field spectra $s_V(\omega)$ can be generated for which

$$s_V(\omega) \le 2S_Q(\omega) \ . \tag{3.10}$$

$s_V(\omega)$ and $S_Q(\omega)$ are, of course, necessarily non-negative.

Conversely, when the inequality (3.10) is satisfied one finds at once from Eq. (3.9) that

$$-1 \le \mu_Q(\omega) \le 1 \ . \tag{3.11}$$

Since the inequality (3.11) is the only constraint that the degree of spectral coherence $\mu_Q(\omega)$ must satisfy we see from Eq. (3.10) , that *any reduced field spectrum $s_V(\omega)$ which does not exceed twice the magnitude of the source spectrum $S_Q(\omega)$ at any frequency ω, can, in principle, be generated by this mechanism.*

We now demonstrate how source correlations can give rise to various types of spectral changes.

3.3   Change in spectral linewidth

Let us assume first that the source spectrum consists of a single spectral line of a Lorentzian profile, viz. ,

$$S_Q(\omega) = \frac{A_0}{\Gamma_0^2 + (\omega - \omega_0)^2} \ , \tag{3.12}$$

(ω_0, Γ_0, A_0 are positive constants and $\Gamma_0 \ll \omega_0$). Suppose that we wish to produce a reduced field spectrum that consists also of a line of Lorentzian profile centered on the same frequency ω_0, but is of a different width and of different strength, say

$$s_V(\omega) = \frac{A_1}{\Gamma_1^2 + (\omega - \omega_0)^2} \; , \tag{3.13}$$

(Γ_1, A_1 are positive constants and $\Gamma_1 \ll \omega_0$). On substituting from Eqs.(3.12) and (3.13) into the inequality (3.10) we find that we must have

$$\frac{A_1}{A_0} \big[f_0(\omega) \big]_{max} \le 2 \; , \tag{3.14}$$

where $\big[f_0(\omega) \big]_{max}$ is the maximum value, in the range $0 < \omega < \infty$, of the function

$$f_0(\omega) = \frac{\Gamma_0^2 + (\omega - \omega_0)^2}{\Gamma_1^2 + (\omega - \omega_0)^2} \; . \tag{3.15}$$

Straightforward calculation shows that for all (positive) frequencies ω,

$$\left(\Gamma_0 / \Gamma_1 \right)^2 \le f_0(\omega) < 1 \qquad \textit{when} \qquad \Gamma_1 > \Gamma_0 \; ,$$

$$\tag{3.16}$$

$$1 < f_0(\omega) \le \left(\Gamma_0 / \Gamma_1 \right)^2 \qquad \textit{when} \qquad \Gamma_1 < \Gamma_0 \; .$$

Using these inequalities we deduce at once from (3.14) that we must have
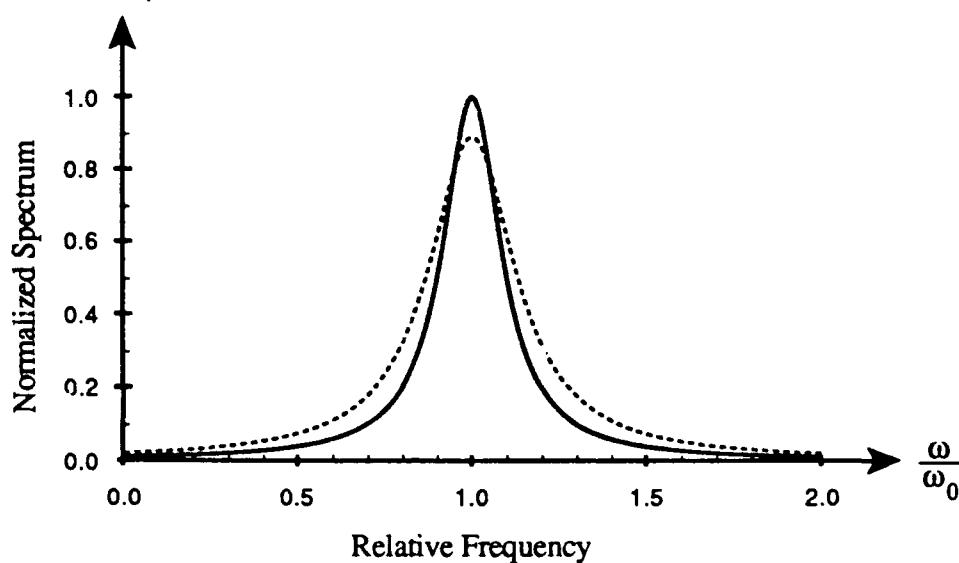
Figure 3.2: An example of line broadening by source correlations. The source spectrum (solid line) and the reduced field spectrum (dashed line) are lines of Lorentzian profiles and the curves are normalized so that the source spectrum has the value unity at the center frequency. The relative linewidths used are $\Gamma_0/\omega_0 = 0.1$, $\Gamma_1/\omega_0 = 0.15$.

$$\frac{A_1}{A_0} < 2 \qquad when \qquad \Gamma_1 > \Gamma_0 \ ,$$

$$\frac{A_1}{A_0} \leq 2(\Gamma_1/\Gamma_0)^2 \qquad when \qquad \Gamma_1 < \Gamma_0 \ . \qquad (3.17)$$

In the first case $(\Gamma_1 > \Gamma_0)$ the emitted (reduced) spectral line is broader than the spectral line of the source; in the second case $(\Gamma_1 < \Gamma_0)$ it is narrower.

With the conditions (3.17) assumed to be satisfied, the degree of spatial coherence that will produce the reduced field spectrum (3.13) from the source spectrum (3.12) is obtained at once on substituting from these equations into the formula (3.9). One then finds that the required degree of spatial coherence is given by
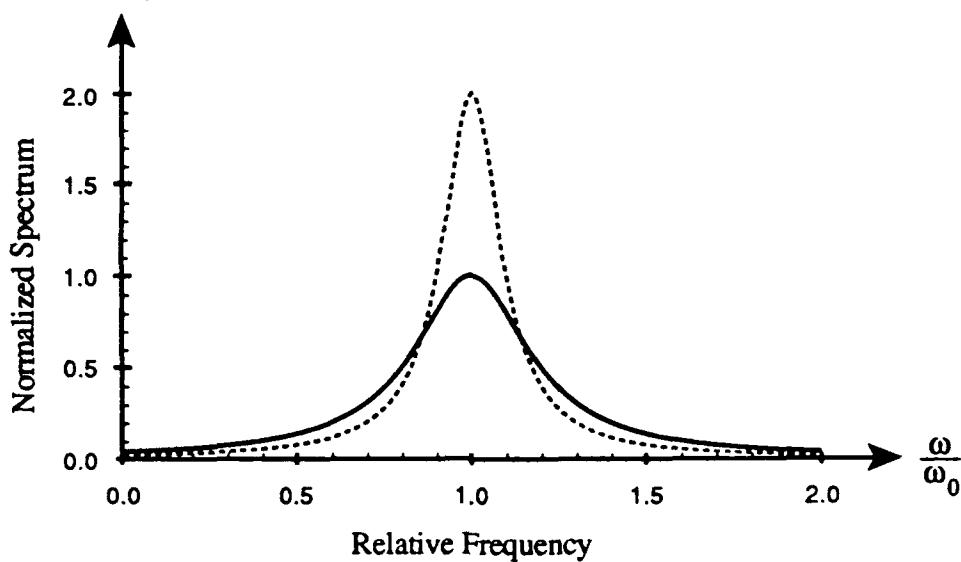
Figure 3.3: An example of line narrowing by source correlations. The source spectrum (solid line) and the reduced field spectrum (dashed line) are lines of Lorentzian profiles and the curves are normalized so that the source spectrum has the value unity at the center frequency. The relative linewidths used are $\Gamma_0/\omega_0 = 0.2$, $\Gamma_1/\omega_0 = 0.1$.

$$\mu_Q(\omega) = \frac{A_1}{A_0} \frac{\Gamma_0^2 + (\omega - \omega_0)^2}{\Gamma_1^2 + (\omega - \omega_0)^2} - 1 \ . \tag{3.18}$$

In Figs. 3.2 and 3.3 we show examples of line broadening and line narrowing with Lorentzian lineshapes. The spatial correlation that produces the reduced field spectrum depicted in Fig. 3.3 is plotted as a function of frequency in Fig. 3.4.

The method of producing Lorentzian field spectra of a controlled linewidths can also be applied to Gaussian lineshapes.[3] The source spectrum then has the form

$$S_Q(\omega) = A_r \exp\left[-(\omega - \omega_0)^2 / 2\delta_0^2\right] \ . \tag{3.20}$$
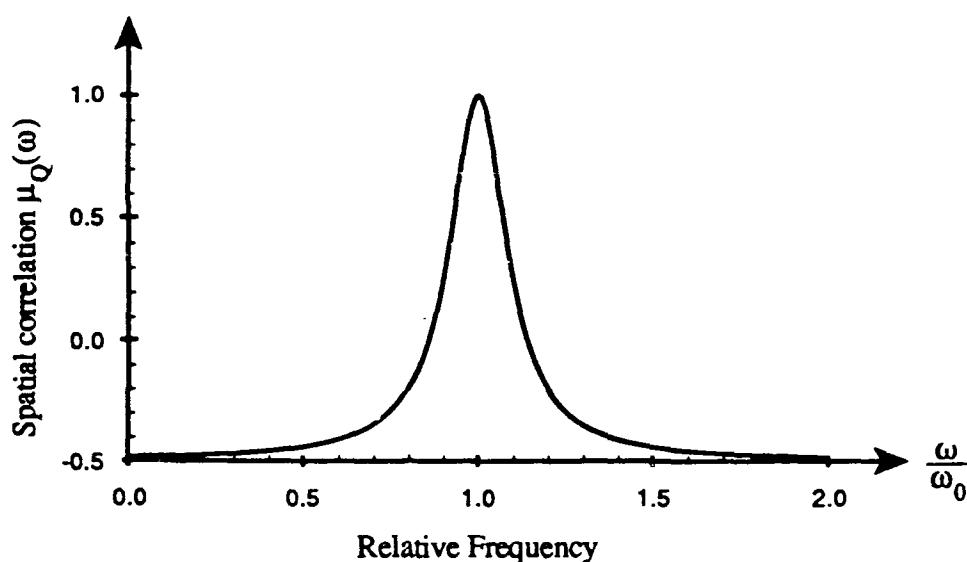
Figure 3.4: The degree of spatial coherence giving rise to the reduced field spectrum of a narrower profile shown in Fig. 3.3.

(ω_0, δ_0, A_0 are positive constants and $\delta_0 \ll \omega_0$). We now consider the possibility of producing a reduced field spectrum that also consists of a line of Gaussian profile, centered at the same frequency ω_0 but of different width and different strength, say

$$s_V(\omega) = A_1 \exp\left[-(\omega - \omega_0)^2/2\delta_1^2\right] \qquad (3.21)$$

(δ_1, A_1 are positive constants and $\delta_1 \ll \omega_0$). On substituting from Eqs.(3.20) and (3.21) into the inequality (3.10) we deduce at once that the following condition must be satisfied:

$$\frac{A_1}{A_0}[g(\omega)]_{max} \leq 2 , \qquad (3.22)$$

where $[g(\omega)]_{max}$ is the maximum value, in the range $0 < \omega < \infty$ of the function

$$g(\omega) = \exp\left[-(\omega - \omega_0)^2 / 2\Delta\right] , \tag{3.23}$$

where

$$\frac{1}{\Delta} = \frac{1}{\delta_1^2} - \frac{1}{\delta_0^2} . \tag{3.24}$$

Consider first the case when $\delta_1 < \delta_0$ (line narrowing). In this case $\Delta > 0$ and evidently $[g(\omega)]_{max} = g(\omega_0) = 1$. Hence the realizability condition (3.22) becomes

$$A_1 / A_0 \leq 2 . \tag{3.25}$$

On the other hand when $\delta_1 > \delta_0$, Δ becomes negative and $g(\omega)$ has then no upper bound in the range $0 < \omega < \infty$. Hence a broader line of Gaussian profile, centered at the same frequency ω_0, cannot be produced by this mechanism. However, in practice one is unlikely to be interested in situations where the spectra $S_Q(\omega)$ and $s_V(\omega)$ have Gaussian forms for all frequencies. If one requires that the reduced field spectrum has a Gaussian shape only over a finite range around frequency ω_0, say

$$\omega_0 - \alpha \leq \omega \leq \omega_0 + \beta , \tag{3.26}$$

where α and β are positive constants, the inequality (3.22) needs only be satisfied when the maximum of $g(\omega)$ is taken over the restricted range (3.26). Instead of the inequality (3.22) we then have the constraint
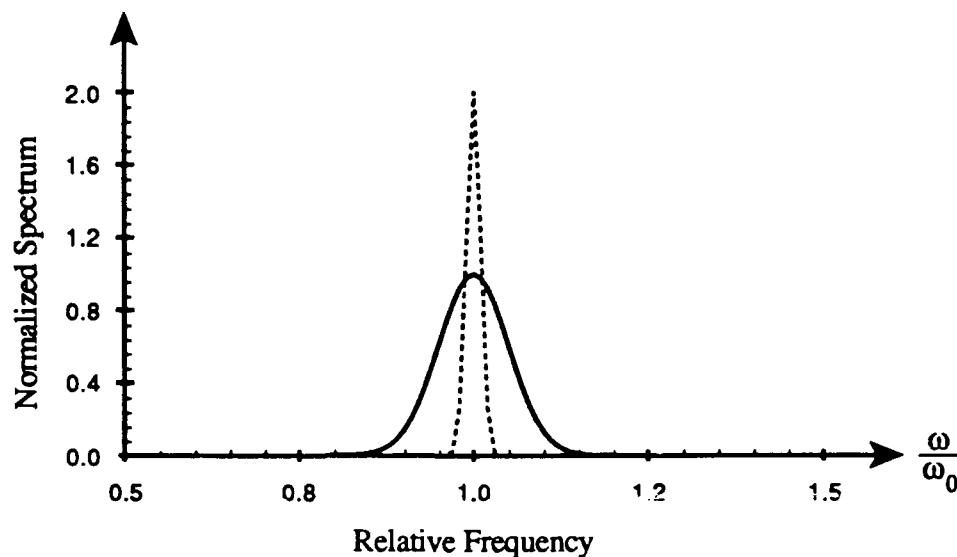
Figure 3.5: An example of line narrowing by source correlations. The source spectrum (solid line) and the reduced field spectrum (dashed line) are lines of Gaussian profiles and the curves are normalized so that the source spectrum has the value unity at the center frequency. The relative linewidths used are $\delta_0/\omega_0 = 0.05$, $\delta_1/\omega_0 = 0.01$.

$$\frac{A_1}{A_0}\exp\left(\gamma^2/2|\Delta|\right) \le 2 \ , \tag{3.27}$$

where γ is the largest of the constants α, β.

Returning to the first case ($\delta_1 < \delta_0$), the degree of spatial coherence needed to achieve this modification of the spectral line is according to Eqs.(3.9), (3.20) and (3.21) given by

$$\mu_Q(\omega) = \frac{A_1}{A_0}\exp\left[-(\omega - \omega_0)^2/2\Delta\right] - 1 \ , \tag{3.28}$$
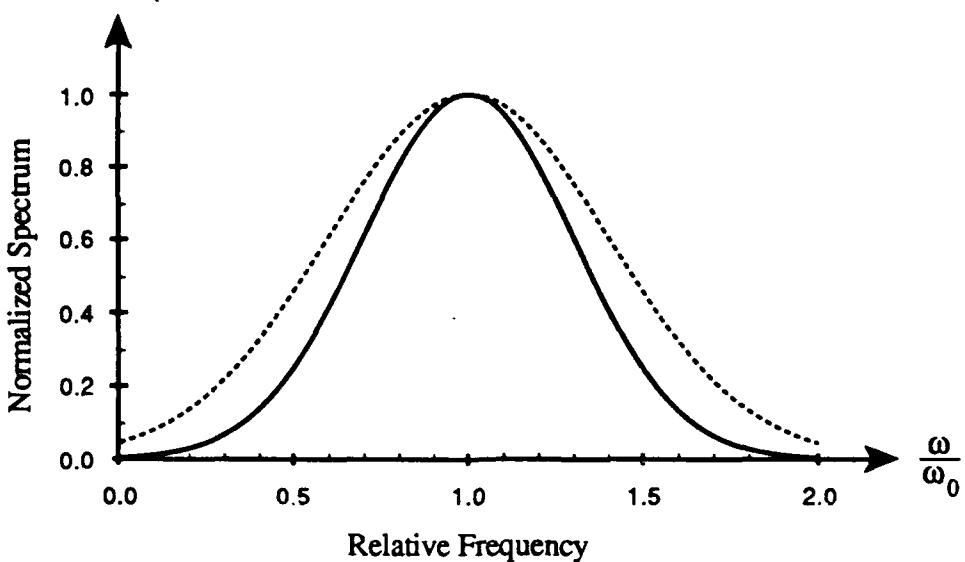
Figure 3.6: An example of line broadening by source correlations. The source spectrum (solid line) and the reduced field spectrum (dashed line) are lines of Gaussian profiles and the curves are normalized so that the source spectrum has the value unity at the center frequency. The relative linewidths used are $\delta_0/\omega_0 = 0.5$, $\delta_1/\omega_0 = 0.7$.

where Δ is defined by Eq.(3.24). In the second case ($\delta_1 > \delta_0$) the degree of spatial coherence is given by Eq.(3.28) only for frequencies that are within the range (3.26); for frequencies outside this range the degree of spatial coherence can take on arbitrary values, subject to the constraint expressed by Eq. (3.11). Line narrowing and line broadening of Gaussian profiles are illustrated in Figs. 3.5 and 3.6.

3.4 Spectral lineshifts

We now consider the possibility of changing not only the width of the line but also its center frequency, from ω_0 to ω_1 say. Suppose that the source spectrum $S_Q(\omega)$ is again the single spectral line (3.13) of Lorentzian profile, but that the reduced field spectrum,
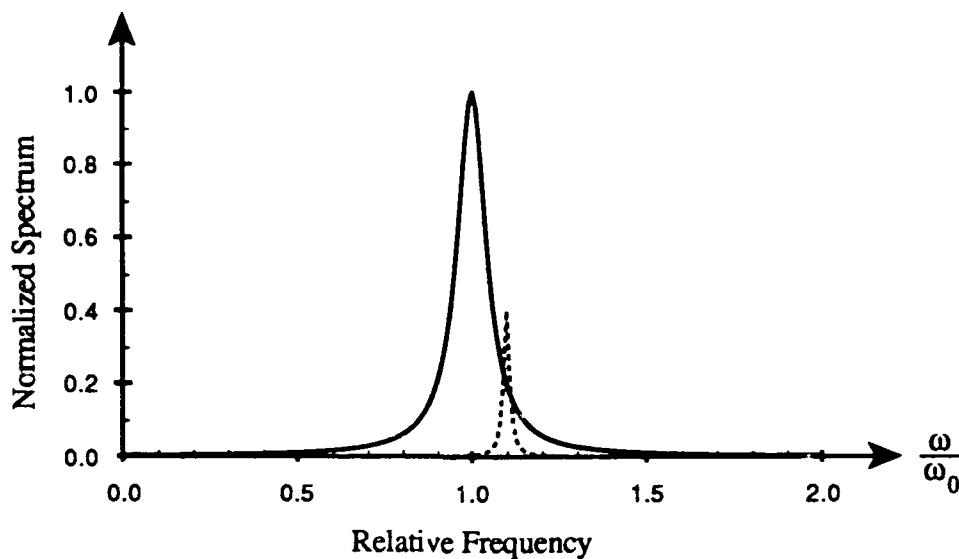
Figure 3.7: Spectral shift and line narrowing with Lorentzian profiles. The source spectrum (solid curve) has a relative linewidth $\Gamma_0/\omega_0 = 0.05$ giving rise to a reduced field spectrum (dashed line) of relative linewidth $\Gamma_1/\omega_0 = 0.01$ centered at frequency $\omega = 1.1\omega_0$.

whilst also a line of Lorentzian profile, is centered at a different frequency $\omega_1 \neq \omega_0$, i.e. that

$$s_V(\omega) = \frac{A_1}{\Gamma_1^2 + (\omega - \omega_1)^2} \, ,$$

(3.29)

$(\omega_1, \Gamma_1, A_1$ are positive constants, $\Gamma_1 \ll \omega_1)$. On substituting from Eqs. (3.12) and (3.29) into Eq. (3.10) we find that the following inequality must now be satisfied:

$$\frac{A_1}{A_0}\left[f_1(\omega)\right]_{max} \leq 2 \, .$$

(3.30)

Here $[f_1(\omega)]_{max}$ is the maximum value in the range $0 < \omega < \infty$ of the function
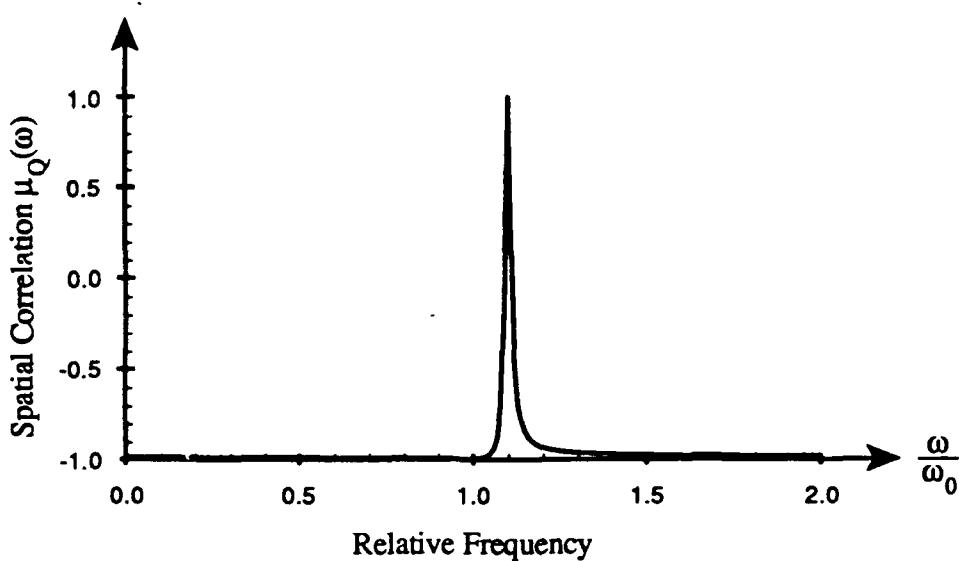
Figure 3.8: The degree of correlation that gives rise to the frequency-shifted reduced field spectrum shown in Fig. 3.7.

$$f_1(\omega) = \frac{\Gamma_0^2 + (\omega - \omega_0)^2}{\Gamma_1^2 + (\omega - \omega_1)^2} \ .$$ (3.31)

Unlike in the case considered above (when $\omega_1 = \omega_0$) an explicit expression for the maximum value of this function cannot readily be obtained (see Appendix A for details of the numerical method used to determine the maximum value of A_1). However it seems that with suitable choices of the constants that specify the reduced field spectrum (3.29) the inequality (3.30) can be satisfied for all non-negative frequencies ω. The degree of spatial coherence which gives rise to the reduced field spectrum (3.29) is then obtained on substituting from Eqs.(3.29) and (3.12) into Eq.(3.9). The resulting expression is

$$\mu_Q(\omega) = \frac{A_1}{A_0} \frac{\Gamma_0^2 + (\omega - \omega_0)^2}{\Gamma_1^2 + (\omega - \omega_1)^2} - 1 \ . \tag{3.32}$$

In Fig. 3.7 we show an example of spectral changes in which both the linewidth and the center frequency are modified by source correlations which are represented by the degree of spatial coherence in Eq. (3.32). Figure 3.8 shows the degree of spatial coherence that gives rise to these spectral changes.

3.5 Modulation of a single spectral line

As a last example we consider the possibility of generating from a source spectrum that consists of a single line of Lorentzian profile a field spectrum that consists of several lines of Lorentzian profile. More specifically, with two sources that have identical spectra given by Eq. (3.12) we wish to generate a field whose reduced spectrum has the form

$$s_V(\omega) = \sum_{n=1}^{N} \frac{A_n}{\Gamma_n^2 + (\omega - \omega_n)^2} \ , \tag{3.33}$$

where N, A_n, ω_n, and Γ_n are positive constants and $\Gamma_n \ll \omega_n$ ($1 \le n \le N$). For this to be possible the following condition obtained on substituting Eqs. (3.33) and (3.12) into Eq. (3.10) must be satisfied:
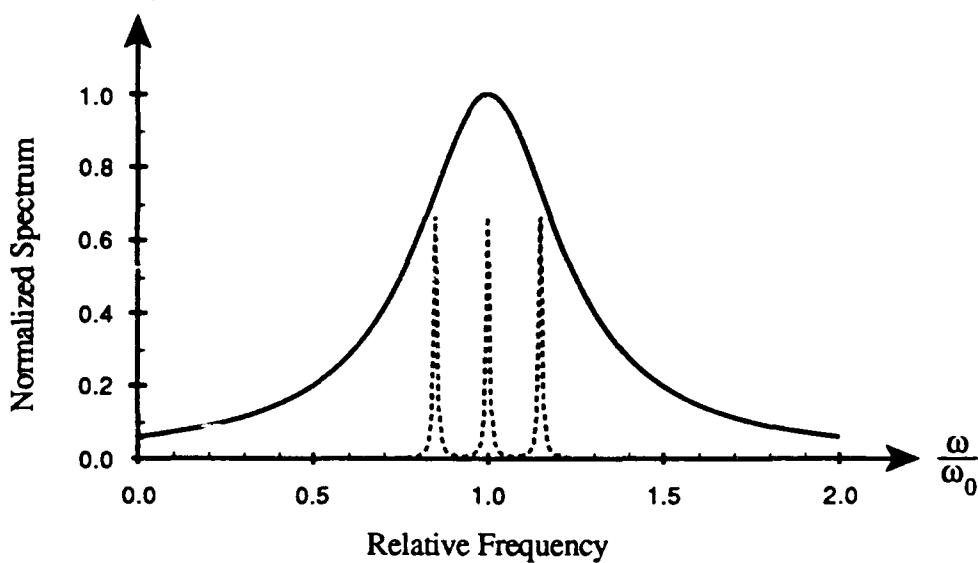
Figure 3.9: Generation of three spectral lines from a single spectral line, all of Lorentzian profiles. The source spectrum consists of a single line whose relative width is $\Gamma_0/\omega_0 = 0.25$ and the three spectral lines are all of relative width $\Gamma/\omega_0 = 0.05$.

$$\frac{1}{A_0}\sum_{n=1}^{N}A_n\big[f_n(\omega)\big]_{\max}\leq 2 \ . \tag{3.34}$$

Here $[f_n(\omega)]_{\max}$ is the maximum value, in the range $0 \leq \omega < \infty$, of the function

$$f_n(\omega)=\frac{\Gamma_0^2+(\omega-\omega_0)^2}{\Gamma_n^2+(\omega-\omega_n)^2} \ . \tag{3.35}$$

Assuming that the constraint (3.34) is satisfied, the degree of spatial coherence needed for generating the reduced field spectrum (3.33) is obtained at once on substituting from Eqs. (3.33) and (3.12) into Eq. (3.9). One then finds that
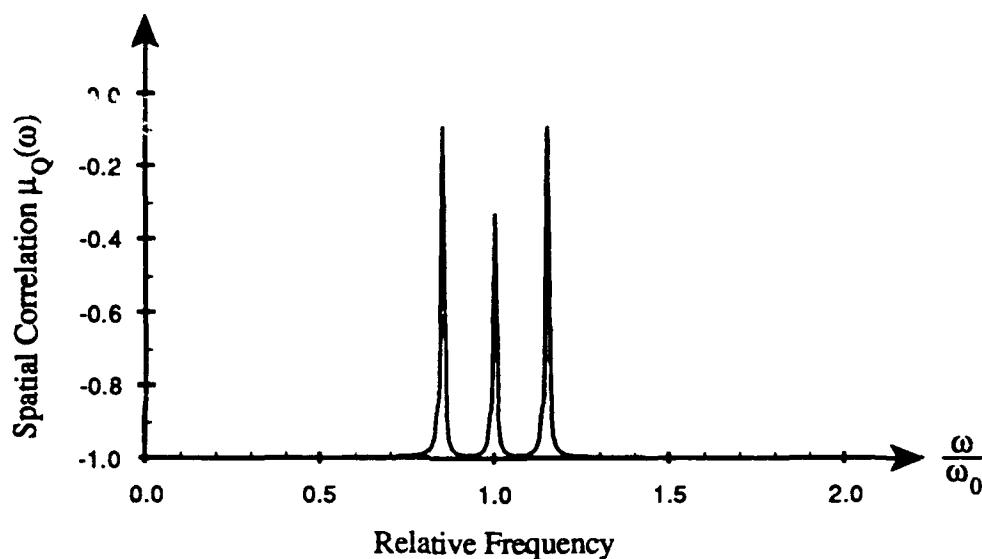
Figure 3.10: The spatial correlation for generation of three spectral lines from a single spectral line.

$$\mu_Q(\omega) = \frac{1}{A_0} \sum_{n=1}^{N} A_n \frac{\Gamma_0^2 + (\omega - \omega_0)^2}{\Gamma_n^2 + (\omega - \omega_n)^2} - 1 \ . \tag{3.36}$$

An example of generation of a field spectrum consisting of three lines from a source spectrum consisting of a single line is illustrated in Fig 3.9. Figure 3.10 shows the degree of correlation which gives rise to this spectrum.

3.6 The spectrum produced by an array of partially coherent sources

So far we have considered a very simple radiating system consisting of two small sources with identical spectra and we showed that by appropriately correlating them,
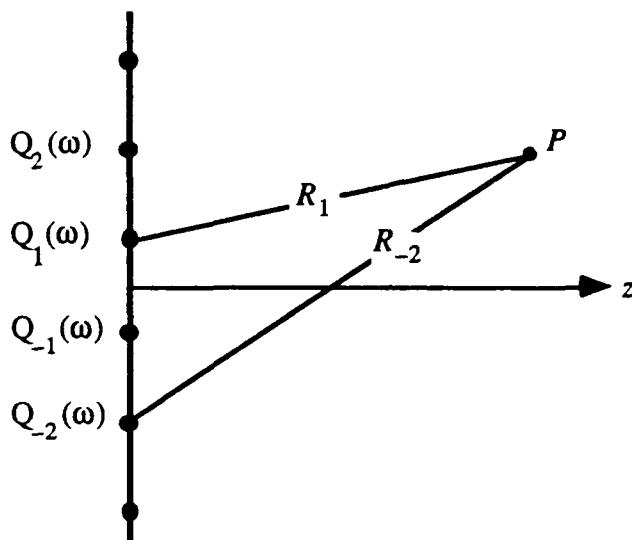
Figure 3.11: The notation for an array of scalar sources

the spectrum of the emitted radiation can take on many different forms. With systems consisting of a larger number of radiating sources one can, of course, produce more diverse spectral changes than those considered above. A simple extension of the system which we considered is an array of $2N$ equally spaced small fluctuating sources[4] (see Fig. 3.11). The field produced by the array is given by [cf. Eq. (3.2)]

$$V(P;\omega) = \sum_{i=-N}^{N} Q_i(\omega)\frac{e^{ikR_i}}{R_i} \,. \tag{3.37}$$

Using Eq. (3.37), the spectrum of the field at the point P is readily found to be

$$S_V(P;\omega) = S_Q(\omega)\left[\sum_{i=-N}^{N} R_i^{-2} + \sum_{i\neq j}\sum \mu_{ij}(\omega)\frac{e^{ik\left(R_j-R_i\right)}}{R_i R_j} \right]. \tag{3.38}$$

Equation (3.38) shows some interesting new features. Even for observation points on the axis, the exponential factor, does not, in general, reduce to a constant which is independent of frequency.[5] As a result, it follows that the spectrum of the field will no longer be proportional to the spectrum of the sources when the fluctuations are fully correlated, $\mu_{ij}(\omega) = 1$. Specifically, the presence of the wavenumber k in the exponential causes some modulation of the spectrum that is proportional to the magnitude of the degree of correlation.[6] On the other hand, when the source fluctuations are uncorrelated, $\mu_{ij}(\omega) = 0$ when $i \neq j$ and we then have

$$S_V(P;\omega) = S_Q(\omega) \sum_{i=1}^{2N} R_i^{-2} \ . \tag{3.39}$$

The spectrum of the field is now seen to be proportional to the spectrum of the source for all points of observation.

3.7 General remarks on spectral modulation

In this chapter we presented simple examples of partially coherent radiating systems in which the field spectrum is modified by the degree of correlation of the source fluctuations. As is evident from Eqs. (3.3) and (3.38), this mechanism does not produce any new frequencies but just increases or decreases their relative contributions to the observed spectrum. This fact implies that in order to generate field spectrum of a particular shape, the source must possess all the required spectral components. For this

reason, it is convenient to choose broad t .nd sources for theoretical and experimental illustration of the spectral effects which we discussed in this thesis.

The basic question that we have not addressed in this chapter is how to produce the prescribed spatial correlations. Several methods for generating and modifying source correlations, at least for secondary sources, have been developed in recent years. They include the use of scattering by liquid crystals under the influence of an external D.C. field[7], the use of rotating ground glass plates[8] and of holographic filters[9], interaction of light with ultrasonic waves[10] by imaging and lensless feedback systems and by the use of achromatic Fourier transform lenses.[11]

The most notable method and experimental demonstration of spectral modulation by control of source correlation was reported by G. Indebetouw[1a]. His technique makes use of spatial masks which produce a secondary source of prescribed frequency dependent degree of correlation.

References

[1] a. G. Indebetouw, "Synthesis of polychromatic light sources with arbitrary degrees of coherence: Some experiments", J. Mod. Opt. **36**, 251-259 (1989).

   b. H. C. Kandpal, J. S. Vaishya and K. C. Joshi, submitted to Opt. Commun.

[2] We follow here the presentation in, E. Wolf, "Red shifts and blue shifts of spectral lines emitted by two correlated sources", Phys. Rev. Lett. **58**, 2646-2648 (1987).

3   In this method of spectral modulation it is usually wise to avoid sources whose spectra consist of Gaussian profiles because of the rapid attenuation of the spectrum away from line center.

4   In this notation there is no source corresponding to Q_0.

5   The only exception is when the sources are correlated symmetrically about the axis, i.e. when $\mu_{ij}(\omega) = 0$ unless $j = -i$.

6   This modulation is equivalent to the formation of interference fringes on light diffraction from multiple pinholes. The visibility of the fringes can be related to the degree of correlation. A discussion of this situation can be found in E. Wolf, "Young's Interference Fringes with Narrow-band Light", Opt. Lett. **8**, 250-252 (1983).

7   a.   F. Scudieri, M. Bertolotti and R. Bartolino, "Light scattered by a liquid crystal: a new quasi-thermal source", Appl. Opt. **13** 181 (1974).

             b.   M. Bertolotti, F. Scudieri and S. Verginelli, "Spatial coherence of light scattered by media with large correlation length of refractive index", Appl. Opt. **15**, 1842 (1976)

8   a.   P. de Santes, F. Gori, G. Guattari and C Palma, "An example of a Collett-Wolf source", Opt. Commun. **29**, 256 (1979).

b. J. D. Farina, L. M. Narducci and E. Collet, "Generation of highly directional beams from a globally incoherent source", Opt. Commum. **32**, 203 (1980).

9 D. Courjon and J. Bulabois, "Modification of coherence prpperties of a light beam: application in optical processing", Proc. S. P. I. E. **194**, 129 (1979).

10 a. Y. Ohtsuka and Y. Imai, "Partial coherence controlled by a progressive ultasonic wave", J. Opt. Soc. Amer. **69**, 684 (1979).

b. Y. Imai and Y. Ohtsuka, "Optical coherence modulation by ultrasonic waves. 1: Dependence of partial coherence on ultasonic parameters", Appl. Opt. **19**, 542 (1980).

c. Y Ohtsuka, "Modulation of optical coherence by ultasonic waves", J. Opt. Soc. Amer. **A3**, 1247 (1986).

11 a. J. Deschamps, D. Courjon and J. Bulabois, "Gaussian Schell-model sources: an example and some perspective", J. Opt. Soc. Amer. **73**, 256 (1983).

b. G. M. Morris and D. Faklis, "Effects of source correlations on the spectrum of light", Opt. Commun. **62**, 5-11 (1987).

Appendix A: The method used in determining the maximum value of A_1

Starting from Eqs. (3.30) and (3.31) we have the constraint

$$\frac{A_1}{A_0} \frac{\Gamma_0^2 + (\omega - \omega_0)^2}{\Gamma_1^2 + (\omega - \omega_1)^2} \leq 2 \ . \tag{A 1}$$

First we set

$$A_0 = \Gamma_0^2 / \omega_0^2 \tag{A 2}$$

to normalize the source spectrum to the value of unity at $\omega = \omega_0$. Next we set the frequency $\omega = \omega_1$ in Eq. (A 1). This choice is made *only for computation purposes* and should not be mistaken as a statement that the function $f_1(\omega)$ in Eq. (3.30) is maximized at $\omega = \omega_1$. It follows from Eqs. (A 1) and (A 2) that the upper bound on A_1 in this case is given by

$$\left[A_1\right]_{\max} = \frac{2\Gamma_0^2 \Gamma_1^2}{\Gamma_0^2 + (\omega_1 - \omega_0)^2} \ . \tag{A 3}$$

This method for determining the value for A_1 was used with numerous choices of the constants Γ_0, Γ_1, ω_0, ω_1 and the resulting degree of correlation has alwas satisfied the constraint (3.11).

4

Spatial and Spectral effects with electromagnetic sources

Introduction

The effects of source correlations on the spectrum of emitted radiation have been treated so far only in the framework of scalar theory. In the previous chapter we considered a simple system consisting of two scalar sources and we examined some of the spectral effects that may be produced on the axis by controlling the correlations between the two sources. In this chapter we consider a system of two partially correlated linear dipoles. First, we derive expressions for the observed spectrum at an arbitrary point in the far zone. We then examine how the degree of correlation of the dipole polarization fluctuations affects the spectrum of the field observed in particular directions. We also consider the effects of the degree of correlation on the angular distribution of the radiant intensity for fixed frequencies. In Secs. 4.4 and 4.5 we present expressions for the total radiated power and for the directivity of the system as a function of the degree of correlation and the spatial separation between the two dipoles. We also compare our results for the partially correlated dipoles with results in the well known limiting cases of fully correlated and uncorrelated dipoles.[1] This comparison gives a valuable measure for the range of possible spatial and spectral modulation effects which can be produced by controlling source correlations.

4.2 Far zone spectrum of partially correlated dipoles

Consider two linear dipoles, situated at points $\pm y_0$ and vibrating in the z direction as shown in Fig. 4.1.

Let

$$P_1(r,t) = p_1(t)\delta(r - y_0\hat{y})\hat{z},$$

(4.1)

$$P_2(r,t) = p_2(t)\delta(r + y_0\hat{y})\hat{z},$$

be the electric polarization vectors of the two dipoles. Here $p_j(t)$, (j = 1, 2), specify the polarization fluctuations of the dipoles as functions of time and $\hat{y}$ and $\hat{z}$ are unit vectors in the positive y and z directions respectively. We assume that $p_j(t)$ are random functions of time, characterized by stationary ensembles.

In the space-frequency representation, the electric Hertz potential of the field produced by the dipoles is given by

$$\Pi_e(r;\omega) = \hat{z}\left[\tilde{p}_1(\omega)\frac{e^{ikR_1}}{R_1} + \tilde{p}_2(\omega)\frac{e^{ikR_2}}{R_2}\right],$$

(4.2)

where $R_1 = |r - y_0\hat{y}|$, $R_2 = |r + y_0\hat{y}|$, and[2]
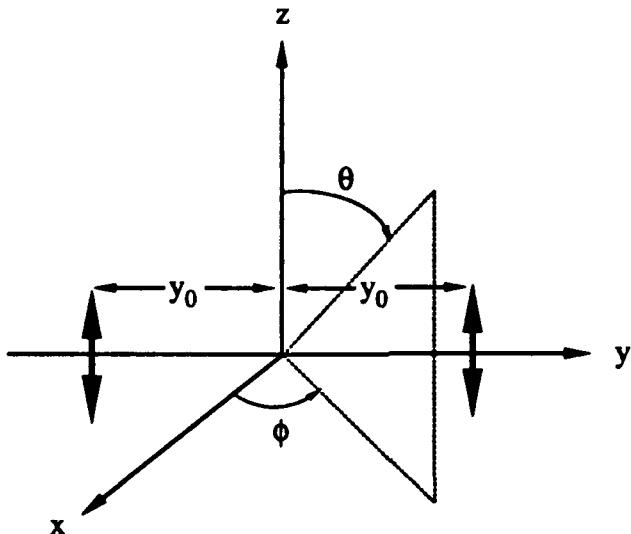
Figure 4.1: Illustrating the configuration and the notation. The two dipoles are marked by the heavy vertical arrows are separated by a distance $2y_0$ from each other.

$$\tilde{p}_j(\omega) = \int_{-\infty}^{\infty} p_j(t)e^{i\omega t} dt \qquad (j = 1, \ 2). \qquad (4.3)$$

In order to calculate the spectral intensity in the far zone, it is sufficient to evaluate the magnetic field only; it is given by the expression:

$$B(r; \omega) = -ik\nabla \times \Pi_e(r; \omega). \qquad (4.4)$$

Since $\Pi_e(r; \omega)$ is a vector along the z-direction, it follows that

$$\nabla \times \Pi_e(r; \omega) = \left[\frac{\partial}{\partial y}\hat{x} - \frac{\partial}{\partial x}\hat{y} \right] \Pi_e(r; \omega). \qquad (4.5)$$

On substituting Eq. (4.2) in Eq. (4.5) and calculating the partial derivatives, we obtain the formula

$$\nabla \times \Pi_e(r; \omega) = \tilde{p}_1(\omega) \frac{e^{ikR_1}}{R_1} \left(ik - \frac{1}{R_1} \right) \left(\frac{y - y_0}{R_1}\hat{x} - \frac{x}{R_1}\hat{y} \right)$$

$$+ \tilde{p}_2(\omega) \frac{e^{ikR_2}}{R_2} \left(ik - \frac{1}{R_2} \right) \left(\frac{y + y_0}{R_2}\hat{x} - \frac{x}{R_2}\hat{y} \right). \qquad (4.6)$$

For field points $r = ru$ in the far zone $kR_j \gg 1$ (j = 1, 2) and we have
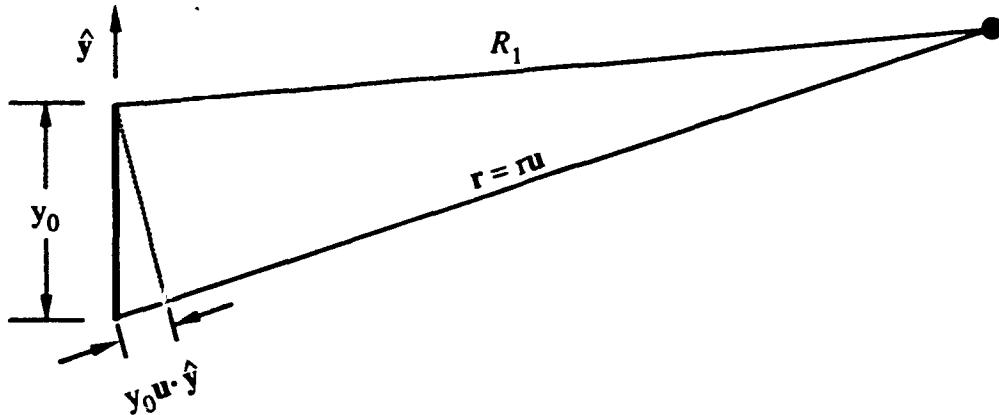
Figure 4.2: Graphical representation of the approximation for R_1 made in Eq. (4.7).

$$R_1 \sim r - y_0(u \cdot \hat{y}),$$
$$R_2 \sim r + y_0(u \cdot \hat{y}), \qquad (4.7)$$

where u is a unit vector in the direction of observation (see Fig. 4.2).

Using Eqs. (4.6) and (4.7), we may express the far zone B-field in the form

$$B(ru;\omega) \sim -\hat{\Phi} k^2 \frac{e^{ikr}}{r} \sin\theta$$
$$\left[\tilde{p}_1(\omega)\exp\left(-iky_0 u \cdot \hat{y}\right) + \tilde{p}_2(\omega)\exp\left(iky_0 u \cdot \hat{y}\right)\right] \qquad (4.8)$$

$$as \ kr \to \infty.$$

Here, we have used the spherical polar coordinates (r, θ, ϕ) with the polar axis along the z-direction and with $\hat{\Phi} = \sin\theta(\hat{y}\cos\phi - \hat{x}\sin\phi)$.

The radiant intensity $J(u;\omega)$, i.e. the power per unit frequency at frequency ω, per unit solid angle around the direction specified by the unit vector u, is given by

$$J(u;\omega) = \lim_{kr \to \infty} r^2 u \cdot \left\langle S^{(\infty)}(ru;\omega) \right\rangle, \tag{4.9}$$

where $S^{(\infty)}(ru;\omega)$ is the Poynting vector at points in the far zone, and the angular brackets denote the ensemble average. In terms of the B-field, we have

$$J(u;\omega) = \lim_{kr \to \infty} r^2 \frac{c}{8\pi} \Re \left\langle u \cdot \left[\left(B^{(\infty)}(ru;\omega) \times u \right)^* \times B^{(\infty)}(ru;\omega) \right] \right\rangle, \tag{4.10}$$

where $\Re$ denotes the real part and c is the vacuum speed of light. Using the vector identity

$$u \cdot (B \times u)^* \times B = |B \times u|^2, \tag{4.11}$$

we simplify Eq. (4.10) for the radiant intensity to the form

$$J(u;\omega) = \lim_{kr \to \infty} r^2 \frac{c}{8\pi} \left\langle |B(ru;\omega)|^2 \right\rangle. \tag{4.12}$$

Let us now assume that both dipoles have the same spectrum, i.e., that

$$\left\langle |\tilde{p}_1(\omega)|^2 \right\rangle = \left\langle |\tilde{p}_2(\omega)|^2 \right\rangle \equiv S_p(\omega). \tag{4.13}$$

We also introduce the complex degree of spatial coherence at frequency ω, which characterizes the correlation between the two dipoles, by the formula

$$\mu_p(\omega) = \left\langle \tilde{p}_1(\omega)\tilde{p}_2(\omega)\right\rangle \Big/ S_p(\omega). \qquad (4.14)$$

On substituting from Eqs. (4.8), (4.13) and (4.14) in Eq. (4.12), we obtain the following expression for the radiant intensity produced by the two partially correlated dipoles:

$$J(u;\omega) = \frac{ck^4}{4\pi} S_p(\omega)\sin^2\theta \left\{ 1 + \Re\left[\mu_p(\omega)\exp\left(2iky_0\sin\theta\sin\phi\right)\right]\right\}. \qquad (4.15)$$

If we express the degree of correlation in the form

$$\mu_p(\omega) = \left|\mu_p(\omega)\right|e^{i2\psi(\omega)}, \qquad (4.16)$$

where $2\psi(\omega)$ corresponds to the effective steering angle[3], we find that the radiant intensity of the two partially correlated linear dipoles is given by the formula

$$J(u;\omega) = \frac{ck^4}{4\pi} S_p(\omega)\sin^2\theta \left\{ 1 + \left|\mu_p(\omega)\right|\cos\left[2ky_0\sin\theta\sin\phi + 2\psi(\omega)\right]\right\}. \qquad (4.17)$$

4.3 The effects of spatial correlation on the spectrum and the angular distribution of the radiant intensity

We now consider some special cases which will help to illustrate the significance of Eq. (4.17). First let us consider two *uncorrelated* dipoles. In this case $\mu_p(\omega) \equiv 0$, and Eq. (4.17) reduces to

$$[J(u;\omega)]_{uncorr.} = \frac{ck^4}{4\pi} S_p(\omega)\sin^2\theta \ . \tag{4.18}$$

As one may expect, the same spectrum is obtained if the radiation originated from a single dipole located at the origin and having polarization fluctuations equal to the sum of the polarizations of the two dipoles.

Similarly, when the two dipoles are *fully correlated*, i.e. when

$$\left|\mu_p(\omega)\right| \equiv 1 \ , \tag{4.19}$$

the formula (4.17) for the radiant intensity reduces to

$$[J(u;\omega)]_{corr.} = \frac{ck^4}{2\pi} S_p(\omega)\sin^2\theta\cos^2\left[ky_0\sin\theta\sin\phi + \psi(\omega)\right]. \tag{4.20}$$

We observe that for every frequency ω, the phase angle $\psi(\omega)$ and the separation constant ky_0 completely determine the angular distribution of the radiated power.

Returning to the general case when the two dipoles are partially correlated, we note that when the point of observation is on the x-axis ($\theta = \pi/2$, $\phi = 0$), the radiant intensity according to Eq. (4.17) is given by

$$J(\hat{x};\omega) = \frac{ck^4}{4\pi} S_p(\omega)\left[1 + \Re\mu_p(\omega)\right]. \tag{4.21}$$

The result for this special case is in the same form as the corresponding expression for the radiant intensity from two small partially correlated scalar sources [cf. Eq. (3.6)]

$$S_V(P;\omega) = \frac{2}{R^2} S_Q(\omega)\left[1 + \Re\mu_Q(\omega)\right], \qquad (4.22)$$

where P is any point on the perpendicular bisector of the line adjoining the two sources. Aside from the $2/R^2$ factor, the only significant difference is in the factor k^4 appearing in Eq. (4.21), and as a result, the product $k^4 S_p(\omega)$ is shifted to higher frequencies relative to $S_p(\omega)$.

The radiation pattern generated by the partially correlated dipoles differs from the two limiting cases of fully-correlated and of completely uncorrelated dipoles in several ways. If we denote the direction for which the radiant intensity is a maximum by u_m, it can readily be shown that the maximum possible radiant intensity $\left[J(u_m;\omega)\right]_{max}$ produced by the two dipoles is obtained when they are fully correlated, and is given by

$$\left[J(u_m;\omega)\right]_{max} = \frac{ck^4}{2\pi} S_p(\omega). \qquad (4.23)$$

On the other hand when the dipoles are only partially correlated, the maximum radiant intensity is smaller by a factor $\frac{1}{2}\left[1 + |\mu_p(\omega)|\right]$.

In the two limiting cases of fully-correlated dipoles and uncorrelated dipoles, the nulls of the radiant intensity distribution are determined by the factor $\sin^2\theta$ in Eq. (4.18), and by the factor $\sin^2\theta\cos^2\left[ky_0\sin\theta\sin\phi + \psi(\omega)\right]$ in Eq. (4.20). By contrast, it follows from Eq. (4.17) that when the dipoles are partially correlated, $0 < |\mu_p(\omega)| < 1$, there are no nulls outside the plane $\theta = 0$. This fact is significant in connection with the theorems regarding the approximation of desired radiation patterns

by arrays of radiators.[4] Specifically, in cases where the directivity of antennas is important, effort is made to reduce the amount of sidelobes. Typical antennas in which all elements are radiating coherently have several nulls in their radiation pattern and hence there is a latitude of design options allowing for the shifting of these nulls. On the other hand, the system considered here has no nulls in the radiation pattern outside the plane $\theta = 0$ in which the radiation vanishes identically. As a result, no rearrangement of the elements can produce a null in a particular direction as long as the degree of correlation is less than unity.

We now illustrate the angular distribution of the radiant intensity produced by the two partially correlated dipoles. Let the dipole spectrum be a Lorentzian line of width δ_0, centered at frequency ω_0, i.e.,

$$S_p(\omega) = \frac{1}{1 + (\omega - \omega_0)^2 / \delta^2}.$$
(4.24)

We choose a real-valued degree of correlation in the form
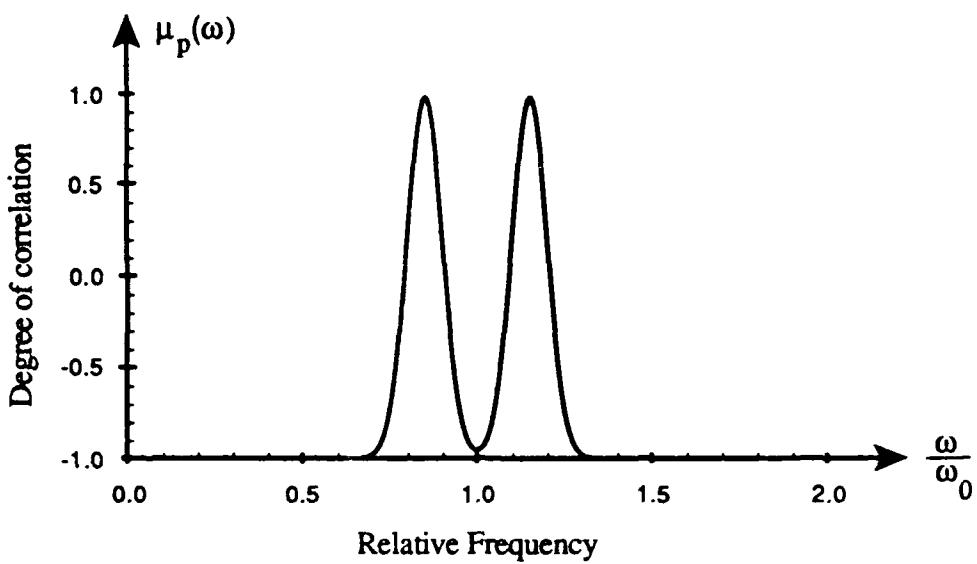
Figure 4.3: The degree of correlation given in Eq. (4.25). The constants used are $\omega_1/\omega_0 = 0.8$, $\omega_2/\omega_0 = 1.2$, $\delta_1 = \delta_2 = 0.05$ and $A_1 = A_2 = 1.98$.

$$\mu_p(\omega) = A_1 \exp\left[-(\omega - \omega_1)^2/2\delta_1^2\right] + A_2 \exp\left[-(\omega - \omega_2)^2/2\delta_2^2\right]. \quad (4.25)$$

Here ω_1, ω_2, δ_1, and δ_2 are positive constants, and we select A_1 and A_2 so that the constraint

$$\left|\mu_p(\omega)\right| \leq 1, \quad (4.26)$$

is satisfied throughout the frequency range of interest. We note that by choosing a real-valued degree of correlation the steering angle is set to zero (i.e., $2\psi(\omega) \equiv 0$) in the following examples.
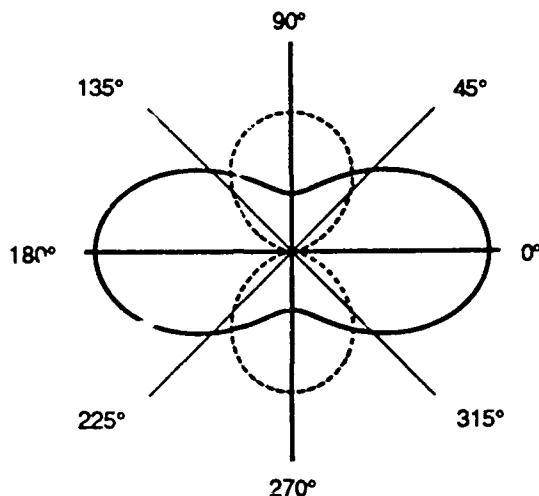
Figure 4.4: Angular distribution of the radiant intensity at frequency $\omega = \omega_0$ for fully correlated dipoles (solid line) and partially correlated dipoles (dashed line). The separation constant is $ky_0 = 1$ and the degree of correlation is given by Eq. (4.25).

Figures 4.4 and 4.5 show the angular distributions of the radiant intensity in the x, y-plane ($\theta = \pi/2$) for two fully correlated dipoles and for partially correlated dipoles whose degree of correlation is given by Eq. (4.25). In Fig. 4.4 the angular

(a)   (b)
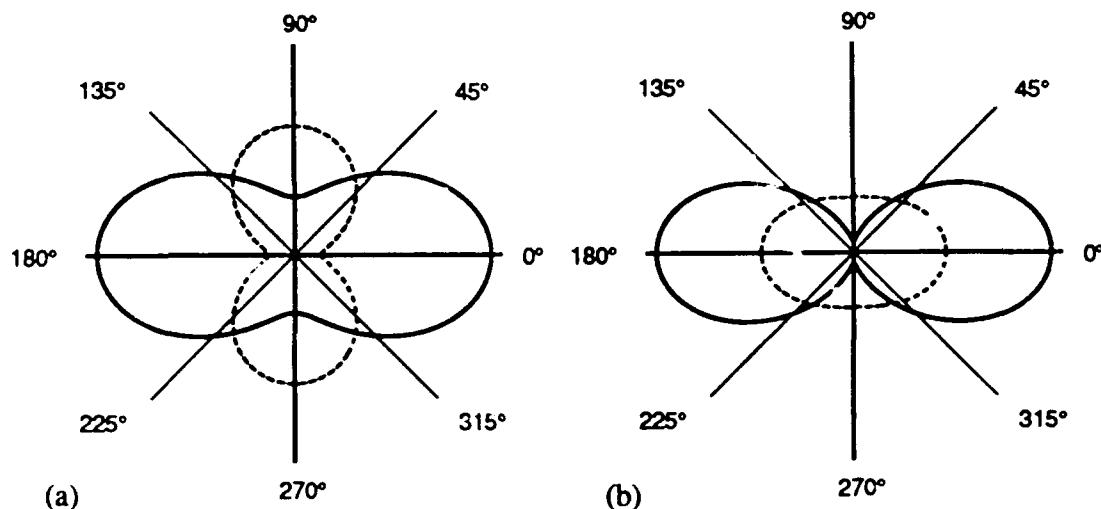
Figure 4.5: The angular distribution of the radiant intensity for fully correlated dipoles (solid line) and partially correlated dipoles (dashed line) and separation constant $ky_0 = 1$. The relative frequencies are $\omega/\omega_0 = 1.05$ [(a)] and $\omega/\omega_0 = 1.1$ [(b)].

distribution is calculated for the center frequency $\omega = \omega_0$ of the polarization spectrum, while Fig. 4.5 shows the angular distributions at different frequencies.

We note that in spite of the fact that the steering angle was fixed, $[\psi(\omega) = 0]$, there is a directional shift in the angular distribution of the radiant intensity produced by partially correlated dipoles.

When the separation between the dipoles increases the lobe structure becomes more complicated. In Figs. 4.6 and 4.7 we show the angular distributions of the radiant intensity for dipole separation $k_0 y_0 = 3$. Comparing the angular distributions for dipole separation $k_0 y_0 = 1$ (Fig. 4.4, 4.5) and $k_0 y_0 = 3$ (Fig. 4.6, 4.7), we note that at each frequency the number of lobes with our two choices of correlations is identical although their angular distributions are somewhat different. In fact, except when the two dipoles are uncorrelated, the number of lobes of the radiant intensity, n, is independent of the degree of correlation and it is given by

$$ n = 4\left[\left|\frac{k y_0}{\pi/2}\right|\right]. \qquad (4.27) $$
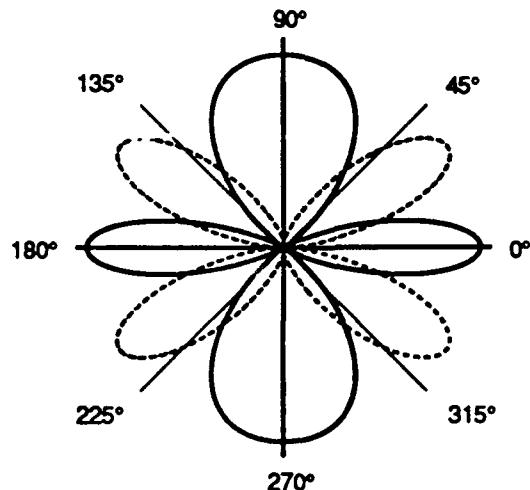
Figure 4.6: The angular distribution of the radiant intensity for fully correlated dipoles (solid line) and partially correlated dipoles (dashed line) and separation constant $k y_0 = 3$. The relative frequency is $\omega/\omega_0 = 1$.
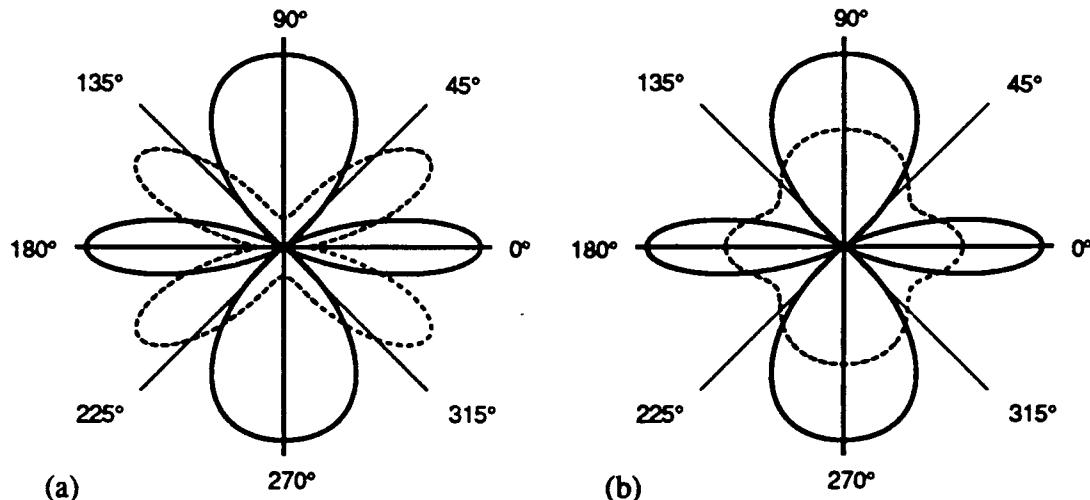
Figure 4.7:   The angular distribution of the radiant intensity for fully correlated dipoles (solid line) and partially correlated dipoles (dashed line) and separation constant $ky_0 = 3$. The relative frequencies are $\omega/\omega_0 = 1.05$ [(a)] and $\omega/\omega_0 = 1.1$ [(b)].

Here the square brackets denote the largest integer which is smaller or equal to the quantity in the brackets.

The two limiting cases of fully correlated and uncorrelated dipoles constitute the limits of possible modification of spectra. In Fig. 4.8 we illustrate the range of modulation that can be achieved at every frequency ω, by the variation of the magnitude of the degree of correlation $\left|\mu_p(\omega)\right|$ and the phase $2\psi(\omega)$. The figure shows four concentric circles, (i) to (iv), representing the relative ranges of the angular distributions of the radiant intensity in the x,y–plane. The external circle (i) corresponds to the limit of fully-correlated dipoles. As one may observe from Eq. (4.20), the radiant intensity of two correlated dipoles may attain any value inside the circle of radius $ck^4 S_p(\omega)/2\pi$. The location of the maximum of the radiant intensity is determined by the choice of the steering angle $2\psi(\omega)$. Similarly it follows from Eq. (4.19) that when the dipoles are uncorrelated, the radiant intensity is constrained to the uniform value on a circle (iii) of radius $ck^4 S_p(\omega)/4\pi$. When the dipoles are partially correlated we see from Eq. (4.17)
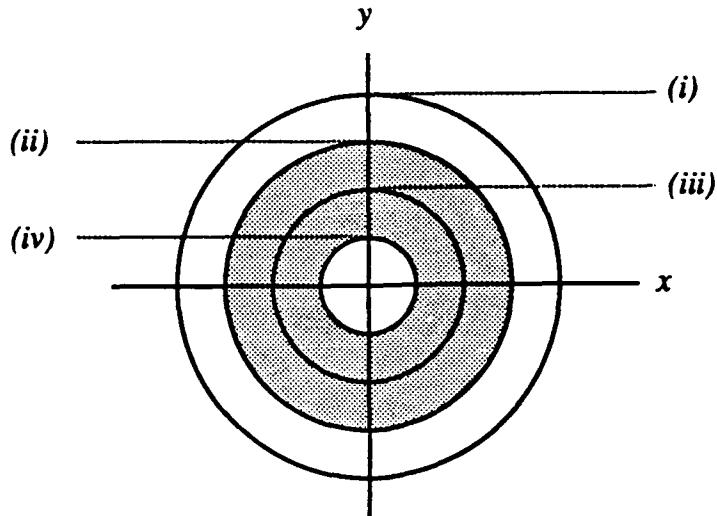
Figure 4.8: The range of possible values of the angular distribution of the radiant intensity. The shaded area indicates the region in which the maxima and minima of the radiant intensity for partially correlated dipoles are found.

that the radiant intensity can have any value in an annular domain bounded by circles (*ii*) and (*iv*). It is also apparent from this representation that unless the two dipoles are fully correlated there are no nulls of the radiant intensity outside the plane $\theta = 0$.

Figure 4.8 gives a symbolic representation of the directivity of the system consisting of two partially correlated linear dipoles. A detailed discussion of the directivity is presented in Sec. 4.5.

4.4 The total emitted power

The total power $P(\omega)$ radiated by the system at frequency ω is given by the expression

$$P(\omega) = \int_{(4\pi)} J(u;\omega) d\Omega, \qquad (4.28)$$

where the integration extends over the whole 4π solid angle. On substituting from Eq. (4.17) in Eq. (4.28) we obtain the expression

$$P(\omega) = \frac{ck^4}{4\pi} S_p(\omega) \int_{(4\pi)} \sin^2 \theta \left\{ 1 + \Re\left[\mu_p(\omega) \exp\left(i2ky_0 \sin\theta \sin\phi\right)\right] \right\} d\Omega. \quad (4.29)$$

After performing the integration in Eq. (4.29) [see Appendix B], we find that

$$P(\omega) = \frac{2}{3} ck^4 S_p(\omega) \left\{ 1 + f(2ky_0) \Re\left[\mu_p(\omega)\right] \right\}, \quad (4.30)$$

where

$$f(z) = \frac{3}{2}\left[j_0(z) - j_1(z)/z \right], \quad (4.31)$$
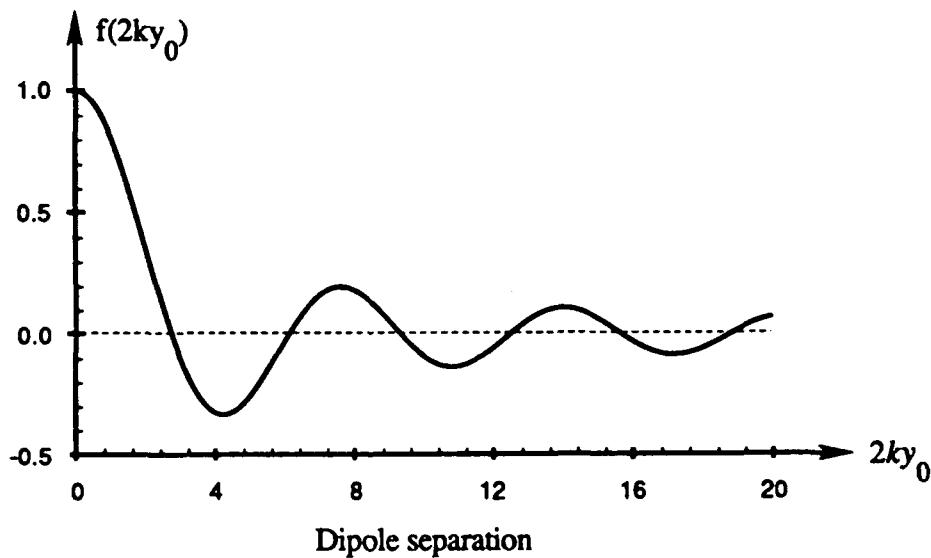
Figure 4.9: The behavior of the function $f(z)$ in Eq. (4.31) as a function of the parameter $z = 2ky_0$.

and $j_0(z)$ and $j_1(z)$ are spherical Bessel functions.

The maximum of the function $f(z)$ can be shown to occur when $z = 0$ where it has the value $f(0) = 1$ (see Fig. 4.9). It follows that the upper bound for the total radiated power is

$$[P(\omega)]_{u.b.} = \frac{4}{3}ck^4 S_p(\omega). \qquad (4.32)$$

In the limiting case when the two dipoles are uncorrelated, the total radiated power is given by

$$[P(\omega)]_{uncorr.} = \frac{2}{3}ck^4 S_p(\omega). \qquad (4.33)$$

On comparing the total power of two partially correlated dipoles $P(\omega)$, and uncorrelated dipoles $[P(\omega)]_{uncorr.}$ we see from Eqs. (4.30) and (4.33) that the ratio between the power emitted by two partially correlated dipoles and two uncorrelated dipoles is given by

$$\frac{P(\omega)}{[P(\omega)]_{uncorr.}} = 1 + f(2ky_0)\Re[\mu_p(\omega)]. \qquad (4.34)$$

Since the function $f(z)$ in Eq. (4.30) decreases rapidly with increasing z, it is evident that the total power emitted by two dipoles that are separated by a distance that is much larger than a wavelength, is equal to the total radiated power from two uncorrelated sources. In other words, when the separation between the two dipoles is large

compared to the wavelength of the radiation, no correlation effects could be deduced from measurements of the total emitted power.

4.5   The directivity of two partially correlated dipoles

The directivity $D(u; \omega)$ of a radiating system is defined by the ratio[5]

$$D(u; \omega) = 4\pi J(u; \omega)/P(\omega), \qquad (4.34)$$

where u is the direction of observation. We are particularly interested in the maximum directivity $D(\omega) \equiv D(u_m; \omega)$ that occurs in a particular direction u_m. It follows from Eqs. (4.23) and (4.30) that the directivity of the two partially correlated dipoles is given by

$$D(\omega) = \frac{3}{2} \frac{1 + |\mu_p(\omega)|}{1 + f(2ky_0)\Re[\mu_p(\omega)]}. \qquad (4.35)$$

When the two dipoles are uncorrelated, $|\mu_p(\omega)| = 0$ and the directivity reduces to the value $D(\omega) = 3/2$, as expected. Similarly, when the dipoles are fully-correlated the directivity is given by

$$D(\omega) = \frac{3}{1 + f(2ky_0)\cos[2\psi(\omega)]}, \qquad (4.36)$$

where $2\psi(\omega)$ denotes again the phase of $\mu_p(\omega)$.

Equations (4.35) and (4.36) also indicate that when the two dipoles are separated by a distance that is much larger than a wavelength, the directivity of partially correlated dipoles approaches the value

$$\lim_{k y_0 \to \infty} D(\omega) = 3\left[1 + \left|\mu_p(\omega)\right|\right]/2, \qquad (4.37)$$

while the directivity of fully correlated dipoles approaches the value

$$\lim_{k y_0 \to \infty} [D(\omega)]_{uncorr.} = 3. \qquad (4.38)$$

We also note that if we use Eq. (4.16) in Eq. (4.35) and differentiate with respect to the magnitude of the degree of correlation $m = \left|\mu_p(\omega)\right|$, we find that

$$\frac{dD(\omega)}{dm} = \frac{3\{1 + f(2k y_0)\cos[2\psi(\omega)]\}}{2[1 + mf(2k y_0)\cos[2\psi(\omega)]]^2} > 0, \qquad (4.38)$$

which implies that for a fixed value of the quantities $f(2k y_0)\cos[2\psi(\omega)]$, the directivity is an increasing function of the magnitude of the degree of correlation. As a result it is clear that the maximum directivity is obtained for fully correlated sources.

4.6   Summary

In this chapter we considered the effect of spatial correlations on the spectrum of the field produced by partially correlated linear dipoles. We showed the changes in the

angular distribution of the radiant intensity and the changes in the spectrum in a fixed direction as a function of correlation of the dipoles polarization.

In examining the total emitted power and the directivity of the system we showed that the maximum radiated power and the maximum directivity are obtained when the dipoles are fully correlated.

References

[1]   a.   J.D. Jackson, *Classical Electrodynamics*, (John Wiley & Sons, 1975), Sec. 9.2.

       b.   Y.S. Shifrin, "Statistical Antenna Theory", Trans. P. Beckmann (The Golem Press 1971).

[2]   We assume that the Fourier transform in Eq. (4.3) exists. See footnote 24 of chapter 1.

[3]   In the case of coherent radiation the quantity $2\psi(\omega)$ is effectively the steering angle. See, for example, R.A. Monzingo and T.W. Miller, *Introduction to Adaptive Arrays* (J. Wiley, New York, 1980) p. 43.

[4]   S.A. Schelkunoff, Bell Sys. Tech. J. **22**, (1943) 80.

[5]   The directivity is defined in the space-frequency domain. This definition is consistent with that used in antenna theory for the harmonic time dependent case: see, for example,

a.   C.H. Papas, *Theory of Electromagnetic Wave Propagation*,(McGraw-Hill, New York, 1965), p. 73.

b.   B. D. Steinberg, *Principles of Aperture and Array System Design*, (J. Wiley, New York, 1976) Chap 6.

Appendix B: Evaluation of the integral in Eq. (4.29) for the total emitted power

We begin with Eq. (4.29), viz.,

$$P(\omega) = \frac{ck^4}{4\pi} S_p(\omega)[I_1 + I_2],$$

(B 1)

where

$$I_1 = \int_{(4\pi)} \sin^2\theta \, d\Omega,$$

(B 2)

$$I_2 = \int_{(4\pi)} \sin^2\theta \, \Re\left[\mu_p(\omega)\exp\left(i2ky_0\sin\theta\sin\phi\right)\right]d\Omega.$$

(B 3)

The value of the first integral is readily found:

$$I_1 = \int_0^{2\pi} d\phi \int_0^{\pi} (1-\cos^2\theta)\sin\theta \, d\theta$$

$$= 2\pi \int_{-1}^{1} (1-x^2)\,dx = \frac{8\pi}{3}.$$

(B 4)

The second integral is given by

$$I_2 = \int_0^{2\pi} d\phi \int_0^{\pi} \sin^3\theta \exp\left(i2ky_0\sin\theta\sin\phi\right)d\theta \, d\phi.$$

(B 5)

In evaluating the second term we first perform the integral[1] over ϕ, giving

$$I_2 = 4\pi \int_0^{\pi/2} \sin^3 \theta \, J_0(2ky_0 \sin \theta) \, d\theta. \tag{B 6}$$

Using the identity

$$\sin^3 \theta = \sin \theta - \sin \theta \cos^2 \theta, \tag{B 7}$$

Eq. (B 6) can be expressed as a sum of two integrals

$$I_2 = 4\pi \int_0^{\pi/2} \sin \theta \, J_0(2ky_0 \sin \theta) \, d\theta + 4\pi \int_0^{\pi/2} \sin \theta \cos^2 \theta \, J_0 2ky_0 \sin \theta) \, d\theta. \tag{B 8}$$

The first integral in Eq. (B 8) has the value[2]

$$4\pi \int_0^{\pi/2} \sin \theta \, J_0(2ky_0 \sin \theta) \, d\theta = 4\pi \, j_0(2ky_0), \tag{B 9}$$

and the second integral in Eq. (B 8) has the value

$$4\pi \int_0^{\pi/2} \sin \theta \cos^2 \theta \, J_0 2ky_0 \sin \theta) \, d\theta = 4\pi \frac{j_1(2ky_0)}{2ky_0}. \tag{B 10}$$

Using Eqs. (B 4), (B 9) and (B 10) in Eq. (B 1) we obtain the following expression for the total emitted power

$$P(\omega) = \frac{2}{3} c k^4 S_p(\omega) \left\{ 1 + f(2ky_0) \Re \left[\mu_p(\omega) \right] \right\}, \qquad \text{(B 11)}$$

where

$$f(z) = \frac{3}{2} \left[j_0(z) - j_1(z)/z \right], \qquad \text{(B 12)}$$

and $j_0(z)$ and $j_1(z)$ are spherical Bessel functions.

---

[1]   I.S. Gradshteyn and I.M. Ryzhik, *Tables of Integrals, series and products*, (Academic Press, New York, 1980) p. 401, #10.

[2]   Ibid, p. 740 #5 and p. 982 #4.

5

Spectral effects in coherent mode representation

Introduction

The theory presented in the previous chapters used model sources for the representation of the cross-spectral density, characterized by a spectral density function and a spatial correlation function. In this chapter we investigate spectral effects which are produced by source correlations using coherent mode representation[1]. This approach emphasizes the role of spatial correlations in generating spectral changes on propagation of partially coherent light, and it clarifies the distinction between diffraction and correlation effects.

We will consider the class of statistically stationary, secondary, partially coherent, planar sources, whose cross-spectral density function consist of a finite sum of Hermite-Gaussian modes. We evaluate the spectral changes which occur on propagation by decomposing the source into its coherent modes and evaluating the contribution of each mode to the observed spectrum. We determine the field spectra for observation points both in the far and in the near zone. A comparison of the calculations shows that, at least in the cases considered in this chapter, most of the spectral changes seen in the far zone are already present in the spectrum that would be observed at very short distances from the source plane. A detailed discussion of the development of spectral changes with propagation distance from the source plane is given in Chapter 6.

Since we are considering sources consisting of Hermite-Gaussian modes and because such modes also represent the transverse modes of certain laser cavities[2], our analysis provides an indication of the type of spectral effects might be expected to arise in fields produced by some multi-mode lasers.

5.2   Coherent-mode representation of partially coherent sources and fields

The cross-spectral density function of a statistically stationary, planar, secondary source of any state of coherence, occupying a finite domain D may be expressed as a sum of coherent modes viz.[3],

$$W^{(0)}(r_1, r_2; \omega) = \sum_{n,m} \lambda_{n,m}(\omega) \chi^*_{n,m}(r_1; \omega) \chi_{n,m}(r_2; \omega). \tag{5.1}$$

Here r_1 and r_2 are position vectors of points in the source domain D, $\lambda_{n,m}(\omega)$ are the eigenvalues and $\chi_{n,m}(r, \omega)$ are the eigenfunctions of the Fredholm integral equation

$$\int_D W^{(0)}(r_1, r_2; \omega) \chi_{n,m}(r_1; \omega) d^2r_1 = \lambda_{n,m}(\omega) \chi_{n,m}(r_2; \omega). \tag{5.2}$$

Here the eigenvalues

$$\lambda_{n,m}(\omega) \geq 0 \qquad (all\ n, m). \tag{5.3}$$

The eigenfunctions (modes) $\{\chi_{n,m}(r; \omega)\}$ of the source are taken to be orthonormal, i.e.,

$$\int_D \chi^*_{i,j}(t; \omega) \chi_{k,l}(r; \omega) d^2r = \delta_{ik} \delta_{jl}, \tag{5.4}$$

where δ is the Kronecker symbol.

The spectrum of the field at a typical observation point r is given by

$$S(r;\omega) = \sum_{n,m} \lambda_{n,m}(\omega) \left| \psi_{n,m}(r;\omega) \right|^2, \tag{5.5}$$

where $\psi_{n,m}(r;\omega)$ is given by

$$\psi_{n,m}(r;\omega) = \int_D \chi_{n,m}(r';\omega) G(r,r';\omega) d^2r', \tag{5.6}$$

and $G(r, r';\omega)$ is the Green's function, which characterizes propagation from the source point r' to the field point r.

It is evident from Eq. (5.5) that each term[4] contributes to the total spectrum independently of all the others, i.e. there are no cross-terms. Moreover, since each term under the summation is necessarily non-negative, the strength of the resulting spectrum at an arbitrary frequency cannot be smaller than the strength of the weakest one at that frequency.

The coherence properties of the source are manifested by the distribution of the eigenvalues $\{\lambda_{n,m}(\omega)\}$. In the case of a one-dimensional Gaussian Schell-model source, for example[5],

$$\frac{\lambda_n}{\lambda_0} = \left\{ \beta^2/2 + 1 + \beta\left[(\beta/2)^2 + 1\right]^{1/2} \right\}^{-n}, \tag{5.7}$$

where β is a relative correlation length

$$\beta = \frac{\sigma_\mu(\omega)}{\sigma_I(\omega)}. \tag{5.8}$$

Here $\sigma_I(\omega)$ is the r.m.s. width of the intensity distribution and $\sigma_\mu(\omega)$ is the r.m.s. correlation length of the field distribution in the source plane.

In this chapter we only consider sources which contain a finite number of modes, N. Let us choose a source with eigenvalues whose frequency-dependence is of the form

$$\lambda_{n,m}(\omega) = s^{(0)}(\omega)\Lambda_{n,m}. \tag{5.9}$$

Here $s^{(0)}(\omega)$ is proportional to the source spectrum $S(x, y, z = 0;\omega)$, and the Λ_n are constants. Explicitly,

$$s^{(0)}(\omega) = \int_D S(x,y;\omega)\,dx\,dy \Big/ \sum_{n,m} \Lambda_{n,m}. \tag{5.10}$$

We also choose the modes to be independent of the frequency ω, i.e.,

$$\chi_{n,m}(r;\omega) \equiv \chi_{n,m}(r). \tag{5.11}$$

Since the domain D lies in a plane it is convenient to consider modes that are separable in the two Cartesian directions, say x and y, i.e. modes of the form

$$\chi_{n,m}(x,y) = \phi_n(x)\phi_m(y). \tag{5.12}$$

For the functional form of the modes we choose for n = 0, 1, 2...

$$\phi_n(x) = \left(\frac{2d_x}{\pi}\right)^{1/4} \frac{1}{\sqrt{2^n n!}} H_n\left(x\sqrt{2d_x}\right)\exp\left(-d_x x^2\right), \tag{5.13}$$

where H_n is the Hermite polynomial of order n and d_x is a constant that determines the spatial distribution of the mode in the x-direction [cf. Ref. 5, Eq. (2.13)]. We use a strictly analogous expression for $\phi_m(y)$.

The choice of frequency-independent modes isolates the frequency dependent factors in the expression for the cross-spectral density of the field in the source plane; consequently, for an arbitrary source spectrum $s^{(0)}(\omega)$ we may analyze the effect of the distribution of the constants $\{A_n\}$ on the resulting field spectrum. This is equivalent to examining the effects of spatial correlations of the source fluctuations on the spectrum of the field that the source produces.

If the source spectrum and the field spectrum each consist of a single line centered at frequencies ω_0 and ω'_0 respectively, one may characterize the spectral change occurring on propagation by the parameter

$$Z = \frac{\omega'_0 - \omega_0}{\omega'_0} . \tag{5.14}$$

However, even when the source spectrum consists of a simple line such as a Lorentzian or a Gaussian, the resulting field spectrum is, in general, a distorted line. A comparison between the spectral lines may then be made on the basis of peak frequencies or the centroids of the line. In the following sections we choose the later approach for calculating the new center frequency ω', i.e., we define ω' by the formula

$$\omega' = \frac{\int \omega S^{(\infty)}(\omega)\, d\omega}{\int S^{(\infty)}(\omega)\, d\omega} . \tag{5.15}$$

5.3   Far-zone spectra

The far-zone field $\psi_{n,m}$ of a typical source mode $\chi_{n,m}$ can be obtained by substituting Eq. (5.12) into Eq. (5.6) and using the asymptotic form of the Green's function. We then obtain

$$\psi_{n,m}(r u;\omega) = \frac{2\pi k \cos\theta}{r} \tilde{\phi}_n(k u_x)\tilde{\phi}_m(k u_y),\qquad(5.17)$$

where θ is the angle between the direction of observation and the normal to the source plane and $\tilde{\phi}_n(f)$ denotes the one-dimensional spatial Fourier transform of the function $\phi_n(x)$,

$$\tilde{\phi}_n(f) = \frac{1}{2\pi}\int_{-\infty}^{\infty}\phi_n(x)e^{-ifx}\,dx.\qquad(5.18)$$

On substituting Eq. (5.13) into Eq.(5.18) and using the identity[6]

$$\int_{-\infty}^{\infty}H_n(x)e^{-x^2/2}\,e^{ixy}\,dx = i^n\sqrt{2\pi}\,H_n(y)e^{-y^2/2},\qquad(5.19)$$

we obtain the following expression for the far field produced by the mode $\chi_{n,m}$:

$$\psi_{n,m}(ru;\omega) = \frac{(-i)^{n+m}k\cos\theta/r}{\sqrt{\pi 2^{n+m}n!m!}}\sqrt{k/\sqrt{2d_x}}\sqrt{k/\sqrt{2d_y}}$$

$$\times H_n\left(\frac{ku_x}{\sqrt{2d_x}}\right)H_m\left(\frac{ku_y}{\sqrt{2d_y}}\right)\exp\left\{-\frac{1}{2}\left[\left(\frac{ku_x}{\sqrt{2d_x}}\right)^2 + \left(\frac{ku_y}{\sqrt{2d_y}}\right)^2\right]\right\}. \qquad (5.20)$$

The far-zone spectrum[7] of the field is now obtained by substituting Eq. (5.9) into Eq. (5.5),

$$S^{(\infty)}(u;\omega) = s^{(0)}(\omega)\sum_{n,m}\Lambda_{n,m}\left|\psi_{n,m}(u;\omega)\right|^2, \qquad (5.21)$$

with $\psi_{n,m}$ given by Eq. (5.20). We may now express the formula (5.21) in the following form, which clearly indicates the various contributions to the far-zone spectrum:

$$S^{(\infty)}(u;\omega) = s^{(0)}(\omega)\frac{\cos^2\theta}{r^2}M(u;d_x;d_y;\omega). \qquad (5.22)$$

Equation (5.22) shows that the far-zone spectrum is a product of the source spectrum, a geometrical factor, and a "spectral modifier" $M(u; d_x, d_y; \omega)$. This factor is given by

$$M(u;d_x;d_y;\omega) = \frac{1}{\pi}\frac{k}{\sqrt{2d_x}}\frac{k}{\sqrt{2d_y}}\exp\left\{-\left[\left(\frac{ku_x}{\sqrt{2d_x}}\right)+\left(\frac{ku_y}{\sqrt{2d_y}}\right)\right]\right\}$$

$$\times\sum_{n,m}\frac{\Lambda_{n,m}}{2^{n+m}n!m!}\left[H_n\left(\frac{ku_x}{\sqrt{2d_x}}\right)H_m\left(\frac{ku_y}{\sqrt{2d_y}}\right)\right]. \qquad (5.23)$$

To examine the effect of the spectral modifier on the spectrum in the far zone, let us consider sources whose spectrum consist of a single spectral line, centered at frequency ω_0. We define the relative frequency α as $\alpha = \omega/\omega_0$, and the characteristic mode lengths $\xi = k_0 / \sqrt{2d_x}$, $\eta = k_0 / \sqrt{2d_y}$. With these definitions Eq. (5.23) may be expressed in the form

$$M(u;d_x,d_y;\omega) = \frac{1}{\pi} \xi\eta\alpha^2 \exp\left\{-\alpha^2\left[\left(\xi u_x\right)^2 + \left(\eta u_y\right)^2\right]\right\}$$

$$\times \sum_{n,m} \frac{\Lambda_{n,m}}{2^{n+m}n!m!}\left[H_n(\xi u_x)H_m(\eta u_y)\right]^2. \tag{5.24}$$

For a fixed direction of observation the spectral modifier M is seen to contain an envelope factor

$$F = \frac{\xi\eta\alpha^2}{\pi} \exp\left\{-\alpha^2\left[\left(\xi u_x\right)^2 + \left(\eta u_y\right)^2\right]\right\} \tag{5.25}$$

and a weighted sum of contributions from the individual modes. As we indicated earlier this sum does not involve any cross-mode terms. It is, therefore, possible to determine the spectral changes directly from the knowledge of the spectral modifiers denoted by $M_{n,m}$, of the individual modes:

$$M_{n,m}(u;d_x,d_y;\omega) = \frac{\Lambda_{n,m}}{\pi 2^{n+m}n!m!}\xi\eta\alpha^2$$

$$\times\left[H_n(\xi u_x)H_m(\eta u_y)\right]^2 \exp\left\{-\alpha^2\left[\left(\xi u_x\right)^2 + \left(\eta u_y\right)^2\right]\right\}. \tag{5.26}$$

To illustrate the behavior of the spectral modifier of individual modes, and its effects on the observed spectra, we consider sources for which there is only one-mode contribution in the y-direction, i.e.,

$$\chi_{n,m}(x,y) = \phi_n(x)\phi_0(y).$$
(5.27)

We also limit our observation points to the plane $y = 0$, where the spectral modifier takes the form

$$M_{n,0}(u_x;\xi,\eta;\alpha) = \frac{\Lambda_{n,0}}{\pi 2^n n!}\xi\eta\alpha^2\left[H_n(\alpha\xi u_x)\right]^2 \exp\left[-(\alpha\xi u_x)^2\right].$$
(5.28)

In Figs. 5.1 and 5.2 we show examples of spectral modifiers of single modes for selected values of the index n and a fixed direction of observation. One can see by inspection that the spectral modifiers of modes specified by n = 4, 6, 9, 11, give rise to blue shifts while the spectral modifiers for modes specified by n = 5, 10, 12, 14 give rise to red shifts.
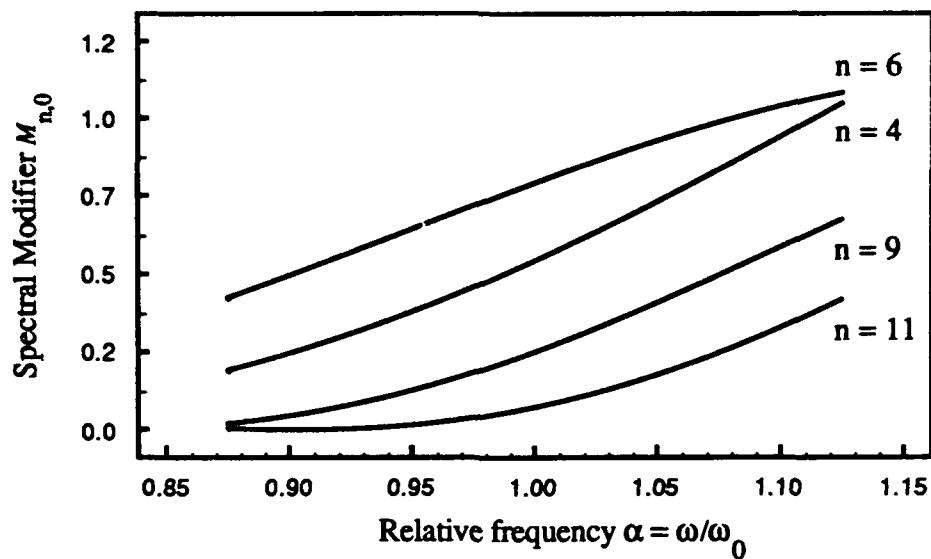
Figure 5.1:   The spectral modifier $M_{n,0}$ for the modes $n = 4, 6, 9, 11$ as a function of the relative frequency α. The positive slope of the curves imply a blueshift on propagation.

In order to determine the type of spectral shift due to an arbitrary mode n_a, we note from Eq. (5.28) that the fine detail in the spectral modifier is due to the square of the Hermite polynomial. The behavior of one such factor is shown in Fig. 5.3. We
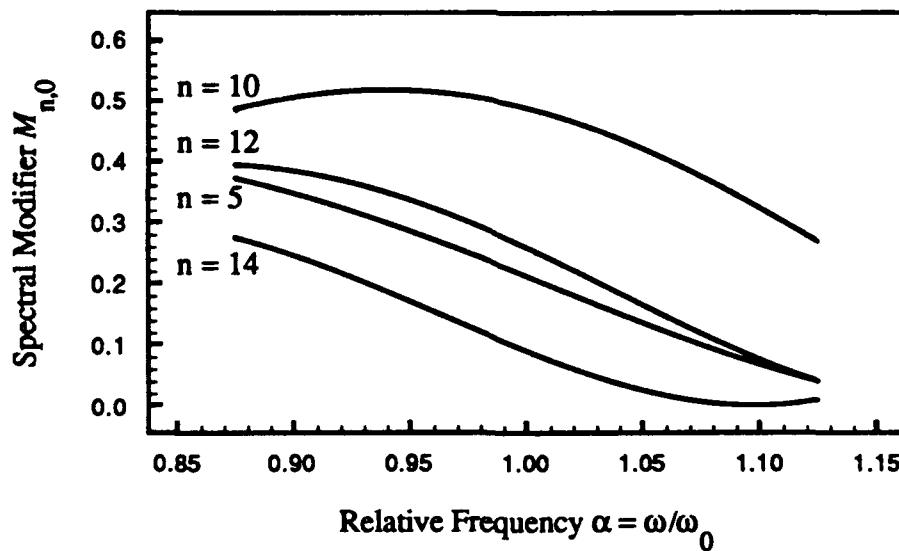
Figure 5.2:   Spectral modifier $M_{n,0}$ for the modes $n = 5, 10, 12, 14$ as a function of the relative frequency α. The negative slopes of the curves imply a redshift on propagation.

Spectral effects in coherent mode representation
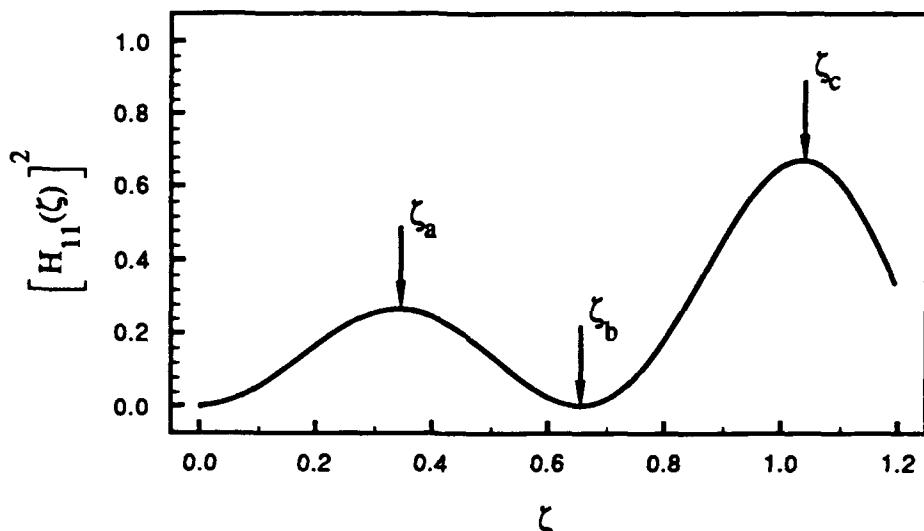
Figure 5.3: An example of the detail in the spectral modifier due to the square of the Hermite polynomial shown here for n = 11. The points ζ_a, ζ_b, ζ_c, denote boundaries of regions giving rise to particular spectral changes.

note that at the center frequency $\alpha = 1$, the behavior of $[H_n(\zeta)]^2$ reflects its dependence on the product ξu_x. When ξu_x lies between the points marked by the symbols ζ_a and ζ_b, this factor produces a red shift, whereas for values of ξu_x between ζ_b and ζ_c it produces a blue shift. When the values of ξu_x correspond to the point ζ_a, the resulting spectral line is narrowed while for values of ξu_x corresponding to the point ζ_b, it is broadened. It is clear from the example shown in Figs. 5.3 that the type of spectral effect observed for a fixed value of ξu_x is determined by the value of ξu_x compared with the nearest zero of the Hermite polynomial. Specifically, let $\zeta_1 < \zeta_2$ be two consecutive zeros of the Hermite polynomial, and let ζ_m be the value at which $[H_n(\zeta)]^2$ attains its maximum value in the interval (ζ_1 , ζ_2); evidently, $\zeta_1 < \zeta_m < \zeta_2$. With these definitions we have

Blue shift	$\zeta_1 < \xi u_x < \zeta_m$
Red shift	$\zeta_m < \xi u_x < \zeta_2$
Line splitting	$\xi u_x = \zeta_2$

Table 5.1: The dependence of spectral changes on ξu_x.

Spectral effects in coherent mode representation
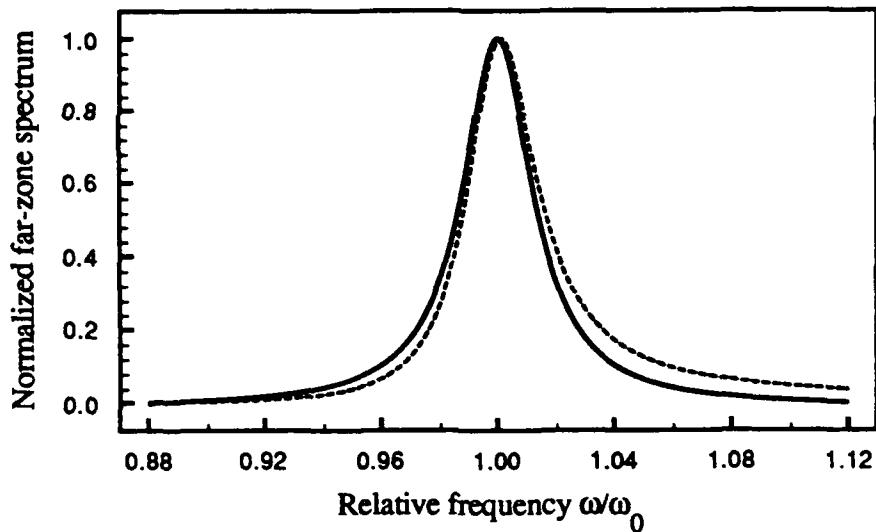
Figure 5.4: Normalized far-zone spectra for the mode n = 7, with $\xi u_x = 1.0$, resulting in a blue-shifted line with $Z = -0.011$.

Examples of the three cases are shown in Figs. 5.4-5.6. The source spectrum in these examples was taken to be a Lorentzian line,
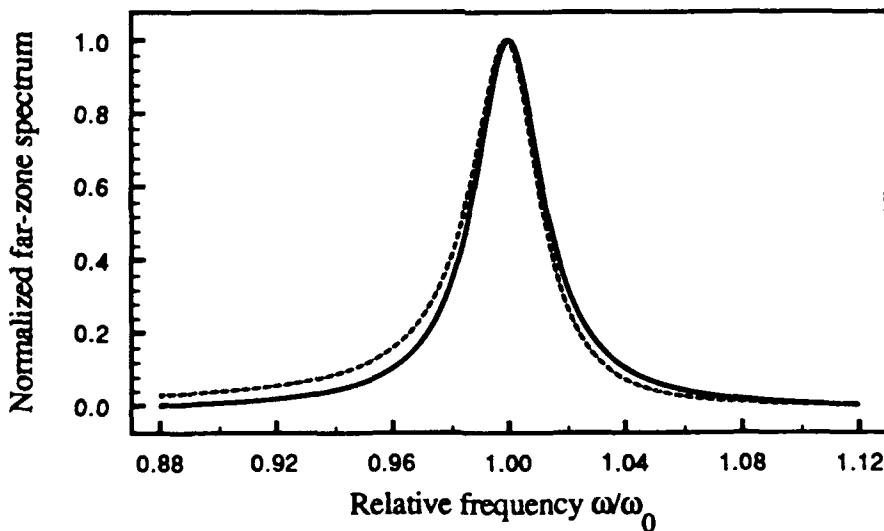
Figure 5.5: Normalized far-zone spectra for the mode n = 7, with $\xi u_x = 0.7$, resulting in a red-shifted line with $Z = 0.0093$.

Spectral effects in coherent mode representation
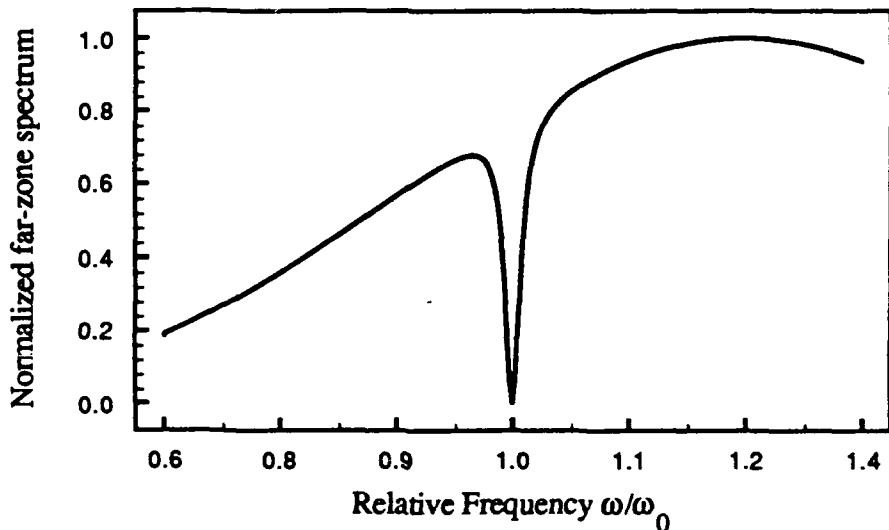
Figure 5.6:   Normalized far-zone spectra for the mode n = 7, with ξu_x = 0.816 corresponding to a zero of the Hermite polynomial. Line splitting is evident as a result of taking ξu_x close to the zero of H_7.

$$s^{(0)}(\alpha;\delta) = 1/\left[1 + (\alpha - 1)^2/\delta^2\right],$$ (5.29)

with δ = 0.06.

5.4   The dependence of field spectra on the relative mode strengths

The spectral changes which occur for a single coherent mode is a consequence of wave propagation. Such effects must be distinguished from the spectral changes due to source correlations. When the source is spatially fully coherent it consists of a single coherent mode. The spectral effects which then arise on propagation were described in the previous section. However, when the source is partially coherent, several modes are present and the resulting field spectrum then also depends on the relative strength of the modes or, equivalently, on the distribution of the constants $\{\Lambda_{n,m}\}$.
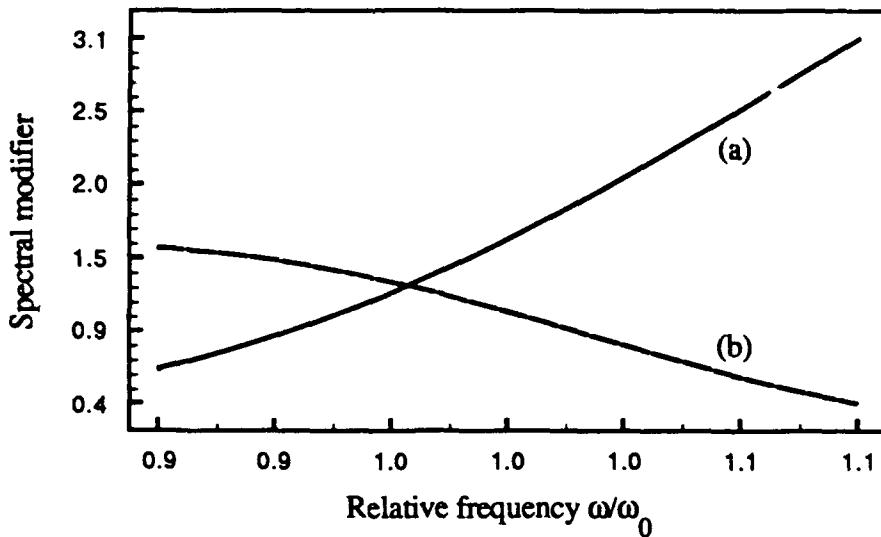
Figure 5.7: Spectral modifiers for sources characterized by the spectral modifiers $M = M_{4,0} + M_{6,0} + M_{9,0} + M_{11,0}$ (a), and $M = M_{5,0} + M_{10,0} + M_{12,0} + M_{14,0}$ (b).

Let us first consider a source consisting of two coherent modes (n_1, m_1) and (n_2, m_2). It follows from Eqs. (5.22) and (5.26) that the spectral modifier for this source is just the sum of the spectral modifiers of the two modes, i.e.,

$$M(u; \xi, \eta; \alpha) = M_{n_1, m_1}(u; \xi, \eta; \alpha) + M_{n_2, m_2}(u; \xi, \eta; \alpha). \qquad (5.30)$$

In terms of the cross-spectral density Eq. (5.1), the degree of correlation of the source fluctuations is given by

$$\mu(r_1, r_2; \omega) = \frac{W^{(0)}(r_1, r_2; \omega)}{\sqrt{W^{(0)}(r_1, r_1; \omega)} \sqrt{W^{(0)}(r_2, r_2; \omega)}}. \qquad (5.31)$$

Spectral effects in coherent mode representation

In Fig. 5.7 we show examples of spectral modifiers for sources consisting of

four modes. The degree of correlation $\mu(r_1, r_2; \omega)$ for the corresponding sources is

shown in Figs. 5.8 and 5.9 for points along the x-axis, with $r_1 = (0, 0)$ and
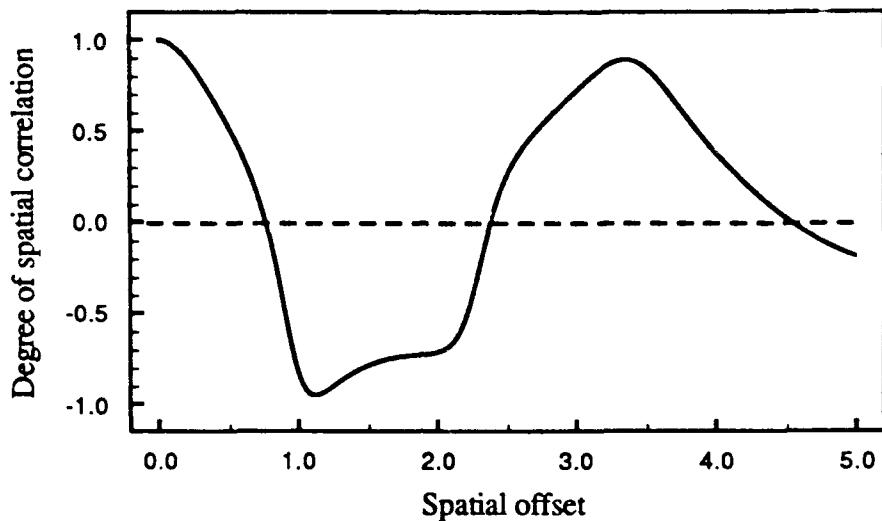
Fig. 5.8:   Degree of spatial correlation $\mu(0, \delta x)$ of the two sources shown in Fig. 5.7 (a),
where the spatial offset is $\delta x = x\sqrt{2d_x}$.
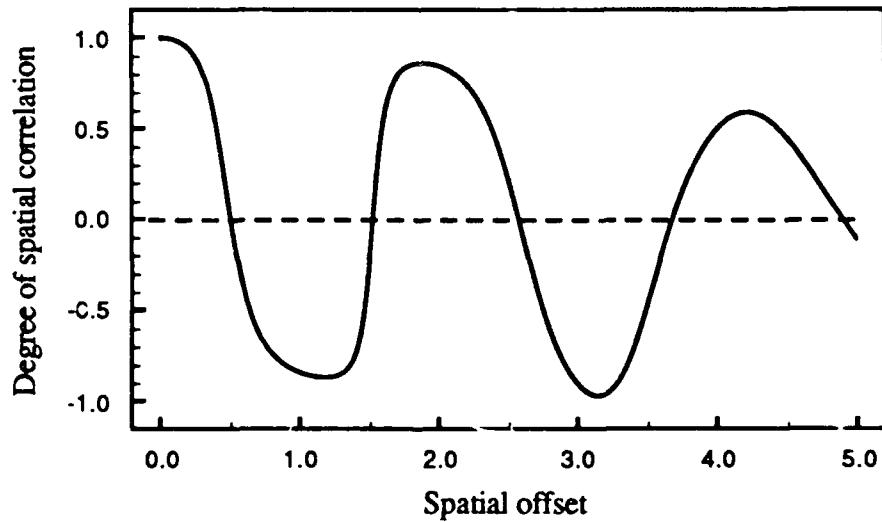
Fig. 5.9:   Degree of spatial correlation $\mu(0, \delta x)$ of the two sources shown in Fig. 5.7 (b),
where the spatial offset is $\delta x = x\sqrt{2d_x}$.
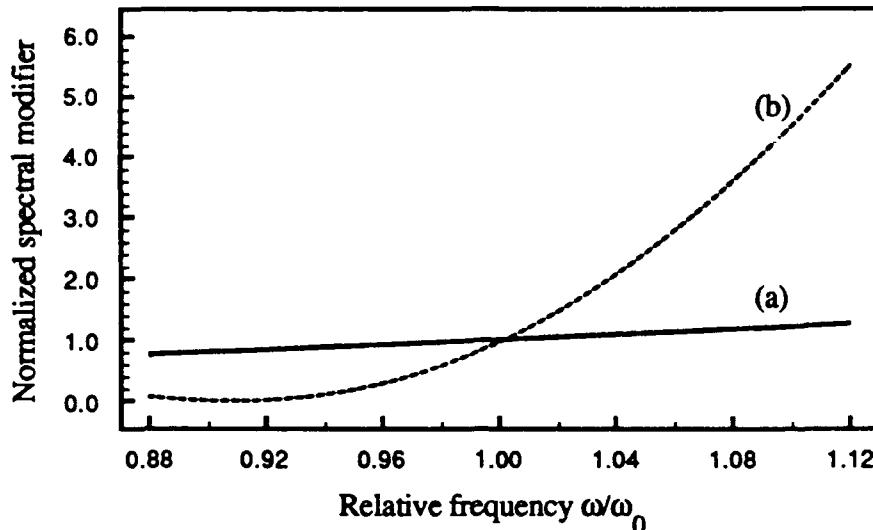
Figure 5.10: Comparison of the spectral modifiers for a source consisting of modes 0-30 (a) and a source consisting of the single mode [n = 9, m = 0] (b). The normalization ensures that both modifiers have the same magnitude at the center frequency.

$r_2 = (x, 0)$. In some cases the degree of correlation may approach a constant value with increasing separation between the two source points. This result is well known for Gaussian Schell-model beams[8].

When the source consists of many modes taken with equal weights, it is equivalent to a spatially incoherent source [cf. ref. 5]. Figure 5.10 shows the spectral modifier for a source consisting of modes n = 0 through n = 30. For comparison we also show the spectral modifier for a source consisting of the single mode n = 9. It can be seen from this figure that when the source consists of many modes, the spectral modifier is relatively constant and consequently the far-zone spectrum produced by this source cannot differ appreciably from the source spectrum.

5.5 Spectral changes in the near zone

The spectrum of the field throughout the half-space $z > 0$ may be evaluated by using the angular spectrum representation for each one of the modes, i.e.,

$$\psi_{n,m}(r;\omega) = \int\limits_{-\infty}^{\infty}\!\!\int A_{n,m}(p,q;\omega)e^{ik(px+qy+mz)}\,dp\,dq. \tag{5.32}$$

In Eq. (5.32) $r = (x, y, z > 0)$,

$$A_{n,m}(p,q;\omega) = \left(\frac{k}{2\pi}\right)^2 \int\limits_{D} \chi_{n,m}(x,y,z=0)e^{-ik(px+qy)}\,dx\,dy, \tag{5.33}$$

and

$$m = \begin{cases} \sqrt{1-p^2-q^2} & \text{when} \quad p^2+q^2<1 \quad (a) \\[3mm] i\sqrt{p^2+q^2-1} & \text{when} \quad p^2+q^2\geq 1. \quad (b) \end{cases} \tag{5.34}$$

It can be shown by numerical evaluation that when $kz > 100$ one may neglect, to a good approximation, the contributions from evanescent waves, i.e. waves for which $p^2 + q^2 > 1$. The infinite domain of integration in Eq. (5.32) can then be replaced by the finite domain $p^2 + q^2 \leq 1$.

To simplify the calculation we consider the source modes given by Eq.(5.12) in Eq. (5.33). The integration over the domain D may be carried out in closed form by extending the domain of integration over the whole x,y-plane and using the identity (5.19). One then finds that

$$A_{n,m}(p,q;\omega) = \frac{k^2}{2\pi}\left(\frac{4d_x d_y}{\pi^2}\right)^{1/4}\frac{(i)^n}{\sqrt{2^n n!}}$$

$$\times H_n\left(\frac{kp}{\sqrt{2d_x}}\right)\exp\left\{-\frac{1}{2}\left[\left(\frac{kp}{\sqrt{2d_x}}\right)^2 + \left(\frac{kq}{\sqrt{2d_y}}\right)^2\right]\right\} . \tag{5.35}$$

The fields $\psi_{n,m}(r;\omega)$ are obtained by substituting from Eq. (5.35) in Eq. (5.32) and letting $d_x = d_y = d$. The result is:

$$\psi_{n,m}(x,y,z;\omega) = \left(\frac{k}{2\pi}\right)^2\sqrt{\frac{2\pi}{d}}\frac{i^n}{\sqrt{2^n n!}}$$

$$\times \iint\limits_{p^2+q^2\leq 1} e^{-k^2(p^2+q^2)/4d} H_n\left(\frac{kp}{\sqrt{2d}}\right)e^{ik(px+qy+mz)}\,dp\,dq . \tag{5.36}$$

The integral (5.36) has been evaluated by many authors within the accuracy of the paraxial approximation[9]. It has also been evaluated under more general conditions or by making use of cylindrical symmetry[10] Because we are interested in observation points that may lie outside the paraxial region, we evaluated the integrals (5.5) numerically for selected values of the mode index n.

In Table 5.2 we compare the relative frequency shifts calculated for the near zone and for the far zone.

Mode	Near zone center frequency	Near zone Z-shift	Far zone center frequency	Far zone Z-shift	$\left\| Z_{f.z.} - Z_{n.z.} \right\|$
5, 0	0.992737	-0.007316	0.992654	-0.007399	0.000083
9, 0	1.020491	0.020079	1.021117	0.020681	0.000602
11, 0	1.011317	0.01119	1.011482	0.011352	0.000162
12, 0	0.993354	-0.00669	0.993168	-0.006879	0.000189
13, 0	1.007263	0.007211	1.007341	0.007288	0.000077
14, 0	0.985337	-0.014881	0.9845217	-0.015722	0.000841
15, 0	1.004433	0.004414	1.0044527	0.004433	0.000019

Table 5.2: The Z-numbers (relative frequency shifts) for observation points in the far and in the near zone, for selected modes.

The rightmost column in Table 5.2 indicates that, at least for the modes considered here, most of the spectral shift is already present for observation points in the near zone. This observation is confirmed in Chapter 6.

5.6   Summary

In this chapter we employed the coherent-mode representation to analyze the changes in the spectrum of light which is generated by a class of secondary, partially coherent, planar, secondary sources. Our treatment isolated the spectral effects due to the individual modes and has demonstrated that even coherent fields exhibit a non-negligible spectral shifts for some directions of observation. These may have to be taken into account in various applications, for example, in determining the speed of moving objects from reflected light on the basis of spectral line shifts.

The effect of the state of coherence of the source on the observed field spectra was examined by varying the eigenvalues $\Lambda_{n,m}$. We found that when the source consists of many coherent modes with the same eigenvalues (corresponding to the incoherent limit), the spectrum of the field does not differ appreciably from that of the source.

The changes in the spectrum of the field on propagation from the immediate neighborhood of the source plane to the far zone were studied by calculations of the spectrum for distance $kz = 100$ and for $kz \rightarrow \infty$. We found that in the case we studied, the spectrum close to the source ($kz = 100$) already possesses most of the features that are present in the spectrum of the field in the far zone.

The evaluation of the near zone spectrum in Sec. 5.5 is computationally intensive. In Chapter 6 we use the paraxial approximation to perform this calculation. The paraxial approximation significantly reduces the difficulty involved in the computation which gives a genuine insight into the development of spectral changes with propagation distance.

References

1   a.   E. Wolf, "New theory of partial coherence in space-frequency domain. Part I: spectra and cross spectra of steady-state sources", J. Opt. Soc. Amer. 72, (1982) 343.

        b.   "Part II: Steady-state fields and higher-order correlations", ibid. A 3, (1986) 76.

2   a.   G.D. Boyd and J.P. Gordon, "Confocal Multimode resonator for Millimeter Through Optical Wavelength Masers", Bell Sys. Tech. J. 40 (1961) 489-508.

        b.   G. S. Agarwal and E. Wolf, "Coherence Theory of Laser Resonator Modes", J. Opt. Soc. Amer. A 1, 541-546 (1984).

3   See the relevant discussion in Chapter 1.

4   In general, the field ψ is not an eigenfunction of the cross-spectral density of the field at the observation point. It is worth mentioning that in the special case that the source consists of Hermite-Gaussian modes, so does the far-zone cross-spectral density of the field.

5   A. Starikov and E. Wolf, "Coherent-mode representation of Gaussian Schell-model sources and of their radiation fields", J. Opt. Soc. Amer., 72, (1982) 923.

6   E.C. Titchmarsh, Introduction to the theory of Fourier integrals, (Chelsea, New York 1986), p 81.

7   Here we refer to the radiant intensity as the far-zone spectrum. The two quantities differ only by a factor of $1/r^2$ which is irrelevant to the present discussion.

[8]   A.T. Friberg and R.J. Sudol, "The spatial coherence properties of gaussian Schell-model beams", Opt. Acta, 30, (1983) 1075-1097.

[9]   See, for example, F. Gori, "Collett-Wolf sources and multimode lasers", Opt Commun. 34, (1980) 301.

[10]   See, for example, G.P. Agrawal and D.N. Pattanayak, "Gaussian beam propagation beyond the paraxial approximation", J. Opt. Soc. Amer, 69, (1979) 575.

6

Spectral changes on propagation of partially coherent light in media

6.1 Introduction

The work described in the previous chapters has focused on light propagation in free space or in a rarefied scattering medium. In this chapter we examine the changes in the spectrum of the field occurring on propagation through homogeneous and inhomogeneous dispersive media. In particular, we investigate the development of the spectrum as a function of the propagation distance and its dependence on the state of coherence of the source in both homogeneous and inhomogeneous media. The inhomogeneous medium considered here is a graded-index medium whose refractive index varies quadratically in the radial direction[1]. Such a medium is readily available for experiments in the form of so-called Selfoc fibers.

The changes in the coherence properties of light propagating through various types of waveguides have been investigated by many authors[2]. In most of the work encountered in the literature, the state of coherence is characterized by the mutual coherence function. As we explained in Chapter 1, this approach is not very suitable for the examination of spectral changes. Agrawal *et al.* [Ref. 2 (a)] considered how the cross-spectral density of the incident light changes on propagation in such multimode fibers. We use the analysis of that reference to derive a closed-form expression for the spectrum of the field at an arbitrary distance from the source.

The general expression derived for a graded-index medium can be used to analyze the spectral changes occurring in a dispersive homogeneous medium in the appropriate limit. The later result reduces to the well known free-space result[3] in the limit in which the refractive index is unity. Our expression is, however, valid for arbitrary propagation distances and allows us to examine how the spectrum evolves from the near-field to the far-field region. We illustrate our results by using physical parameters that apply in many practical configurations. In particular, we show how the

spectrum of light can be shifted toward the shorter or the longer wavelength, depending on the propagation distance and the state of coherence of the source. Our results indicate that the spectral shift occurring in the far-zone region is considerably enhanced in a homogeneous medium, with the enhancement factor depending on the index of refraction of the medium.

We examine the evolution of spectral shifts from the near to the far zone by deriving an alternative expression for the field spectrum that is valid, within the paraxial approximation, for an arbitrary propagation distance in free space. We use this expression to obtain the spectral shift for optical fields generated by a Gaussian Schell-model source, and to study how the shift changes during transition from the near to the far zone.

6.2 Propagation of the spectrum in graded index fibers

In this section we derive expressions for the propagation of the cross-spectral density of the field in graded-index fibers. We establish the notation and derive an expression for the field spectrum.

Consider a graded-index fiber with the axis of symmetry along the z-direction (see Fig. 6.1). The fiber is characterized by an index of refraction having the parabolic profile

$$n^2(x, y; \omega) = \begin{cases} n_0^2(\omega)\left[1 - \alpha^2(\omega)\left(x^2 + y^2\right)\right] & for \quad x^2 + y^2 \leq R_0^2 \quad (a) \\ n_0^2(\omega)\left[1 - \alpha^2(\omega)R_0^2\right] & for \quad x^2 + y^2 > R_0^2, \quad (b) \end{cases} \quad (6.1)$$
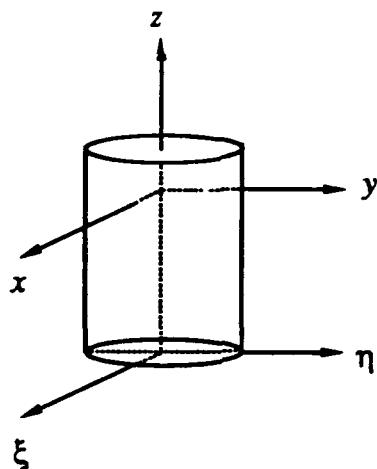
Figure 6.1: Illustrating the geometry and the notation.A point in the source plane $z = 0$ is denoted by (ξ, η) and an observation point is denoted by (x, y, z).

where R_0 is the core radius, n_0 is the index of refraction at the center of the fiber, α is the radial gradient of the index, and $\omega = kc$ (c = vacuum speed of light) is the frequency associated with the free-space wavenumber k.

To obtain an expression for field propagation in this medium[4] we first make the assumption that Eq. (6.1a) is valid for all x and y. It follows that the differential equation governing the propagation of a field V in this fiber is in the form

$$\left\{ \nabla^2 + k_0^2 \left[1 - \alpha^2 \left(x^2 + y^2 \right) \right] \right\} V(x,y,z) = 0 . \tag{6.2}$$
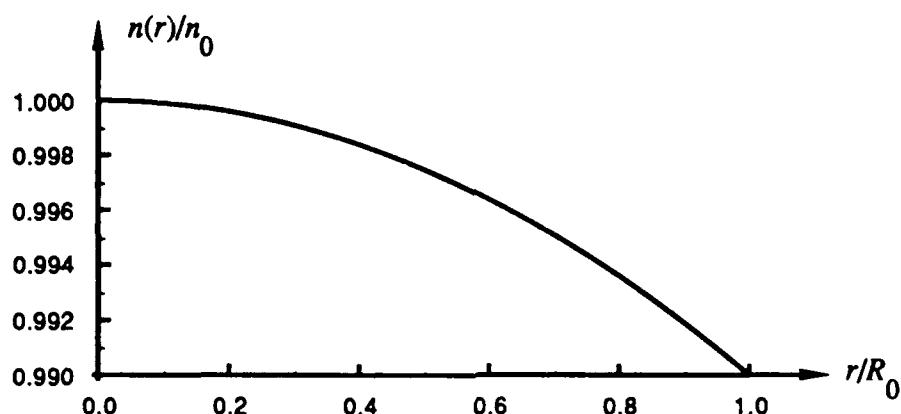
Figure 6.2: The parabolic index profile of Eq. (6.1) with $\alpha = 0.1$.

Spectral changes on propagation of partially coherent light in media

Its solution can be expressed as an infinite series of Hermite Gaussian functions[5]

$$V(x,y,z) = \sum_{n,m=0}^{\infty} a_{n,m} H_n\left(\frac{\sqrt{2}x}{w_0}\right) H_m\left(\frac{\sqrt{2}y}{w_0}\right) \exp\left(i\beta_{n,m}z\right), \tag{6.3}$$

where w_0 is the spot size

$$w_0 = \sqrt{2/k\alpha}, \tag{6.4}$$

and $\beta_{n,m}$ are the propagation constants given by

$$\beta_{n,m} = \sqrt{k^2 - 2k\alpha(n+m+1)}. \tag{6.5}$$

In Eq. (6.3) the coefficients $a_{n,m}$ are determined from the boundary value of the field incident on the fiber $V(\xi,\eta, 0)$ using the orthogonality of the Hermite-Gaussian functions. One then finds that

$$a_{n,m} = \frac{2}{\pi w_0^2} \frac{1}{2^{n+m} n! m!}$$

$$\times \int_D V(\xi,\eta,0) H_n\left(\frac{\sqrt{2}\xi}{w_0}\right) H_n\left(\frac{\sqrt{2}\eta}{w_0}\right) \exp\left(-\frac{\xi^2+\eta^2}{w_0^2}\right) d\xi\, d\eta, \tag{6.6}$$

where ξ and η are the coordinates in the input plane D.

If follows from Eqs. (6.3) and (6.6) that the field $V(r)$ after propagation to any plane $z > 0$ may be expressed in the form

$$V(r) = \int_D V(\xi,\eta,0)K(r;\xi,\eta)d\xi\,d\eta, \qquad (6.7)$$

where the propagation kernel $K(r,\xi,\eta)$ is given by

$$K(r;\xi,\eta) = \frac{k}{2\pi i}e^{i\phi(r)}\frac{\alpha}{\sin\alpha z}\exp\left\{\frac{ik\alpha}{\sin\alpha z}\left[\frac{1}{2}\cos\alpha z\left(\xi^2+\eta^2\right)-\left(\xi x+\eta y\right)\right]\right\}, \qquad (6.8)$$

and

$$\phi(r) = k\left[z+\frac{1}{2}\frac{\alpha}{\sin\alpha z}\cos\alpha z\left(x^2+y^2\right)\right]. \qquad (6.9)$$

When the medium is homogeneous, $\alpha = 0$ and Eq. (6.8) reduces to

$$K(r,\xi,\eta) = \frac{k}{2\pi i z}e^{ikz}\exp\left\{\frac{ik}{2z}\left[(x-\xi)^2+(y-\eta)^2\right]\right\}, \qquad (6.10)$$

which is also the propagation kernel for the paraxial Fresnel approximation.

Using Eqs. (6.7) and (6.8), the cross-spectral density of the field for any two points in the fiber is given by

$$W(r_1,r_2;\omega) = \iint_D K^*(r_1,\rho_1;\omega)K(r_2,\rho_2;\omega)W(\rho_1,\rho_2;\omega)d^2\rho_1\,d^2\rho_2, \qquad (6.11)$$

where $W(\rho_1,\rho_2;\omega)$ is the cross-spectral density in the source plane and $\rho_j = (\xi_j,\eta_j)$ is a radius vector in that plane. The spectrum[6] of the field is obtained by setting $r_1 = r_2 = r$ in Eq. (6.11), i.e.,

$$S(r;\omega) = \iint K^*(r,\rho_1;\omega)K(r,\rho_2;\omega)W(\rho_1,\rho_2;\omega)d^2\rho_1\, d^2\rho_2. \qquad (6.12)$$

On substituting from Eqs. (6.8) and (6.9) into Eq. (6.12) we obtain the following expression for the spectrum of the field:

$$S(\mathbf{r};\omega) = \left(\frac{k\alpha}{2\pi\sin\alpha z}\right)^2 \iint \iint d\xi_1\, d\xi_2\, d\eta_1\, d\eta_2 W(\rho_1,\rho_2;\omega)$$

$$\times \exp\left\{\frac{ik\alpha}{\sin\alpha z}\left[\frac{\cos\alpha z}{2}\left(\xi_2^2 - \xi_1^2 + \eta_2^2 - \eta_1^2\right) - x\left(\xi_2 - \xi_1\right) - y\left(\eta_2 - \eta_1\right)\right]\right\}. \qquad (6.13)$$

Equation (6.13) can be used to obtain the field spectrum at any point r for a given form of the cross-spectral density of the incident field in the source plane $z = 0$. We will choose a Gaussian Schell-model for the cross-spectral density in the source plane, viz.,

$$W(\rho_1,\rho_2;\omega) = S^{(0)}(\omega)\exp\left[-\frac{\left(\xi_1^2 + \xi_2^2\right) + \left(\eta_1^2 + \eta_2^2\right)}{4\sigma_I^2}\right]$$

$$\times \exp\left[-\frac{\left(\xi_2 - \xi_1\right)^2 + \left(\eta_2 - \eta_1\right)^2}{2\sigma_g^2}\right], \qquad (6.14)$$

where σ_I is the r.m.s width of the Gaussian intensity distribution [Full-Width-Half-Maximum(FWHM) = 2.35 σ_I] and σ_g is the r.m.s width of the spatial correlation. On substituting Eq. (6.13) into Eq. (6.14) and performing the integration [see Appendix C] we obtain the following expression for the spectrum of the field:

$$S(\mathbf{r};\omega) = S^{(0)}(\omega)M(\mathbf{r};\alpha;\omega),\tag{6.15}$$

where the spectral modifier M is given by

$$M(\mathbf{r};\alpha;\omega) = \frac{1}{z^2}\left(\frac{k\sigma_I}{\Delta}\right)^2 \exp\left[\frac{k^2(x^2+y^2)/z^2}{2\Delta^2}\right].\tag{6.16}$$

In Eq. (6.16) we have used the notation

$$\Delta = 2ab\sigma_I \sin\alpha z/\alpha z ,\tag{6.17}$$

$$a^2 = \frac{1}{8\sigma_I^2} + \frac{1}{2\sigma_g^2} ,\tag{6.18}$$

and

$$b^2 = \frac{1}{2\sigma_I^2} + \left(\frac{k\alpha\cos\alpha z}{2a\sin\alpha z}\right)^2.\tag{6.19}$$

Equations (6.15) and (6.16) are general expressions, valid within the paraxial approximation, for the spectrum of the field produced by planar secondary Gaussian Schell-model sources. In particular, Eq. (6.15) is valid at any distance z from the

source plane and for any range of real valued $n(\omega)$ and $\alpha(\omega)$. It can be easily verified that $S(r; \omega)$ reduces to $S^{(0)}(\omega)\exp\left(-r^2/2\sigma_I^2\right)$ in the limit $z \to 0$, as one might expect. In the limit when $\alpha \to 0$ our formulation corresponds to the case of dispersive homogeneous media. The spectral modifier for homogeneous media M_h is given by

$$M_h(r;\omega) = \frac{1}{1+\left(z/z_d\right)^2}\exp\left[-\frac{x^2+y^2}{2\sigma_I^2}\frac{1}{1+\left(z/z_d\right)^2}\right], \qquad (6.20)$$

where

$$z_d = \frac{2k\sigma_I^2}{\sqrt{1+4\sigma_I^2/\sigma_g^2}}. \qquad (6.21)$$

The parameter z_d is analogous to the so-called diffraction length or the Rayleigh range[7] encountered in propagation of coherent Gaussian beams and reduces to it in the coherent limit ($\sigma_g \gg \sigma_I$).

Equation (6.20) is also applicable to paraxial free-space propagation if we set $n(\omega) = 1$; then $k = k_0$. Since we have examined in the previous chapter the spectral changes that occur on free-space propagation, we consider this case first. Later we will consider the general case in which $n(\omega) > 1$ and $\alpha > 0$. In order to make our results readily available for experimental verification, we assume that the source spectrum $S^{(0)}(\omega)$ corresponds to that of a Gallium Phosphide (GaP) visible light source[8], which is well approximated by a Lorentzian line centered at 564 nm ($v_0 = \omega_0/2\pi \cong 532$ THz) and having a FWHM of 36 nm ($\cong 34$ THz). All the numerical results in this chapter pertain to this source spectrum.

6.3   Free-space propagation

In the previous chapters we examined the changes in the spectrum of light on propagation in free space and we reviewed the relevant published work. So far there has not been a clear understanding of the development of the spectral changes with increasing propagation distance from the source, a fact that may be due to the complexity of the computations involved[9]. Our analysis provides a relatively simple way for understanding the transition from near to far field within the paraxial approximation.

In our notation the spectrum of the field after propagating a distance z in free-space is given by

$$S_f(\mathbf{r};\omega) = S^{(0)}(\omega)M_f(\mathbf{r};\omega) , \qquad (6.22)$$

where M_f is the spectral modifier for free-space propagation that is obtained from M_h of Eq. (6.20) by setting $k = k_0$.

The expression for the spectrum of the field in the far-zone is obtained in the limit $k_0 z \rightarrow \infty$ (with fixed direction of observation), and it is given by

$$S_f^{(\infty)}(\mathbf{r};\omega) = S^{(0)}(\omega)\left(\frac{k_0\sigma_I}{\sqrt{2}az}\right)^2 \exp\left[-\frac{k_0^2\sigma_I^2(x^2+y^2)/z^2}{4a^2}\right] , \qquad (6.23)$$

where the superscript (∞) indicates the far-zone limit. Equation (6.23) is in agreement, within the paraxial approximation, with a known result for far-zone radiant intensity of Gaussian Schell-model sources[3].
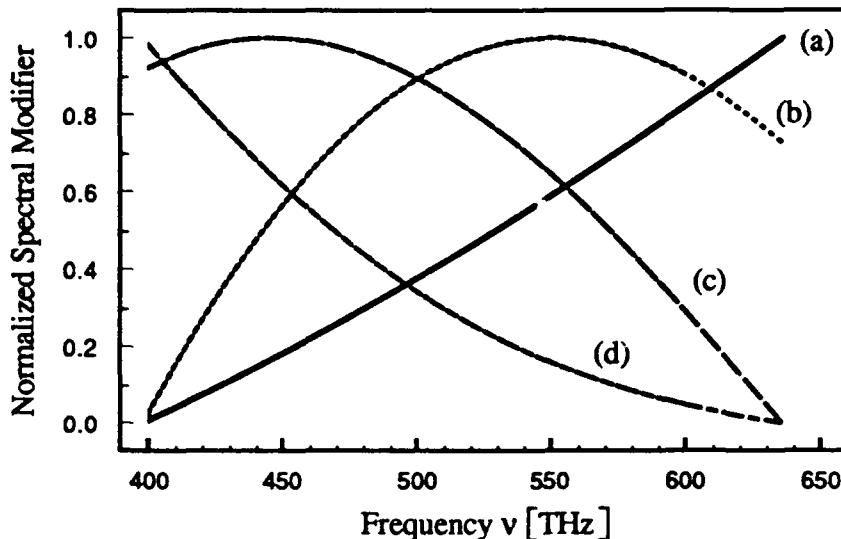
Figure 6.3: Normalized spectral modifier M_f for propagation distance $k_0 z = 100$ in free space. The spectral modifier is shown as a function of frequency v for $k_0\sigma_I = 20$ and four different values of the correlation length; $k_0\sigma_g = 1.0$ (a), $k_0\sigma_g = 8.0$ (b), $k_0\sigma_g = 10$ (c) and $k_0\sigma_g = 20$ (d). The direction of the spectral shift is determined by the slope of M_f at the center frequency of the source.

We now return to the general expression for the spectrum of the field in free space [Eq. (6.20)], and evaluate the spectral modifier M_f for sources with different states of coherence, governed by the values of σ_g and σ_I.

Figure 6.3 shows the variation of the spectral modifier M_f with the frequency $v = \omega/2\pi$ for several choices of σ_g and σ_I, when the propagation distance is $z = 1000\lambda_0/2\pi$ (i.e., when $k_0 z = 1000$), and the observation direction makes an angle of $10°$ with the z-axis. Each one of the curves is normalized so that its maximum value is unity. It follows from Eq. (6.20) that when the spectral modifier, considered as a function of v, has a positive slope at $v = v_0$, the resulting line is blue-shifted while a negative slope of the spectral modifier at that frequency results is a red-shifted spectrum. If the spectral modifier is not uniform throughout the frequency range of the source spectrum, the nature of the spectral changes may be more complicated (for more
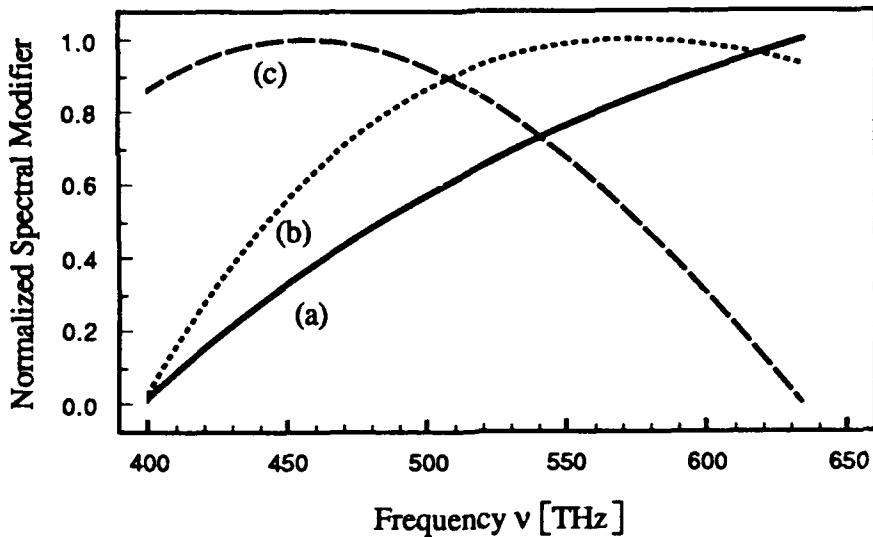
Figure 6.4: Normalized spectral modifier M_f for propagation distances $k_0 z = 100$ (a), $k_0 z = 250$ (b), and $k_0 z = 600$ (c) in free space for $k_0 \sigma_I = 20$, $k_0 \sigma_g = 10$. At $v_0 = 532$ THz a blue shift is obtained for $k_0 z = 100$ and a red shift for $k_0 z = 600$.

details see Sec. 5.3). The examples shown in Fig. 6.3 correspond to a blue shift for $k_0 \sigma_g < 9$ and red shift for $k_0 \sigma_g \geq 10$ for GaP source for which $v_0 \cong 532$ THz.

For a given state of coherence the spectral shift also depends on the propagation distance. This is shown in Fig. 6.4 where we compare the spectral modifier for different propagation distances from sources with $k_0 \sigma_I = 20$ and $k_0 \sigma_g = 10$. The spectral shift is to vard higher frequencies for $k_0 z = 100$ (positive slope at $n = n_0$), and toward lower frequencies for $k_0 z = 600$ (negative slope at $n = n_0$). Figure 6.5 shows the spectra of the GaP source when $k_0 z = 10$ (i.e. in the near zone) and when $k_0 z = 1000$ (in the far zone) with $k_0 \sigma_I = 20$ and $k_0 \sigma_g = 20$. The source spectrum exhibits a red shift in the far zone, and a slight blue shift in the near zone. It should also be noted that the spectrum becomes asymmetric as a result of propagation.

We quantify the magnitude of the spectral shift by defining a parameter Δv that corresponds to the shift of the spectral peak from from the location of the peak of the
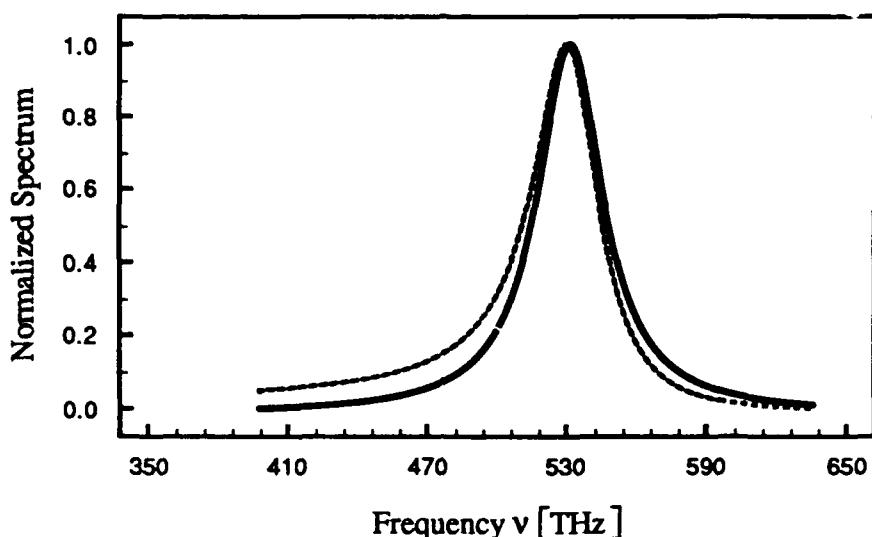
Figure 6.5: Normalized field spectrum for observation at an angle of 10° off axis and a propagation distance k_0z = 1000. The source is characterized by $k_0\sigma_I$ = 20 and $k_0\sigma_g$ = 20. The solid line shows the original source spectrum and the dashed line shows the red-shifted field spectrum.

source spectrum. In Fig. 6.6 we show the spectral shift Δv as a function of the propagation distance k_0z, for k_0s_I = 20 and several values of $k_0\sigma_g$. We note that when the source is relatively incoherent ($k_0\sigma_g \leq 1$) the spectral shift, which is towards the blue for this angle of observation, develops rapidly with propagation distance. When the source is relatively coherent ($k_0\sigma_g \gg 1$) an initial blue shift turns into a red shift with increasing k_0z.

For the states of coherence considered in this paper, the transition from the blue shift to the red shift takes place when $k_0z \sim 100$. In all cases the frequency shift in the far zone approaches an asymptotic value which depends on $k_0\sigma_g$. The constant value . The frequency shift for $k_0\sigma_g$ = 25 [curve (d) in Fig. 6.6] is about 10% of the source spectral width (FWHM $\cong$ 34 THz).
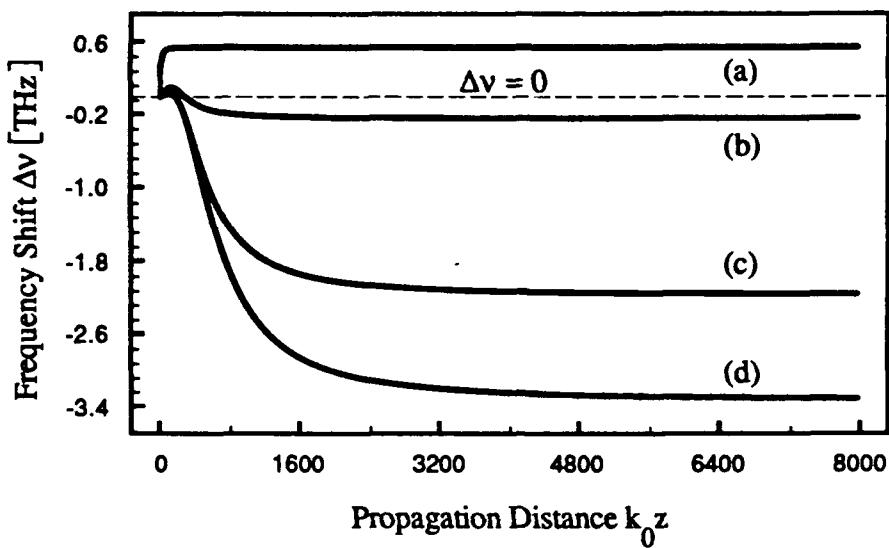
Figure 6.6: Frequency shifts Δv versus propagation distance for sources char acterized by the same value of $k_0\sigma_I = 20$ and different values of $k_0\sigma_g$: $k_0\sigma_g = 1$ (a), $k_0\sigma_g = 10$ (b), $k_0\sigma_g = 20$ (c) and $k_0\sigma_g = 25$ (d).

6.4. Spectral changes in homogeneous media

In the previous section we showed that the changes in the spectrum on propagation in free space depend on the state of coherence and on the propagation distance from the source. In this section we consider propagation through homogeneous media for which the index of refraction $[n(\omega) > 1]$ is independent of position in space. We assume that the index of refraction is frequency dependent, a feature that indicates the dispersive nature of the homogeneous medium. The wave number is then given by

$$k = n(\omega)\frac{\omega}{c}. \qquad (6.24)$$

On substituting Eq. (6.24) in Eq. (6.20) we obtain the expression for the spectral modifier for dispersive homogeneous media. When the refractive index $n(\omega)$ is nearly constant over the source spectral width, the medium acts as a non-dispersive homogeneous medium of constant refractive index $n_0 = n(\omega_0)$, where ω_0 is the central frequency of the source spectrum. We will consider the non-dispersive case first.

It is evident from Eq. (6.20) that the spectral modifier M_h for a non-dispersive homogeneous medium is identical to that of free space if k_0 is replaced by $n_0 k_0$. Thus, the free space results for the spectral modifier shown in Figs. 6.3 and 6.4 apply, provided that the scaling factor k_0 is appropriately modified. The spectral changes can be quite different as a result of the scaling. The comparison between the spectral changes occurring on propagation in free-space and on propagation in homogeneous non-dispersive media must be considered separately for distances short and long compared with z_d. For a short propagation range $(z \ll z_d)$

$$\frac{1}{1+\left(z/z_d\right)^2} \approx 1 ,$$

(6.25)

and the spectral modifier M_h becomes independent of n_0. Hence for such propagation distances we expect no difference between the spectral changes occurring in dispersive homogeneous media and free space. For long propagation distances $(z \gg z_d)$ the approximation

$$\frac{1}{1+\left(z/z_d\right)^2} \sim \left(\frac{z_d}{z}\right)^2$$

(6.26)

holds, and the spectral modifier for propagation in homogeneous media $[n(\omega) > 1]$ then differs by a multiplicative factor

$$f = n_0^2 \exp\left[-\frac{x^2+y^2}{2\sigma_I^2}\left(\frac{z_0}{z}\right)^2\left(n_0^2-1\right)\right]$$ (6.27)

in comparison with the spectral modifier for free-space propagation. In Eq. (6.27) z_0 is given by the expression

$$z_0 = \frac{2k_0\sigma_I^2}{\sqrt{1+4\sigma_I^2/\sigma_g^2}} .$$ (6.28)

The extent of the spectral changes taking place under these circumstances depends on the value of n_0. Figure 6.7 gives a comparison of spectral shifts in free space ($n_0 = 1$) and in two non-dispersive homogeneous media of refractive indices $n_0 = 1.5$ and 2.0 when $k_0\sigma_I = 20$ and $k_0\sigma_g = 10$. The most notable feature is that the far-zone value of the spectral shift increases with increasing refractive index n_0. This is an important feature which shows that the spectral changes are enhanced in a homogeneous medium.
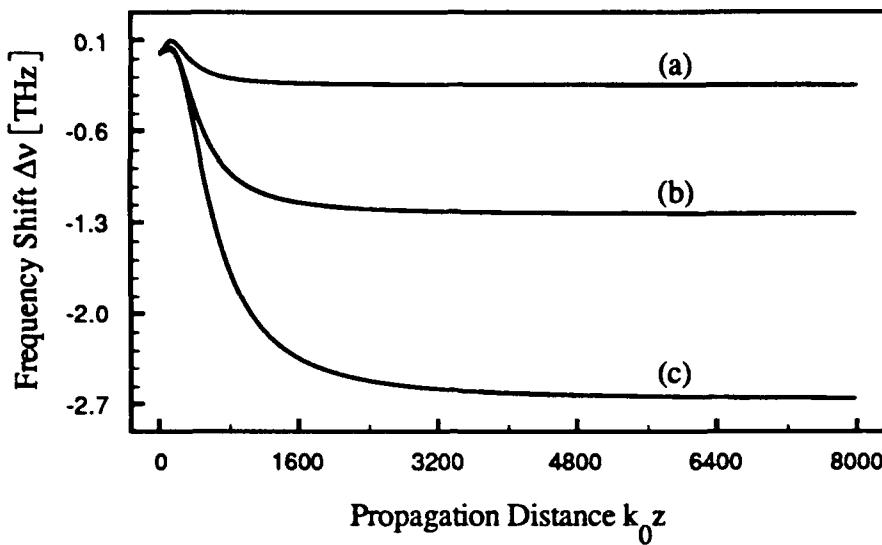
Figure 6.7: Comparison of frequency shifts for propagation in non-dispersive homogeneous media. The frequency shifts for a fixed angle of observation (10°) are shown for propagation in free space (a), for propagation in a homogeneous medium of an index of refraction $n(\omega_0) = 1.5$ (b) and for propagation in a medium of index of refraction $n(\omega_0) = 2.0$ (c). The observation angle is 10° and the source parameters are $k_0 \sigma_I = 20$ and $k_0 \sigma_g = 10$.

We next consider propagation in dispersive homogeneous media. As in the case of non-dispersive media, we must consider the changes in the spectrum for short and long propagation distances separately. For short propagation distances ($z \ll z_d$), the quantity $1/\left(1 + z^2/z_d^2\right)$ is again independent of the index of refraction and the spectral effects are identical to those encountered in free-space propagation. For long propagation distances ($z \gg z_0$),

$$f(\omega) = n_0^2(\omega) \exp\left\{-\frac{x^2 + y^2}{2\sigma_I^2}\left(\frac{z_0}{z}\right)^2\left[r_0^2(\omega) - 1\right]\right\}$$ (6.29)

and hence the difference in the spectral effects in this medium from those generated in free-space depend on the variation of $n(\omega)$ in the frequency range covered by the source
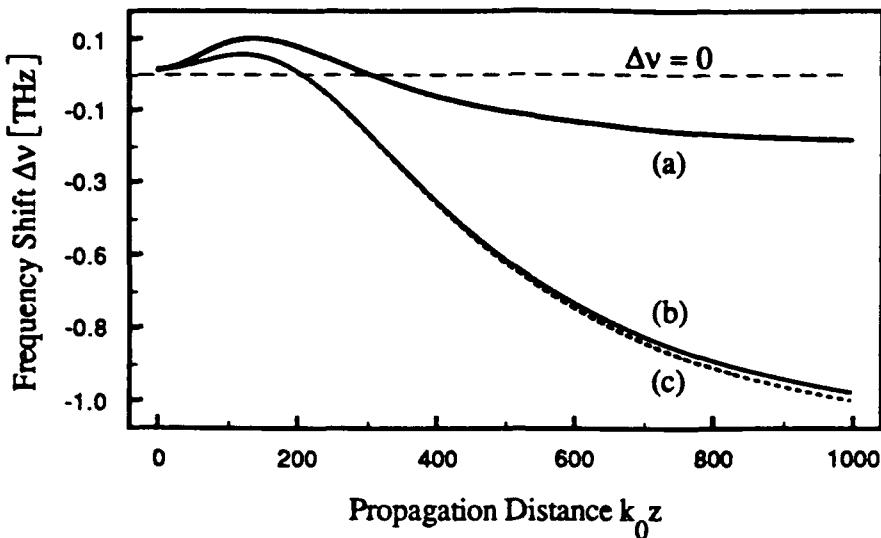
Figure 6.8: Comparison of frequency shifts for dispersive homogeneous media. Δv is shown as a function of $k_0 z$ for propagation in free space (a), propagation in pure silica (b), and propagation in silica doped with 7.9% GeO_2 (c). The observation angle is $10°$ and the source parameters are $k_0 \sigma_I = 20$ and $k_0 \sigma_g = 10$.

spectrum [cf. Eq. (6.27)]. We illustrate our results by using a slab of silica glass as an example of dispersive homogeneous medium.

Figure 6.8 shows the frequency shift Δn obtained after light from GaP source propagates through a slab of silica glass of various thicknesses. The source parameters are $k_0 \sigma_I = 20$ and $k_0 \sigma_g = 10$. The frequency dependence of $n(\omega)$ was obtained by using the well-known Sellmeier formula[10]

$$n^2(\omega) = 1 + \sum_{j=1}^{3} \frac{B_j \omega_j^2}{\omega_j^2 - \omega^2} .$$ (6.30)

For pure silica $B_1 = 0.6961663$, $B_2 = 0.4079426$, $B_3 = 0.8974794$, $\lambda_1 = 0.0684043$, $\lambda_2 = 0.1162414$, $\lambda_3 = 9.896161$ mm, where $\lambda_j = 2\pi c/\omega_j$.

The effect of dopants on the spectral shift can be easily included in our analysis. For example, the refractive index $n(\omega)$ of silica glass can be increased by doping it with

germania (GeO$_2$). The refractive index $n(\omega)$ is still given by the Sellmeier formula but the parameters B_j and ω_j are different and depend on the amount of the dopant. As an example, we consider silica glass doped with 7.9% GeO2, for which the parameters are $B_1 = 0.7136824$, $B_2 = 0.4254807$, $B_3 = 0.8964226$, $\lambda_1 = 0.0617167$, $\lambda_2 = 0.1270814$, $\lambda_3 = 9.896161$ mm. Figure 6.8 shows the expected change (dashed curve) in the frequency shift. The shift is slightly larger for doped silica since the dopant increases the refractive index by a small amount. In both cases (pure silica and slightly doped silica) the frequency shifts in the far zone are much larger than those that would be produced in free space.

The main conclusion of this section is that correlation-induced spectral shifts are enhanced in a homogeneous medium of refractive index $n(\omega) > 1$. The frequency dependence of the refractive index $n(\omega)$ is not critical as the enhancement is found to occur even when n is frequency independent. The origin of the enhancement factor for large propagation distances can be understood by referring to Eq. (6.20) and using the formula $k = \omega n(\omega)/c$ in Eq. (6.21). The Gaussian factor in Eq. (6.20), plotted as a function of ω, is narrower for a homogeneous medium than for free space. It is this feature of the spectral modifier that is responsible for a larger spectral shift when $n(\omega) > 1$.

6.5 Propagation in inhomogeneous media

In this section we return to the general expression for the spectrum of light in a graded-index fiber [Eqs. (6.15)-(6.19)]. In this case the parameter α is non-zero; it depends on the fiber design. In particular we consider a fiber whose core is made of doped silica (7.9% GeO$_2$ at the core center) and a cladding made of pure SiO$_2$. If $n_1(\omega)$ is the
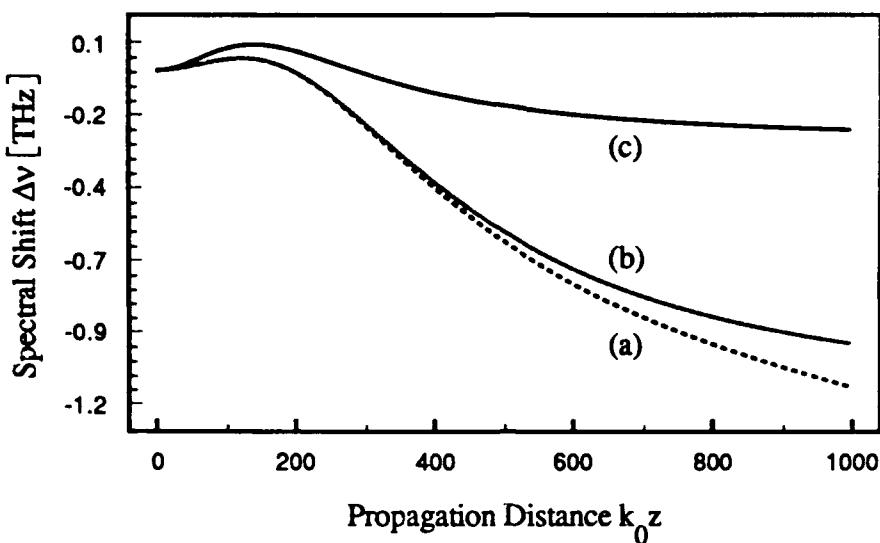
Figure 6.9: Frequency shift Δv versus the propagation distance $k_0 z$ in a dispersive graded-index medium (a). Curve (b) shows Δv when the inhomogeneous nature of the medium is ignored by setting $\alpha = 0$. Curve (c) shows the corresponding result for free-space propagation. The observation angle is $10°$ and the source parameters were chosen to be $k_0 \sigma_I = 20$ and $k_0 \sigma_g = 10$.

refractive index at the core center $(r = 0)$ and $n_2(\omega)$ is the refractive index at the boundary $(r = R_0)$, the parameter α is given by

$$\alpha(\omega) = \frac{1}{R_0} \sqrt{1 - n_2^2(\omega)/n_1^2(\omega)} \ . \tag{6.31}$$

Since $n_1(\omega)$ and $n_2(\omega)$ can be obtained by using Eq. (6.29), the frequency dependence of $\alpha(\omega)$ is readily determined. In the following calculations we take the core radius to be $R_0 = 25 \ \mu m$.

Figure 6.9 shows the frequency shift as a function of the propagation distance for $\alpha \neq 0$ in such a medium, and the shifts generated in a homogeneous medium of refractive index n_1. We note that in the range of propagation distances shown in the figure, the frequency shift is larger for a graded-index medium than in the

homogeneous medium. This enhancement of the frequency shift is due to the inhomogeneous nature of the medium and depends on the functional form of the inhomogeneity.

Although the frequency shift Δv tends to a constant (far-zone) in a homogeneous medium, no such limit exists in the graded-index medium considered here. This feature is due to the imaging property of a medium with a quadratic variation of the refractive index. Such a medium reproduces the incident field periodically, with a period given by $\Delta z = 2\pi/\alpha$, a feature that is due to the periodic nature of the propagation kernel, Eq. (6.8). One would thus expect that the spectrum $S(r; \omega)$ given by Eq. (6.12) also reduces to the source spectrum for $z = 2m\pi/\alpha$, where m is a positive integer. We show in Appendix D that this is indeed the case. Furthermore, we find that the source spectrum is reproduced not only at $z = 2m\pi/\alpha$, but also at $z = (2m + 1)\pi/\alpha$, except for a spatial inversion of the intensity distribution. For a symmetric intensity profile such as a Gaussian, $S(r, \omega)$ is reproduced periodically with a period $z_p = \pi/\alpha$.

It would appear from this discussion that the spectral shift should follow a periodic evolution pattern with period z_p. However, this is not the case, as is evident from the solid curve in Fig. 6.10 where the spectral shift is plotted as a function of $k_0 z$ for propagation distances covering three periods (with $k_0 z_p \sim 6600$) for $k_0 \sigma_I = 20$, $k_0 \sigma_g = 10$, and α obtained by using Eq. (6.31). Figure 6.10 is drawn for a fixed radial distance from the fiber axis ($\rho = 10$) rather than for a fixed observation angle. This choice is made because for large propagation distances the radial distance would exceed the fiber dimensions if the observation angle were kept fixed. Figure 6.10 also shows that the frequency shift indeed becomes zero for $z_p = \pi/\alpha_0$ [$\alpha_0 = \alpha(\omega_0)$], but its maximum and minimum values become larger for successive periods.
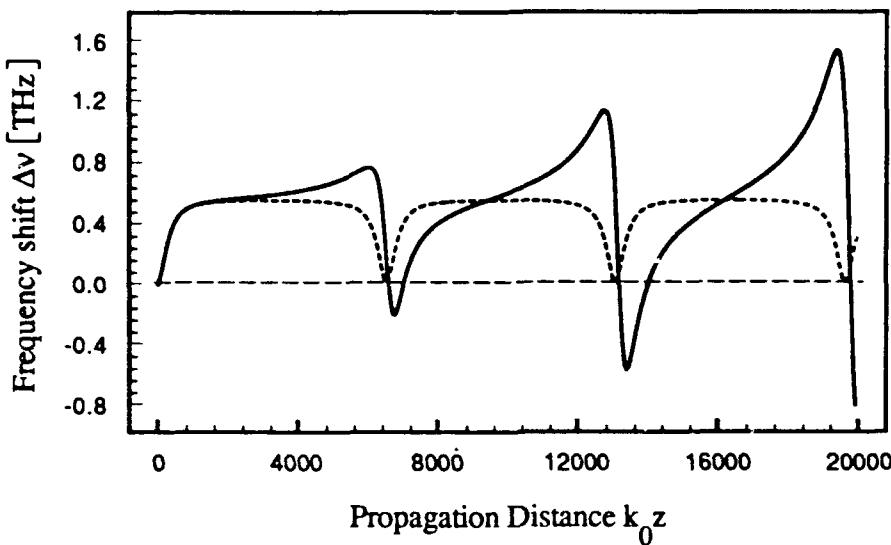
Figure 6.10: Frequency shift Δv as a function of propagation distance in a graded-index fiber (solid line). The frequency shifts are calculated for observation at a fixed distance $10/k_0$ from the center of the fiber and $k_0\sigma_I = 20$ and $k_0\sigma_g = 10$. The dashed line shows the frequency shifts when the frequency dependence of α is ignored by setting $[\alpha(\omega_0)/k_0 = 0.00048]$.

The physical origin of the non-periodic nature of the frequency shift can be traced back to the dispersive nature of the graded-index media that makes α frequency dependent. Indeed, if α is replaced by α_0, we obtain the behavior indicated by the dashed curve in Fig. 6.10. It is clear from this curve that when the frequency dependence of α is ignored, the frequency shift Δv shows periodic behavior with period π/α_0. When α is allowed to vary with frequency, Δv becomes non-periodic. This feature may be understood by noting that the period $z_p = \pi/\alpha$ itself becomes frequency dependent. Since the argument αz of the trigonometric functions appearing in Eqs. (6.17) and (6.19) is frequency-dependent, we may expect z-dependent changes in the frequency shift. Thus we conclude that the spectral shifts occurring in an inhomogeneous medium are strongly affected by the dispersive nature of the medium.

References

1   A. Ghatak and K. Thyagarajan, "Graded Index Optical Waveguides: A Review", in *Progress In Optics* XVIII, E. Wolf ed. (North Holland, Amsterdam, 1980), pp. 1-126.

2   a.   G.P. Agrawal, A. K. Ghatak and C.L. Metha, "Propagation of a partially coherent beam through selfoc fibers", Opt. Commun. 12, 333-337(1974).

     b.   P. Spano, "Connection between spatial coherence and modal structure in optical fibers and semiconductor lasers", Opt. Commun., 33, 265-270 (1980).

     c.   S. Piazzola and P. Spano, "Spatial coherence in incoherently excited optical fibers", Opt. Commun., 43, 175-179 (1982).

     d.   M. Imai and Y. Ohtsuka, "The influence of mode-coupling on the degree of coherence in an optical fiber", Opt. Commun., 45, 331-335 (1983).

     e.   M. Imai, S. Satoh and Y Ohtsuka, "Complex degree of spatial coherence in an optical fiber: theory and experiment", J. Opt. Soc. Amer. A, 3, 86-93 (1986).

3   See, for example, in a different notation, E. Wolf and E. Collett, "Partially coherent sources which produce the same far-field intensity distribution as a laser", Opt. Commun. 25, 293-296 (1978).

[4]   Our analysis here is based on G.P. Agrawal, A. K. Ghatak and C.L. Metha, "Propagation of a partially coherent beam through selfoc fibers", Opt. Commun. 12, 333-337(1974).

[5]   D. Marcuse, *Light Transmission Optics*, (Van Nostrand Reinhold Comp., New York, 1972), p. 267.

[6]   Here the field spectrum $S(r; \omega)$ is taken to be the diagonal component $W(r; r; \omega)$ of the cross-spectral density. Strictly speaking, the spectral intensity should be identified with the magnitude of the flux vector associated with the optical field. However, in the paraxial approximation these two quantities are proportional to each other.

[7]   A.E. Siegman, *Lasers*, (University Science Books, Mill Valley, California, 1986), p 668.

[8]   See, for example, Texas Instruments type TIL211, Bulletin No. DS-S 7412095, March 1974.

[9]   a.   Z. Dacic and E. Wolf, "Changes in the spectrum of a partially coherent light beam propagating in free space", J. Opt. Soc. Amer. A 5, 1118-1126 (1988).

        b.   A. Gamliel, "Mode analysis of spectral changes in light propagation from sources of any state of coherence", J. Opt. Soc. Amer. A, in press.

10   G.P. Agrawal, *Nonlinear fiber optics*, (Academic Press, New York 1989), pp. 7-8.

Appendix C: Derivation of the expression for the spectrum of the field Eq. (6.15)

The spectrum of the field at any point r is given by the expression

$$S(r;\omega) = \iint K^*(r;\rho_1;\omega)K(r;\rho_2;\omega)W(r_1,r_2;\omega)d^2\rho_1 d^2\rho_2 \ . \qquad (C\,1)$$

Here $K(r;\rho;\omega)$ is the propagator, given by Eqs. (6.8), and $W(\rho_1;\rho_2;\omega)$ is the cross-spectral density in the source plane, given by Eq. (6.14). On substituting from Eq. (6.14) into Eq. (C 1) we find that

$$S(r;\omega) = S^{(0)}(\omega)\left(\frac{k\alpha}{2\pi\sin\alpha z}\right)^2 B(x;\omega)B(y;\omega) \ , \qquad (C\,2)$$

where

$$B(x;\omega) = \iint \exp\left\{-\frac{\xi_2^2 + \xi_1^2}{4\sigma_I^2} - \frac{(\xi_2 - \xi_1)^2}{2\sigma_g^2}\right\}$$

$$\times \exp\left\{\frac{ik\alpha}{\sin\alpha z}\left[\frac{\cos\alpha z}{2}(\xi_2^2 - \xi_1^2) - x(\xi_2 - \xi_1)\right]\right\}d\xi_1 d\xi_2 \ . \qquad (C\,3)$$

To perform the two-dimensional integration we introduce the average and difference variables

$$\gamma_1 = \frac{1}{2}(\xi_2 + \xi_1), \qquad (C\,4)$$

$$\gamma_2 = \xi_2 - \xi_1 \ . \qquad (C\,5)$$

Equation (C 3) then takes the form

$$I(x;\omega) = \int d\gamma_1 \exp\left[-\gamma_1^2/2\sigma_I^2\right]$$

$$\times \int d\gamma_2 \exp\left\{-\gamma_2^2\left[\frac{1}{8\sigma_I^2} + \frac{1}{2\sigma_g^2}\right] + \frac{ik\alpha\gamma_2}{\sin\alpha z}\left[\gamma_1\cos\alpha z - x\right]\right\}. \qquad \text{(C 6)}$$

If we define the parameter a by the formula

$$a^2 = \frac{1}{8\sigma_I^2} + \frac{1}{2\sigma_g^2}, \qquad \text{(C 7)}$$

and use the relation[1]

$$\int_{-\infty}^{\infty} \exp\left[-p^2 x^2 \pm qx\right] dx = \frac{\sqrt{\pi}}{p}\exp\left(\frac{q^2}{4p^2}\right), \qquad \text{(C 8)}$$

Eq. (C 6) may be written as

$$I(x;\omega) = \frac{\sqrt{\pi}}{a}\exp\left[-x^2\left(\frac{k\alpha}{2a\sin\alpha z}\right)^2\right]$$

$$\times \int d\gamma_1 \exp\left\{-\gamma_1^2\left[\frac{1}{2\sigma_I^2} + \left(\frac{k\alpha\cos\alpha z}{2a\sin\alpha z}\right)^2\right] + 2\gamma_1 x\cos\alpha z\left(\frac{k\alpha}{2a\sin\alpha z}\right)^2\right\}. \qquad \text{(C 9)}$$

Next we define

$$b^2 = \frac{1}{2\sigma_I^2} + \left(\frac{k\alpha\cos\alpha z}{2a\sin\alpha z}\right)^2 , \qquad \text{(C 10)}$$

and use Eq. (C 8) again. We then find

$$I(x;\omega) = \frac{\pi}{ab}\exp\left\{-x^2\left(\frac{k\alpha}{2a\sin\alpha z}\right)^2\left[1-\left(\frac{k\alpha\cos\alpha z}{2ab\sin\alpha z}\right)^2\right]\right\} . \qquad \text{(C 11)}$$

We note that

$$\left[1-\left(\frac{k\alpha\cos\alpha z}{2ab\sin\alpha z}\right)^2\right] = \frac{1}{(2ab\sin\alpha z)^2}\left[(2ab\sin\alpha z)^2 - (k\alpha\cos\alpha z)^2\right] , \quad \text{(C 12)}$$

which, by Eq. (C 10) can be simplified to the form

$$\left[1-\left(\frac{k\alpha\cos\alpha z}{2ab\sin\alpha z}\right)^2\right] = \frac{1}{2b^2\sigma_I^2} . \qquad \text{(C 13)}$$

On substituting from Eq. (C 11) and Eq. (C 13) into Eq. (C 2) and using a similar expression for $B(y; \omega)$ we obtain the expression

$$S(r;\omega) = S^{(0)}(\omega)\left(\frac{k\alpha}{2ab\sin\alpha z}\right)^2\exp\left\{-\frac{x^2+y^2}{2}\left(\frac{k\alpha}{2ab\sigma_I\sin\alpha z}\right)^2\right\} , \qquad \text{(C 14)}$$

which can be written in the form

$$S(r;\omega) = S^{(0)}(\omega)\left(\frac{k\sigma_I}{z\Delta}\right)^2\exp\left\{-\frac{k^2}{2\Delta^2}\frac{x^2+y^2}{z^2}\right\} , \qquad \text{(C 15)}$$

with

$$\Delta = 2ab\sigma_I \frac{\sin \alpha z}{\alpha z} \ . \qquad\qquad (C\ 16)$$

---

[1]   I.S. Gradshteyn and I.M. Ryzhik, *Table of Integrals, Series, and Products*, (Academic Press, New York, 1980), § 3.323.2.

Appendix D: Proof of the periodic reproduction of the source spectrum

When the propagation distance satisfies the condition $\alpha z = m\pi$ for a positive integer m, some of the factors in Eq. (6.13) become singular. However, the spectrum of the field at such propagation distances remains well defined. In this appendix we use the method of stationary phase to evaluate the spectrum in the limit as $z \to m\pi/\alpha$. We start with Eq. (6.13) and rewrite it as

$$S(r;\omega) = \left(\frac{k\alpha\Lambda}{2\pi}\right)^2 \iint \iint d\xi_1\, d\xi_2\, d\eta_1\, d\eta_2\, W(\xi_1,\xi_2,\eta_1,\eta_2;\omega)$$

$$\times \exp\left\{ik\alpha\Lambda\left[\frac{\cos\alpha z}{2}\left(\xi_2^2 - \xi_1^2 + \eta_2^2 - \eta_1^2\right) - x\left(\xi_2 - \xi_1\right) - y\left(\eta_2 - \eta_1\right)\right]\right\},$$

(D 1)

where

$$\Lambda = \frac{1}{\sin\alpha z}.$$

(D 2)

Since $\Lambda \to \infty$ as $z \to m\pi/\alpha$, we can evaluate the integral using the method of stationary phase[1]. According to this method, if

$$I(\Lambda) = \int f(t)\exp[i\Lambda\phi(t)]dt,$$

(D 3)

one has, under fairly general conditions

$$I(\Lambda) \sim \exp[i\Lambda\phi(d)]f(d)\sqrt{\frac{2\pi}{\Lambda|\phi''(d)|}}\exp\left(\frac{\pi i\mu}{4}\right) + O\left(\Lambda^{-3/2}\right) \quad as \quad \Lambda \to \infty. \quad (D 4)$$

Here d is a zero of $\phi'(t)$ [assuming there is only one] and $\mu = \text{sgn}[\phi''(d)]$. Applying these formulas to Eq. (D 1), with the definitions

$$\phi(\xi_2) = k\alpha\left[\frac{\cos\alpha z}{2}\xi_2^2 - x\xi_2\right] , \tag{D 5}$$

and

$$f(\xi_2) = W(\xi_1, \xi_2, \eta_1, \eta_2; \omega) , \tag{D 6}$$

we find that

$$I(\Lambda) \sim \sqrt{\frac{2\pi}{\Lambda k\alpha}}\exp\left(\frac{i\pi\mu}{4}\right)$$

$$\times\exp\left\{\frac{ik\alpha}{\cos\alpha z}x^2\left(\frac{1}{2} - \frac{1}{\cos\alpha z}\right)\right\}W(\xi_1, \frac{x}{\cos\alpha z}, \eta_1, \eta_2) + O\left(\Lambda^{-3/2}\right) . \tag{D 7}$$

We repeat the same procedure for the integration over the variables ξ_1, η_1, η_2 and take the asymptotic limit $\Lambda \to \infty$. All the phase factors cancel and the final result is

$$S(r; \omega) = W\left(\frac{x}{\cos\alpha z}, \frac{x}{\cos\alpha z}, \frac{y}{\cos\alpha z}, \frac{y}{\cos\alpha z}; \omega\right) . \tag{D 8}$$

Since $\cos\alpha z = \pm 1$ we see from the last equation that the spectrum of the source is completely reproduced at propagation distances $z = 2m\pi/\alpha$. For propagation distances $z = (2m + 1)\pi/\alpha$ the spectrum of the source is again reproduced but is spatially inverted. For a symmetric intensity profile such as Gaussian, the source spectrum and the intensity

distribution are both reproduced at $z = m\pi/\alpha$. It can be shown that Eq. (D 8) is exact at

$z = m\pi/\alpha$ in spite of our use of an asymptotic approximation for evaluating the integrals in

Eq. (D 1).

---

[1]   N. Bleistein and R.A. Handelsman, *Asymptotic Expansions of Integrals*, (Holt,

Rinehart and Winston, New York, 1975), Chapter 6.

7

Summary

In this thesis we investigated effects of source correlations on the fields radiated by sources of any state of coherence. In particular we studied the effects of spatial correlations of source fluctuations on the total emitted power and on the spatial and spectral distribution and the spectrum of the emitted radiation.

After a general introduction presented in Chapter 1 we reviewed some elements of coherence theory that are essential to the discussion in this thesis. Chapter 2 consists of two parts. In the first part we introduce the concept of radiation efficiency and we discuss the efficiency of planar, secondary, Gaussian Schell-model sources. We show that for sources of this class the radiation efficiency increases with increasing source size and with increasing spatial correlation length of the source fluctuations. We found that when the linear dimensions of the source exceed several wavelengths, the radiation efficiency is typically over 90%, irrespective of the source correlation length[1]. A different result is obtained for the radiation efficiency of three-dimensional primary sources; in this case we find that the radiation efficiency does not increase with increasing source size or with increasing correlation length. In fact, we find, for example, that the radiation efficiency of a uniform, spherically symmetric, coherent and co-phasal source, decreases with increasing source radius.

For a primary partially coherent, three-dimensional sources with a given intensity profile we developed a method which makes it possible to determine the spatial correlation function that maximizes the radiation efficiency. Using this method we showed that the radiation efficiency of an isotropic quasi-homogeneous source is maximized when the degree of spatial coherence is given by $\sin kr'/kr'$. This result is

significant in that it shows from the point of view of coherence theory that the spatial correlation of blackbody radiators gives rise to the maximum radiation efficiency of isotropic quasi-homogeneous sources.

The discussion of the radiation efficiency was formulated using the space-frequency representation and the results therefore apply on a frequency by frequency basis. In chapter 3 we focused our attention on the frequency-dependence of fields generated by partially coherent sources by investigating the effects of source correlations on the spectrum of the radiation. We analyzed a basic physical configuration in which source correlation can be manifested, i.e., that of two small sources. Using this simple example we illustrated possible modifications of field spectra depending on the choice of the correlation function. Our calculations included examples of line narrowing, line broadening, line shifting and line splitting.

The range of possible modification of field spectra can be significantly enhanced by using a system which contains more than two sources. One such system is an array of 2N sources which we also analyzed in the last part of chapter 3.

The discussion in chapter 3 of spectral modulation in scalar theory was extended in chapter 4 to the full electromagnetic case. We considered the effect of correlation on the spectrum of the electromagnetic field produced by partially correlated linear dipoles. In this chapter we were mainly concerned with the dependence of the angular distribution of the radiant intensity and with the shape of the spectrum in various directions of observation. We showed that the the number of lobes of the radiant intensity produced by the partially correlated dipoles are determined, just as in the deterministic case, mainly by the separation distance between the two dipoles, whereas the direction and the shape of the lobes were largely determined by the correlation between the two dipoles.

In the analysis of chapters 3 and 4 we assumed that we can choose certain forms of spatial correlations. In chapter 5 we analyzed the radiation from a source that consisted of a finite number of coherent modes. The spatial correlation of this source then depends both on the number of the modes and on their relative strengths. For sources that consist of Hermite-Gaussian modes we showed the spectral effects in the far and in the near zone and their dependence on the mode composition of the source. We also examined, for comparison, the small spectral shifts that occur on propagation from sources that consist of a single coherent mode. In the analysis of chapter 5 we introduced the concept of "spectral modifier" which is a correlation-dependent factor that determines the spectral changes in the emitted radiation.

Chapters 2-5 pertain to propagation in free space. In chapter 6 we considered propagation of partially coherent light in homogeneous and inhomogeneous media. We also studied how the spectrum changes as a function of the propagation distance from the source plane. Our results show that spectral shifts are er   ced in a medium whose index of refraction is larger than unity. Within a given homogeneous medium th.· spectral shifts usually develop rapidly with increasing propagation distance from the source plane. In the case of a non-dispersive graded-index fiber, we showed that the spectral shifts are periodic along the propagation direction. When dispersion effects are taken into account we showed that there exists deviation of the spectral shifts from the periodic form.

The research described in this thesis ·· s conducted between 1986 and 1989. During this period many other contributions were made in this field by numerous authors. It see.as that there is a great potential for further work in this area, especially in connection with astrophysics, spectroradiometry and scattering.

1   This statement assumes that the correlation length is not less than that of a thermal source.

Appendix E: List of publications

Journal Publications

A. Gamliel, "Radiation Efficiency of Planar Gaussian Schell-Model Sources", Opt. Commun. 60, 333 (1986).

A. Gamliel and E. Wolf, "Spectral Modulation by Control of Source Correlations", Opt. Commun. 65, 91 (1988).

A. Gamliel and N. George, "Radiated Spectrum from Two Partially Correlated Dipoles", J. Opt. Soc. Amer. A 6, 1150(1989).

A. Gamliel, K. Kim, A.I. Nachman and E. Wolf, "A New Method for Specifying Non-radiating, Monochromatic, Scalar Sources and their Fields", J. Opt. Soc. Amer. A, 6, 1388(1989).

A. Gamliel, "Mode analysis of spectral changes in light propagation from sources of any state of coherence", J. Opt. Soc. Amer. A, in press.

A. Gamliel and A.T. Friberg, "Spatial correlations that maximize the radiation efficiency of three-dimensional primary sources", J. Opt. Soc. Amer. A, in press.

A. Gamliel and G.P. Agrawal, "The Wolf effect in homogeneous and inhomogeneous media, J. Opt. Soc. Amer. A, in press.

G.P. Agrawal and A. Gamliel, "Spectrum of partially coherent light: Transition from near to far zone", Opt. Commun., **78**, 1 (1990).

A. Gamliel and G.P. Agrawal, "Spectrum-Enhanced Spreading of Partially Coherent Beams", Opt. Commun., in press.

Other Publications

A. Gamliel, "New Method For Spectral Modulation", Proc. SPIE 976, 137(1988).

A. Gamliel, "Spectral changes in light propagation from a class of partially coherent sources", Proc. Sixth Rochester Conference on Coherence and Quantum Optics (Plenum Publ.), in press.

N. George and A. Gamliel, "Correlation Theory of Electromagnetic Radiation using Multipole Expansions", in Electromagnetic Theory: Recent Advances, Springer Verlag, in press.

Appendix F: List of symbols

Symbol		Page
A_{nm}	Angular spectrum representation for coherent modes	135
A_i	Amplitude of a spectral line	75
$\alpha(\omega)$	Radial gradient of the index of refraction	143
B	Magnetic field produced by the dipoles	98
c	Speed of light	14
$C(\omega)$	The radiation efficiency	34
$\hat{\mathcal{D}}$	Differential propagator	13
$D(\xi)$	Dawson integral	37
$\mathcal{D}$	Domain normalization parameter	42
$D(\mathbf{u}; \omega)$	Directivity (general)	111
$D(\omega)$	Directivity (standard definition)	111
$F(\mathbf{u})$	Directional distribution of the transform of g_Q	54
$f(z)$	Auxiliary function related to the total radiated power	109
$\phi(\omega)$	Total flux at frequency ω	34
ϕ_m	Eigenfunctions of Fredholm integral equation	22
g_Q	Spatial correlation of a primary source	47
$g(\omega)$	Auxiliary function related to the maximum amplitude of a spectrally modified line	79
$\Gamma(\dots)$	Mutual coherence function	10
Γ_i	Spectral line width	75
γ	Degree of coherence	11
$H_n(x)$	Hermite polynomial	124
J	Radiant intensity	15

j_1	Spherical Bessel function	46
k	Wavenumber	14
K_0	Spatial frequency vector at which the radiation efficiency attains its maximum value	59
$K(\ldots)$	Propagator	146
λ	Wavelength of the radiation	14
λ_n	Eigenvalues	22
Λ_{nm}	Frequency independent eigenvalues	122
M	Spectral modifier	125
μ	Spatial (spectral) degree of coherence	17
μ_p	Degree of correlation of polarization fluctuations	100
μ_Q	Degree of correlation of source fluctuations	72
n	Number of lobes in the radiation pattern	106
N	Intensity normalization	42
$n_0,\ n$	Index of refraction for the fiber	143
$P(\omega)$	Total radiated power at frequency ω	15
$p_j(\mathbf{r},t)$	Polarization fluctuations	96
$\tilde{p}_j(\mathbf{r},t)$	Spatial Fourier transform of $p_j(\mathbf{r},t)$	97
Π_e	Electric Hertz vector	96
$Q(\mathbf{r};\omega)$	Scalar source distribution	48
$Q_i(\omega)$	Stationary source distributions	71
$R(\mathbf{r}';\omega)$	Auxiliary source function	47
$S(\mathbf{r};\omega)$	Spectrum at position $\mathbf{r}$	14
S_Q	Spectrum of a source	72
S_V	Spectrum of the field	72
s_V	Reduced field spectrum	74
$S^{(\infty)}(r\mathbf{u};\omega)$	Far-zone spectrum in direction $\mathbf{u}$	99

List of symbols